Separating the contributions of descending pathways to movement

Isabel Stella Glover

Thesis submitted for the degree of

Doctor of Philosophy

Institute of Neuroscience

Newcastle University

Supervisors:

Prof Stuart Baker

Dr Mark Baker

September 2018

Abstract

The corticospinal tract is well established as the dominant descending pathway in primates; however, it does not occupy an exclusive position in its ability to control movement. By lesioning this pathway, Lawrence and Kuypers (1968) demonstrated that a wide range of movements could be mediated by brainstem motor pathways, such as the reticulospinal tract. Fifty years after these experiments, the relative contributions of corticospinal and reticulospinal pathways to movement is still a topic of debate. Animal studies are invaluable in addressing this question and advancing our understanding of the motor system. However, these must be considered in combination with the use of non-invasive techniques in order to translate our findings into humans.

This thesis describes three separate experiments. In the first, the mechanisms underlying transcranial magnetic stimulation (TMS) were investigated by applying TMS to anaesthetised rhesus macaques whilst recordings were made from individual corticospinal axons. Our results differ from the population effects observed in human recordings, emphasising the complexity of the responses evoked by TMS. Secondly, in humans we performed a choice reaction reaching task thought to involve tecto-reticulospinal pathways. By pairing stimuli targeting the reticular formation, we propose that the resulting change in muscle activity represents a modulation of reticulospinal output. Finally, a strength training study was performed in two rhesus macaques and the adaptations in corticospinal and reticulospinal pathways assessed, with EMG and spinal recordings implicating reticulospinal pathways in strength-induced adaptations.

These experiments demonstrate that a comprehensive understanding of the motor system requires consideration of both the human and animal literature, with their respective strengths and limitations. Furthermore, we need to advance beyond the corticospinal-centric view that has dominated the field and instead consider the role of all neural elements in the motor system, including brainstem pathways and interneuron circuits. Only through such means can we further our clinical and scientific understanding of movement.

For Winter and Willow

Acknowledgements

The work presented in this thesis would not have been possible without the help and support of a number people. Although I have listed specific contributions at the start of each chapter, I would like to thank the following individuals for their role in making my PhD such an enjoyable and stimulating experience.

Firstly, I would like to thank my supervisor Stuart Baker for his optimism, enthusiasm and patience. Throughout my PhD he has provided me with a wealth of opportunities both within the lab and further afield, and I am grateful for the challenge these have presented. His commitment and continuous stream of ideas have been an inspiration to me.

Secondly, I would like to thank those in the field who I have been fortunate enough to interact with. This includes Monica Perez, who kindly hosted my visit to her lab in Miami; Hrishikesh Kumar and Supriyo Choudhury, for the adventure they provided in India; Mark Baker, Demetris Soteropoulos and the 'Cheese and Wine' community for their insightful discussions; Steve Edgley, for his tireless efforts at unearthly hours during the acutes; and Ed Hodkin for his camaraderie and unfiltered (but gratefully received) critique.

Thirdly, for the technical and emotional support they provided during the many trials and tribulations faced in the past three years, I would like to thank Terri Jackson and Norman Charlton. I am also grateful to Andrew Atkinson, who rose to the challenge of joining the lab at the height of recordings; and Denise Reed, for her kindness and reassurance.

Finally, I would like to thank my friends and family for their support throughout the last few years.

Contents

List of Figures

Abbreviations

1DI	First dorsal interosseous
AP	Anterior-posterior
BB	Biceps branchii
CM	Corticomotoneuronal
CMEP	Cervicomedullary motor evoked potential
CST	Corticospinal tract
cTMS	Controllable pulse parameter TMS
DLF	Dorsolateral funiculus
EDC	Extensor digitorum communis
EMG	Electromyography
EPSP	Excitatory post-synaptic potential
FCR	Flexor carpi radialis
FDS	Flexor digitorum superficialis
GABA	Gamma-aminobutyric acid
M1	Primary motor cortex
MEP	Motor evoked potential
MLF	Medial longitudinal fasciculus
MVC	Maximum voluntary contraction
PA	Posterior-anterior
PD	Posterior deltoid
PM	Pectoralis major
PSTH	Peri-stimulus time histogram
PT	Pyramidal tract
PTN	Pyramidal tract neuron
RF	Reticular formation
RST	Reticulospinal tract

RuST	Rubrospinal tract
RVR	Rapid visual reaction
SAS	Startling auditory stimulus
TES	Transcranial electrical stimulation
TMS	Transcranial magnetic stimulation
VLF	Ventrolateral funiculus
VMF	Ventromedial funiculus

Publications

Papers

Hodkin EF, Lei Y, Humby J, **Glover IS**, Choudhury S, Kumar H, Perez MA, Rodgers H, Jackson A (2018) Automated FES for upper limb rehabilitation following stroke and spinal cord injury. IEEE transactions on neural systems and rehabilitation engineering: a publication of the IEEE Engineering in Medicine and Biology Society 26: 1067-1074

Abstracts – Oral presentations

Glover IS, Edgley SA & Baker SN. Corticospinal axonal responses to TMS with different coil orientations. *Brainbox Initiative,* London, 2018.

Glover IS, Edgley SA & Baker SN. Corticospinal axonal responses to TMS with different coil orientations. *Society for Neuroscience,* Washington DC, 2017.

Glover IS, Edgley SA & Baker SN. Corticospinal axonal responses to TMS with different coil orientations. *UK Sensorimotor Conference,* Bristol, 2017.

Glover IS & Baker SN. Facilitation of short latency responses in human arm muscles by stimuli targeting the reticular formation. *UK Sensorimotor Conference,* Newcastle upon Tyne, 2016.

Abstracts – Poster presentations

Glover IS & Baker SN. Relative contributions of corticospinal and reticulospinal pathways to strength adaptation in non-human primates. *Society for Neuroscience,* San Diego, 2018.

Glover IS, Edgley SA & Baker SN. Corticospinal axonal responses to TMS with different coil orientations. *Progress in Motor Control,* Miami, 2017. **(Poster prize winner)**

Hodkin EF, Humby J, Lei Y, **Glover IS**, Choudhury S, Kumar H, Perez MA, Rodgers H, Jackson A. Closed-loop functional electrical stimulation for upper limb rehabilitation following SCI and stroke. *Society for Neuroscience,* Washington DC, 2017.

Glover IS & Baker S. Facilitation of short latency responses in human arm muscles by stimuli targeting the reticular formation. *Neural Control of Movement,* Dublin, 2017.

Hodkin EF, Lei Y, **Glover IS**, Choudhury S, Kumar H, Perez MA, Rodgers H, Jackson A. Closed-loop functional electrical stimulation for upper limb rehabilitation following SCI and stroke. *Neural Control of Movement,* Dublin, 2017.

Glover IS & Baker SN. Facilitation of short latency responses in human arm muscles by stimuli targeting the reticular formation. *Society for Neuroscience,* San Diego, 2016.

CHAPTER I

Introduction

Descending pathways

The seminal work of Lawrence and Kuypers has shaped the field of motor neuroscience over the last 50 years by initiating the discussion on the relative contributions of descending pathways to movement (Lawrence and Kuypers, 1968a, b). The authors reported that surgical lesion of the corticospinal tract (CST) in macaques resulted in an initial flaccid paralysis followed by a deficit in independent limb movement. Although the animals largely recovered over a period of weeks, they did not regain independent finger control (Lawrence and Kuypers, 1968b). These findings suggest that despite the CST being the dominant descending pathway in primates (Lemon, 2008), subcortical pathways can also generate a wide range of movements, with the notable exception of manual dexterity. Subsequent lesions of either the ventromedial or lateral brainstem pathways led Lawrence and Kuypers (1968a) to attribute distal function to lateral brainstem pathways such as the rubrospinal tract (RuST), whilst ventromedial pathways including the reticulospinal tract (RST) were proposed to mediate proximal movements. Thus by the end of the 1960s, the RST, RuST and CST had been categorised as pathways for basic movement, independent limb control and independent finger control, respectively. Although aspects of this categorisation stand true today, over the last half a century a concerted effort to study the motor system has produced a more detailed characterisation of these pathways.

The corticospinal tract

Given the little evidence supporting a RuST contribution in man (Nathan and Smith, 1955; Onodera and Hicks, 2010), the literature, which is often centred on hand function, has focussed predominantly on corticospinal contributions to movement. The CST is an axon bundle originating from throughout the motor and somatosensory cortices (Dum and Strick, 2005; Lemon, 2008). The

majority of fibres decussate at the medulla to descend in the contralateral dorsolateral funiculus (DLF), and although approximately 10% descend in the ipsilateral DLF (Liu and Chambers, 1964; Ralston and Ralston, 1985), these cross the midline in the spinal cord and so also form contralateral terminations (Yoshino-Saito et al., 2010). Any ipsilateral corticospinal actions are therefore dependent upon the ~2% of fibres that descend in the ipsilateral ventromedial funiculus (VMF) and the extensive presence of commissural interneurons (Rosenzweig et al., 2009; Yoshino-Saito et al., 2010). Electrophysiological recordings suggest that this contribution is of little functional significance given the scarcity of ipsilateral responses in either muscles or motoneurons to corticospinal stimulation (Soteropoulos et al., 2011). Thus the CST can be considered as a predominantly unilateral pathway, an important distinction from the bilateral ventromedial brainstem pathways.

Corticospinal terminations onto interneurons in the intermediate zone of the cord are well conserved across mammals, thus the main corticospinal drive to motoneurons is mediated by a disynaptic pathway. A notable exception to this is observed in primates in which corticospinal axons can also form monosynaptic corticomotoneuronal (CM) connections (Bernhard and Bohm, 1954). Manual dexterity improves with the emergence of CM connections, both in terms of evolution and developmental maturation (see Kuypers, 1981), suggesting that this monosynaptic pathway endows the primate CST with the characteristic sophisticated movements with which it is associated. Although it should be noted that independent finger movements are not exclusively the domain of CM cells since they persist in the absence of these connections, presumably due to C3/C4 propriospinal interneurons (Sasaki et al., 2004).

The functional division of monosynaptic and disynaptic connections to motoneurons is represented as an anatomical division in the primary motor cortex (M1). Anatomical and electrophysiological studies have revealed that fast-conducting corticospinal axons that form CM connections originate from the region of M1 on the anterior bank of the central sulcus, whereas corticospinal axons that terminate on interneurons, together with slower conducting fibres with CM connections, are found throughout M1 (Rathelot and Strick, 2009; Witham et al., 2016). This has led to the classification of two subdivisions – an evolutionarily new M1, located caudally, from which fast CM cells arise; and an evolutionary old M1, which is located rostrally and characterised by its lack of fast CM cells.

In summary, as a development of the ideas of Lawrence and Kuypers (1968b), the unique ability of the CST to produce independent finger movements has been attributed to CM connections and the caudal region of M1. Furthermore, the relatively limited collateralisation of CM cells (Buys et al., 1986) likely accounts for the role of this pathway in independent limb movements too. Thus, considerable progress has been made in identifying the anatomical substrates responsible for the behavioural observations of Lawrence and Kuypers (1968b).

The reticulospinal tract

In contrast to the widespread attention received by the CST, the RST has been comparatively neglected in the study of primate motor control. This bilateral pathway originates from the nuclei of the reticular formation (RF) and forms both monosynaptic and disynaptic connections with motoneurons (Riddle et al., 2009). Found in mammals as well as more primitive species, the RST has been considered as a phylogenetically old pathway that exerts simple and often reflexive control of movement. In its most basic form, the rudimentary reticulospinal system consists of just two Mauthner cells capable of evoking an escape reflex in fish and amphibians (Korn and Faber, 2005). In the more developed form seen in cats, the RST has been associated with gross movements including locomotion (Drew et al., 1986; Mori et al., 2001), reaching (Schepens and Drew, 2004a, 2006b) and postural control (Deliagina et al., 2008; Schepens et al., 2008). Similarly, primate studies have shown a direct involvement of the RST in upper limb movements such as reaching (Buford and Davidson, 2004; Davidson and Buford, 2004; Davidson and Buford, 2006; Davidson et al., 2007). These functions correspond with the extensive divergence of the RST (Peterson et al., 1975; Matsuyama et al., 1997), supporting its role in the synergistic control of movement.

Only in recent years has a role for the RST in more distal movements been defined. The motivation for these investigations stems from the observation by Lawrence and Kuypers (1968a) that although animals with both CST and RuST lesions had severely impaired manual dexterity, they were still able to climb the bars of their cage, suggesting that the intact RST was able to mediate some degree of hand function. Accordingly, reticulospinal connections to motoneurons innervating wrist and digit muscles have been identified in primates (Riddle et al., 2009), with electrophysiological recordings demonstrating task-dependent modulation of RF neurons during precise index finger movements (Soteropoulos et al., 2012).

On the basis of these findings, our understanding of the RST has developed from the relatively dismissive view that this pathway can mediate only the most basic aspects of movement, to a more modern outlook suggesting that the connectivity exists within the RST to support a wide range of movements. The functional relevance of these connections, both in the healthy state and following the corticospinal damage associated with many neurological conditions, is still a debated subject.

A comparison of pathways

The similarities between the CST and RST in primates, particularly the innervation of distal and proximal muscles by both pathways, raises the question of why two descending pathways exist. The most simplistic view is that the existence of two pathways, which can converge onto the same populations of interneurons and motoneurons (Riddle and Baker, 2010), represents redundancy in the motor system. The phylogenetically newer CST dominates in the healthy state, with its CM cells providing additional dexterity, whereas the RST could be considered as an evolutionary relic. The corticospinal focus in the human motor control literature perhaps reflects this view. However, there is increasing evidence suggesting that the CST and RST are both functionally relevant in primates, with each uniquely contributing to the complex network that is the motor system.

The first observation to make is that the CST and RST do not constitute entirely independent pathways. The interconnectivity of these two pathways can be demonstrated not only by the presence of cortico-reticular projections (Berrevoets and Kuypers, 1975; Jinnai, 1984), but also by the observation that many of these are actually corticospinal collaterals (Keizer and Kuypers, 1989). This relationship is to some extent bidirectional since fibres ascend from the RF to the cortex, although this pathway is largely concerned with conveying sensory information (see Steriade, 1996).

Furthermore, there is considerable overlap in the terminations of the CST and RST, with convergent input to interneurons in cats (Schepens and Drew, 2006b), and both interneurons and motoneurons in primates (Riddle and Baker, 2010). Although this could be taken to imply redundancy in the system, it has instead been proposed that by modulating the excitability of target neurons, the relatively specific corticospinal projections are able to gate the much more dispersed

reticulospinal input in order to produce the required pattern of muscle activation (Schepens and Drew, 2006b).

It could be inferred from such a system that the RST provides the main drive to motoneurons whilst the CST fine tunes this input to produce precise, fractionated movement. This hypothesis is supported by the anatomy of these pathways, with the RST projecting bilaterally and showing extensive collateralisation compared to the less divergent, predominantly unilateral CST (Lemon, 2008). Furthermore, since the lesion studies of Lawrence and Kuypers (1968b), the RST has been specifically implicated in strength due to the authors' report of a progressive increase in strength following corticospinal lesions. Subsequent human studies have shown that when making strong contractions, an increasing number of muscles are activated both ipsilaterally and contralaterally (Zijdewind and Kernell, 2001), which matches with the bilateral and divergent nature of the RST. Further support for the dissociation between the strength and precision of movement can be drawn from human studies of hand function in healthy controls (Perez and Rothwell, 2015), stroke survivors (Xu et al., 2017) and individuals with spinal cord injury (Bunday et al., 2014; Baker and Perez, 2017).

Clinical significance

In addition to furthering our knowledge of the motor system, study of the descending pathways is motivated by the desire to generate clinically relevant therapies for the many neurological conditions characterised by motor deficits. For example, both stroke and spinal cord injury may result in selective lesioning of the CST with the possibility of relative sparing of the RST. Although, as discussed above, the RST does not constitute a parallel pathway to the CST, it is likely that the motor deficits experienced following stroke and spinal cord injury could to some extent be ameliorated by upregulating reticulospinal function (Baker, 2011; Baker et al., 2015).

Reticulospinal adaptation following corticospinal injury has been demonstrated in primate lesion studies (Zaaimi et al., 2012; Darling et al., 2018). Following a stroke, the recovery of movement that occurs matches the anatomy of the RST; survivors can regain considerable motor function but often experience reduced dexterity (Lang and Schieber, 2003, 2004; Raghavan et al., 2006), increased co-contraction of muscles (Bourbonnais et al., 1989; Dewald et al., 1995), and enhanced

mirror movements (Nelles et al., 1998). Similarly, individuals with spinal cord injury show signs of increased reticulospinal function (Baker and Perez, 2017).

Although it appears that plastic changes occur in the RST following corticospinal injury, the full potential of this pathway to compensate for the loss of descending drive associated with conditions such as stroke and spinal cord injury remains to be elucidated. Furthermore, it is not known to what extent the strengthening of reticulospinal connections is detrimental to movement. By better understanding the relative contributions of the CST and RST in the healthy state, we may be able to develop therapies to modulate reticulospinal plasticity following injury and thereby maximise the potential of this pathway to compensate for deficits elsewhere in the motor system.

Non-invasive techniques

Our current knowledge of the relative roles of descending pathways in movement control largely comes from animal experiments, predominantly performed in cats and non-human primates. These studies have proved invaluable in the characterisation of corticospinal and reticulospinal pathways. However, notable differences exist between the motor systems of different species (Lemon, 2008). If the ultimate goal of the field is to translate findings to humans and explore the possibility of clinical interventions, it is necessary to develop non-invasive techniques to study the motor system and in particular, the separate contributions made by its descending pathways.

Structural imaging techniques can be used to draw some comparisons to the animal literature, such as the identification of human corticoreticular projections using diffusion tensor imaging (Yeo et al., 2012). However, a functional understanding of the motor system requires electrophysiological techniques. Non-invasive quantification of the activity of a neural pathway requires the ability to provide an input and record an output. Similarly to the animal studies, electrical stimulation of the motor system is unlikely to excite neurons in an analogous manner to the physiological activation, but nonetheless can provide considerable insight into motor function. Output measures of descending pathways are most easily obtained by recording muscle activity with electromyography (EMG).

Transcranial stimulation

Given that the corticospinal tract originates from the cortex, it is logical that this pathway can be activated by passing current through the motor cortex to excite pyramidal tract neurons. This was first achieved with transcranial electrical stimulation (TES; Merton and Morton, 1980) in which a small current is passed between two electrodes placed on the scalp, typically with the anode over the motor cortex and a large distant cathode (Hern et al., 1962). This stimulus evokes contralateral muscle twitches, known as motor evoked potentials (MEPs). The onset latency of the earliest TES response is 2-2.6ms when recorded epidurally from the high cervical cord (Di Lazzaro et al., 1998b) and approximately 21ms in muscle (Sakai et al., 1997). Comparison of these values to single unit recordings in primates (Patton and Amassian, 1954) led to the suggestion that TES directly excites descending corticospinal axons (Day et al., 1989). Measurement of MEP size can therefore be used to provide a measure of corticospinal output. However, application of TES has been limited by the discomfort associated with its use since the high currents required to penetrate the skull result in painful stimulation of the scalp muscles and sensory receptors in the skin.

The development of transcranial magnetic stimulation (TMS) by Barker et al. (1985) overcame this major drawback of TES by using an electromagnetic coil to generate a magnetic field which can easily penetrate the skull and evoke currents in the brain. TMS was originally used as a non-focal stimulus since the round coils through which it was delivered did not activate neural tissue directly under the coil but instead induced current that spread in an annulus. More recently, with the advent of figure of eight coils, TMS can be used focally since this configuration generates the largest current density directly below the centre of the coil (Ueno et al., 1988). Although all coil types and orientations are capable of producing measurable MEPs in muscles, the onset of these occurs at subtly but consistently different latencies (Sakai et al., 1997; Di Lazzaro et al., 1998b). This is thought to reflect indirect activation of corticospinal axons via circuits of cortical interneurons. Therefore, although TMS is effective in evoking measurable muscle responses which are indicative of corticospinal excitability, interpretation of the MEPs requires caution since the specific neural elements activated by this stimulus are not known.

Non-invasive measures of reticulospinal function

The transcranial stimulation techniques available for the study of the CST are of limited use in deep structures such as the reticular formation (RF). Although TMS can activate reticular neurons (Fisher et al., 2012), is unlikely to provide a reliable reticulospinal assessment since any responses observed are presumably dominated by the much larger corticospinal activation. Instead, reticulospinal function in humans can be inferred by using sensory stimuli thought to target the reticular formation.

Briefly, these include loud auditory stimuli which, via activation of the caudal pontine RF, evoke the startle reflex (Brown et al., 1991) and when delivered as an imperative signal, can dramatically shorten reaction times (Valls-Solé et al., 1995; Valls-Solé et al., 1999). Visual stimuli processed by the superior colliculus can activate the RF via the tecto-reticulospinal tract (Illert et al., 1978; Grantyn and Grantyn, 1982; Werner, 1993; Stuphorn et al., 1999; Philipp and Hoffmann, 2014) and can evoke short-latency EMG activity during fast reaching movements (Pruszynski et al., 2010). Electrical stimulation over the mastoid processes can elicit vestibular sway responses (Fitzpatrick and Day, 2004), which are likely to have a reticulospinal component (Rothwell, 2006). Finally, increasing evidence supports a reticular role in the long latency stretch reflex (Soteropoulos et al., 2012; Kurtzer, 2014) hence quantification of this response may provide another means to assess reticulospinal excitability.

Each of these techniques provides some indication of reticulospinal function, but it is important to note that none provide a pure measure of the RST. Instead they are likely to be contaminated by contributions from other descending pathways including the CST and vestibulospinal tract. Similarly to TMS MEPs, interpretation of experiments using these non-invasive assessments of reticulospinal function requires consideration of the wider motor system.

The requirement for invasive measures

Despite the increasing number of techniques available for the non-invasive study of the motor system, animal experiments are still extremely valuable in the continued effort to characterise descending pathways. These preparations also provide the opportunity to gain mechanistic insight into the non-invasive techniques used in humans, thereby facilitating the interpretation of data

collected with such methods. Only by integrating the knowledge gained from both human and animal experiments, as well as considering the contribution of all descending pathways, can the field move towards its ultimate goal of a complete understanding of the motor system and the development of effective therapies for neurological disorders affecting movement.

Thesis objective

The aim of this thesis is to explore the relative contributions of the CST and RST to movement in primates and humans by investigating the non-invasive techniques available for their study as well as demonstrating the role of the RST in a field previously dominated by the study of corticospinal adaptations.

The application of non-invasive techniques used in humans to animal models can provide a means of studying their specific mechanisms of action. Chapter 2 uses this approach to study the specific neural elements activated by TMS. In anaesthetised macaques, recordings were made from individual corticospinal axons in response to different orientations of TMS delivered over M1. By studying single axons, rather than the population effects observed with epidural or muscle recordings, the origin of a number of these axons was identified. In combination with measurements of the latency of spikes observed in single axons, this enabled mechanistic inferences to be made about TMS and its activation of the CST.

Similarly, the RST can be stimulated using non-invasive techniques. In Chapter 3, reticulospinal pathways were non-invasively studied in healthy human subjects by pairing loud auditory stimuli thought to target the RF with a choice reaction reaching task previously hypothesised to evoke tecto-reticulospinal activity. Recordings from shoulder muscles demonstrate both the ability to modulate this putative reticulospinal output, as well as the induction of plasticity.

Chapter 4 brings together ideas on the relative roles of the CST and RST by comparing the neural adaptations that occur in each of these pathways with strength training. Two macaques were trained to perform a weight lifting task. Over a period of several months, the effects of a strength training intervention on the CST and RST was assessed by recording upper-limb responses to stimulation of each of these pathways. Following completion of the intervention, spinal

adaptations were assessed with bilateral recordings of spinal field potentials. These experiments demonstrated that significant adaptations occur in reticulospinal pathways during strength training.

The experiments presented in this thesis further our understanding of non-invasive techniques available for investigating the motor system, demonstrate the applicability of non-invasive techniques to the study of the RST and elucidate the contributions of descending pathways to strength adaptations. Furthermore, this thesis bring together several ideas about the study of the motor system. Firstly, the importance of understanding the mechanisms underlying non-invasive stimulation, particularly if the aim is to draw specific conclusions from these relatively non-specific techniques. Secondly, the limited number of techniques available for the study of reticulospinal pathways in man and the necessity to develop these if we are to continue to advance our knowledge of the human RST. Thirdly, despite the technical challenges associated with studying different elements of the motor system, the need to move away from a corticospinal-centric view and consider the contributions of other pathways such as the RST.

CHAPTER II

Corticospinal axonal responses to TMS with different coil orientations

The experiments described in this chapter were performed by myself, Stuart Baker and Steve Edgley. They were supported by Norman Charlton, who designed and manufactured the TMS coil manipulator; Terri Jackson, who oversaw the care of the animals; Eisha Joshi, with whom I made the cortical wires; Rogue Research, who kindly lent us their cTMS device and manufactured adaptor cables; and the veterinary team at Newcastle University, who performed the initial stages of surgery and provided assistance throughout the experiments. I performed all data analysis.

Introduction

The study of descending motor pathways in humans requires the use of non-invasive stimulation techniques. Transcranial magnetic stimulation (TMS) is an example of one such technique, but the specific neural elements which it activates are not currently known. TMS generates a magnetic field which can in turn evoke current in the brain; these currents travel parallel to the skull's surface and penetrate only superficially. When delivered through a round coil, the current spreads in an annulus, with no activation of neural tissue directly under the middle of the coil thereby making it a non-focal stimulus. In contrast, TMS with a figure of eight coil constitutes a focal stimulus since the largest current density is generated directly below the centre of the coil (Ueno et al., 1988) and the current direction depends upon the coil orientation.

Measurement of strength-duration time constants suggests that the site of activation for TMS is within the axons of neurons, rather than the cell bodies (Burke et al., 1993). It is well established that in peripheral nerves, electrical stimulation is most effective when the induced currents are directed along the length of the axon (Rushton, 1927; Amassian et al., 1992). However, the situation is much more complex in the cortex where axons can travel in various directions, bend sharply, and cross from grey matter to white matter. A recent modelling study proposed that these

three features represent the most likely sites of activation with TMS (Salvador et al., 2011). Thus for an interneuron that does not cross the grey/white matter boundary and has a relatively straight trajectory, the activation threshold is determined by the orientation of the axon relative to the current. In contrast, pyramidal tract neurons (PTNs) are activated at the bend that occurs as they transition from the grey matter to white matter since the bend generates localised variations in the effective electric field (Amassian et al., 1992) and charge accumulation occurs at the boundary between grey matter and white matter (Miranda et al., 2007). Depending upon the direction of current, these two effects can summate or be in opposition (Salvador et al., 2011). Therefore, for all neurons present within the cortex, activation with TMS depends upon the direction of the current relative to the geometry of the axons.

In primates, the primary motor cortex (M1) extends deep into the central sulcus (Geyer et al., 1996). The orientation of the axons of both interneurons and PTNs relative to the scalp therefore depends on whether they reside in the gyral crown or the anterior bank of the central sulcus. This is particularly important when considering that M1 can be subdivided into a caudal ("new M1") and rostral ("old M1") region, as first reported by Geyer et al. (1996). Subsequent work has demonstrated that fast conducting corticospinal axons making corticomotoneuronal (CM) connections are exclusively located in new M1, whilst slower conducting axons generating both monosynaptic and disynaptic connections to motoneurons originate throughout M1 (Rathelot and Strick, 2009; Witham et al., 2016).

The induction of current within the brain can generate measurable responses in contralateral muscles, known as motor evoked potentials (MEPs), which can be recorded both from surface electromyography (EMG) and single motor units. Descending volleys in the spinal cord can be directly measured using epidural recordings both in anaesthetised patients undergoing spinal surgery (Boyd et al., 1986; Berardelli et al., 1990; Burke et al., 1993), and in awake patients with implanted spinal cord electrodes, as first reported by Nakamura et al. (1996). Furthermore, in animal models, recordings can be made from individual corticospinal axons (Patton and Amassian, 1954; Edgley et al., 1997). All of these methods demonstrate that stimulation of the motor cortex generates waves of activity in the corticospinal tract.

The earliest response evoked by stimulation of the cortex is the D-wave observed with transcranial electrical stimulation (TES). The short latency of this response, in combination with its persistence after removal of the cortical grey matter (Patton and Amassian, 1954) and lack of modulation with muscle contraction (Di Lazzaro et al., 1999a), suggests that it originates from direct activation of corticospinal axons below the level of the initial segment. In contrast, the D-waves evoked with TMS are subject to modulation with cortical excitability and so are thought to originate from closer to the soma (Baker et al., 1995). The later responses, termed I-waves, appear at intervals of approximately 1.5ms and are dependent upon the integrity of the grey matter, implying that they originate from trans-synaptic activation of PTNs by cortical interneurons (Patton and Amassian, 1954). With increasing intensity, each cortical stimulus generates a different pattern of responses. For example, TES and non-focal TMS preferentially evoke D-waves (Hern et al., 1962; Burke et al., 1993; Di Lazzaro et al., 1998b), whereas TMS with a posterior to anterior (PA) current evokes early I-waves at the lowest threshold (Di Lazzaro et al., 1998b), and TMS with an anterior to posterior (AP) current evokes late I-waves, although these are more variable (Di Lazzaro et al., 2001; Sakai et al., 2009). The recent development of controllable pulse parameter TMS (cTMS) (Peterchev et al., 2013), generates the possibility of selectively evoking different I-waves by changing the pulse width of TMS (D'Ostilio et al., 2016).

In order to understand the output generated by TMS, it is paramount that we identify the specific neural elements activated by this stimulus. The aim of this study was to characterise the responses of individual corticospinal axons to PA and AP orientations of TMS, to compare the response profiles of corticospinal axons originating from old M1 and new M1, and to investigate the effects of TMS pulse width on corticospinal axons. We report the first example of recordings from individual primate corticospinal axons in response to focal TMS.

Methods

All animal procedures were performed under UK Home Office regulations in accordance with the Animals (Scientific Procedures) Act (1986) and were approved by the Local Research Ethics Committee of Newcastle University. Recordings were made from six terminally anaesthetised rhesus macaque monkeys (monkeys D, K, L, N, W, and Y; all female).

Surgical preparation

Following sedation with an intramuscular injection of ketamine and induction of anaesthesia with intravenous propofol, animals were intubated and a central venous line inserted. Anaesthesia was then maintained through inhalation of sevoflurane and intravenous infusion of alfentanil. Pulse oximetry, heart rate, blood pressure, core and peripheral temperature, and end-tidal CO_2 were monitored throughout surgery. Hartmann's solution was infused to prevent dehydration, a heating blanket and a source of warm air maintained body temperature and a positive pressure ventilator ensured adequate ventilation. Anaesthetic doses were adjusted as necessary to ensure deep general anaesthesia was maintained.

A craniotomy was performed to expose the left motor cortex and a burr hole drilled to allow access to the left medullary pyramidal tract (PT). Screws were inserted into the anterior and posterior skull to later enable replacement of the stereotaxic frame with plastic bars, as required for TMS. A laminectomy exposed segments C1-T1 and L1, enabling the vertebral column to be clamped at the high thoracic and mid-lumbar levels, and the head was fixed in a stereotaxic frame. Following this initial preparation, the anaesthetic regimen was switched to an intravenous infusion of alfentanil, ketamine and midazolam.

A parylene-insulated tungsten electrode (LF501G, Microprobe Inc, Gaithersburg, MD, USA) was implanted into the medullary PT, rostral to the decussation, to allow stimulation of the corticospinal tract. The double angle stereotaxic technique, described by Soteropoulos and Baker (2006), was used to aim the electrode at the desired target from the craniotomy. The optimal position for the electrode was defined as the site with the lowest threshold for generating an antidromic cortical volley in ipsilateral M1, without eliciting a contralateral M1 volley at 300µA. Cortical and spinal volleys were obtained using silver ball electrodes.

The cortical dura over the left motor cortex was opened and the region mapped to identify the angle of the central sulcus. Custom-made cortical electrodes, consisting of rows of insulated tungsten wire spaced 1.5mm apart, were inserted 4mm and 1.5mm deep, parallel to the sulcus, to target new M1 and old M1, respectively. In monkeys D, K, L and N, 12 electrodes were implanted

into old M1 and 6 into new M1. In monkeys W and Y, 16 electrodes were implanted into old M1 and 8 into new M1.

To enable TMS to be delivered, rigid plastic rods were clamped to the stereotaxic frame and cemented to the skull with dental acrylic so that the metal ear and eye bars could be removed; this ensured that no eddy currents could flow through the fixation system. A small figure of eight TMS coil (25mm loop diameter), mounted on a manipulator, was fixed over the left motor cortex tangential to the cranium and approximately 45 degrees from the midline, corresponding to a PA coil orientation. Attachment of a reversing cable changed the direction of the current so that it was possible to switch between PA and AP stimulation without moving the coil. This was necessary due to the fragility of the recordings. For the same reason, neuromuscular blockade with atracuronium prevented TMS-induced muscle twitches and a bilateral pneumothorax minimised respiratory movements of the chest. To prevent overheating, the TMS coil was cooled with ice throughout the experiment.

In all monkeys, PA and AP TMS were delivered with a Magstim 200 stimulator. In monkeys W and Y, adaptor cables enabled attachment of the same TMS coil to a Brainsight cTMS device (Rogue Research) so that the length of the TMS pulses could be adjusted. Threshold for each TMS orientation and pulse width was determined using epidural volleys recorded with a silver ball electrode placed over the DLF on the cervical cord. Due to the volleys in these recordings being small in amplitude and variable, threshold was defined as the lowest intensity at which an unambiguous volley could be observed in an average of 15 sweeps.

Axon recordings

Recordings from individual axons were made using glass microelectrodes filled with 1M potassium acetate and manipulated with a Burleigh piezoelectric microdrive. After the dura was opened around the level of C5 and a small pial patch made, the microelectrode was inserted into the right DLF (Figure 2-1*a*). A pressure foot was used to reduce the pulsation artefact and improve the stability of recordings. Corticospinal axons were identified by a spike in response to PT stimulation (0.7mA biphasic pulses, 0.2ms per phase, 4Hz repetition rate; Figure 2-1*b*, Figure 2-2). Antidromic responses to stimulation of the lumbar electrode (2.0mA biphasic pulses, 0.2ms per

phase, 4Hz repetition rate; Figure 2-1*c*, Figure 2-2) were recorded. Failure to respond to this stimulus implied that the axon may have terminated in the cervical cord, although it is also possible that the axon had a very high threshold or terminated in the thoracic cord. Similarly, the presence of a response to the lumbar stimulation did not unequivocally mean that the axon terminated in the lumbar cord but simply that it projected at least as far as this point.

Axons were classified as originating from old M1 if responses at D-wave latency (1.4-2.6ms) were evoked by stimulation of the old M1 electrodes, and from new M1 if responses at D-wave latency (1.4-2.6ms) were evoked by stimulation of the new M1 electrodes (0.3-1.0mA biphasic pulses, 0.2ms per phase; Figure 2-1*d*, Figure 2-2). Since both the old M1 and new M1 electrodes spanned a considerable area, it was only necessary for an axon to respond to stimulation of a single electrode to be classified as originating from this region. In cases where both old M1 and new M1 electrodes generated D-waves, presumably due to spontaneous firing or current spread, the current was reduced until D-waves were observed with only one electrode type, and the axon classified as originating from this area.

TMS was delivered in either PA or AP current direction for 1.2x, 1.5x and 2.0x epidural threshold (Figure 2-1*e*, Figure 2-2). After approximately 40 stimuli of each intensity, the current direction was changed using the reversing cable and the sequence repeated. In monkeys W and Y, cTMS was then delivered through the same figure of eight coil in an AP direction for a short-duration (AP30: 30μs positive pulse, 0.2 M-ratio) and long-duration (AP111: 111μs positive pulse, 0.2 M-ratio) pulse. The 111μs pulse was chosen as this was the maximum pulse length achievable with the cTMS device and our coil configuration; however, this limited the stimulator output to 44% so only two intensities were delivered in monkey W (1.2x and 1.5x) and three in monkey Y (1.2x, 1.5x, ~1.8x). The M-ratio is a measure of the ratio of electric field phases and the value of 0.2 was chosen since this resembles the monophasic pulse commonly used in TMS (Sommer et al., 2018).

The PT, cortical and TMS stimuli were delivered in non-orderly sequence to give an overall repetition rate of 4Hz. Axon recordings (25kHz sampling rate, 200x gain, 100Hz to 100kHz band-pass) and stimulation parameters were stored to disc. In many cases, the axons were lost mid-way through the recording and so the full sequence of stimuli was not delivered.

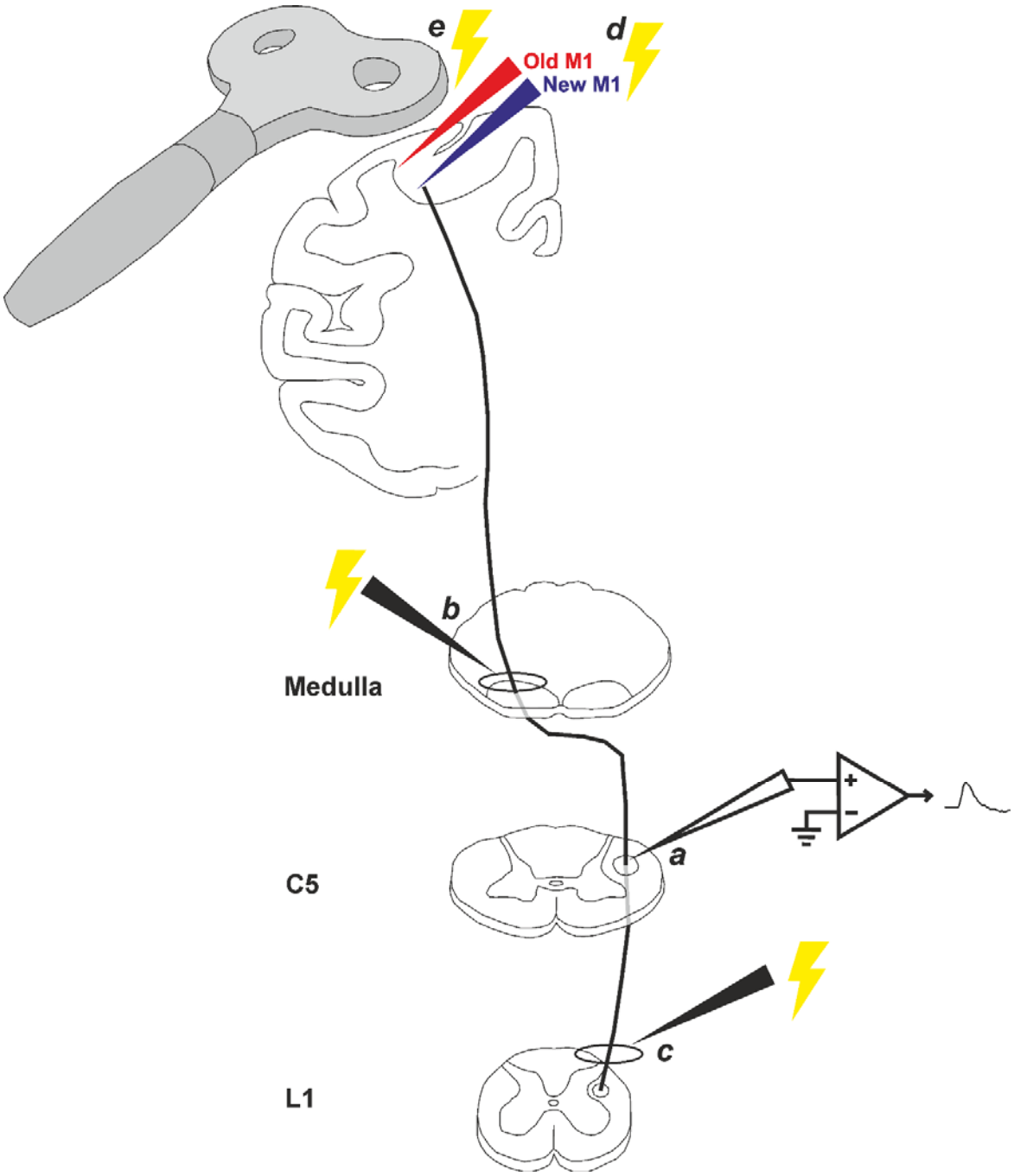

Figure 2-1. Experimental design

Schematic showing the stimulation and recording sites used in the experimental protocol. (***a***) Recordings were made from cervical axons. Stimulation was delivered at (***b***) the medullary PT to identify corticospinal axons, (***c***) the lumbar DLF to distinguish between axons likely to project to upper and lower limbs, (***d***) the cortex to identify the axon origin as old M1, new M1 or unknown, and (***e***) with TMS to identify the pattern of D and I waves generated.

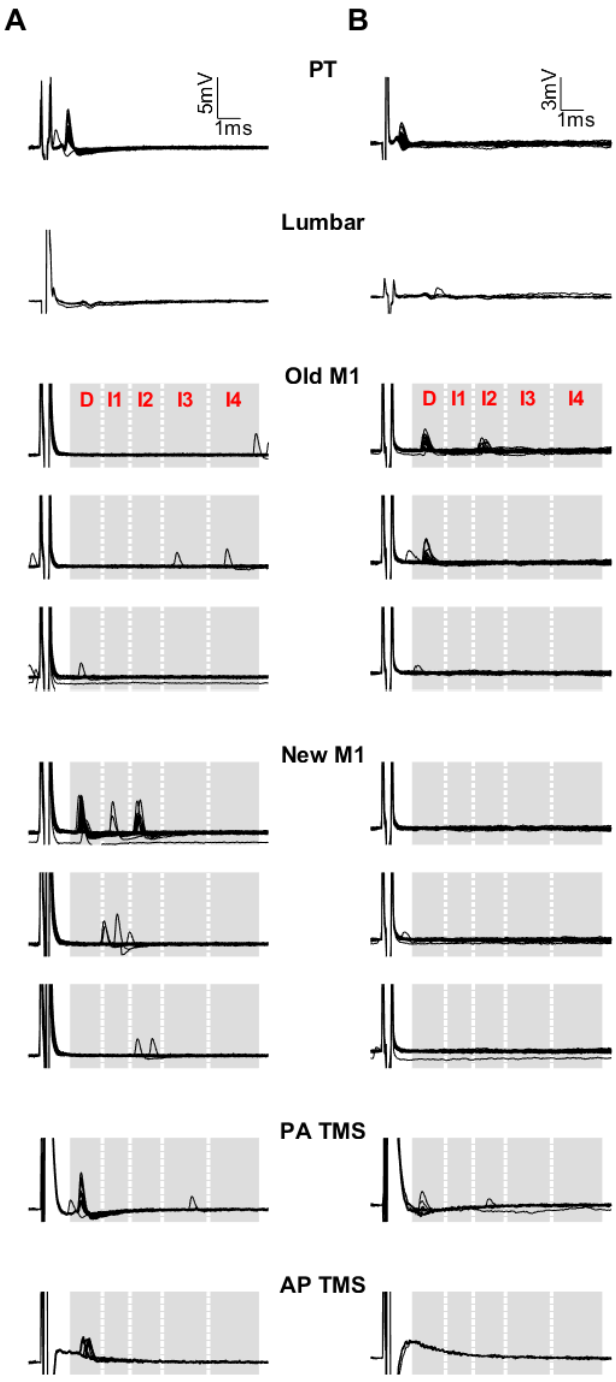

Figure 2-2. "Electroanatomy" methods

Example recordings from individual corticospinal axons, each column presents a different axon (***A, B***) and its responses to PT stimulation, lumbar stimulation, old M1 stimulation through three different electrodes, new M1 stimulation through three different electrodes, and PA and AP TMS at 2x threshold. Each sweep is an individual trial and the windows show the latencies representing D, I1, I2, I3 and I4 waves.

Data analysis

All analysis was performed off-line using custom software written in MATLAB. The presence of PT and lumbar axon potentials were determined by visual inspection. Axons without a clear PT response could not be definitively identified as corticospinal and so were excluded from all subsequent analysis. Due to the relatively low number of axons responding to TMS (see Results), lumbar-responding axons were included in all analyses except those in which comparisons were made between old M1 and new M1 since this division has only been reported for corticospinal axons projecting to upper limb motoneurons (Rathelot and Strick, 2009; Witham et al., 2016).

For the cortical electrodes and TMS responses, spike latencies were measured from stimulus onset to peak and were grouped into 0.2ms bins. Response windows for D and I waves were selected by visual inspection of the data and were applied uniformly to all axons and stimuli. These were as follows, D: 1.4-2.6ms; I1: 2.8-3.8ms; I2: 4.0-5.2ms; I3: 5.4-7.2ms; and I4: 7.4-9.4ms. Due to low levels of spontaneous firing, axons in which responses at D-wave latency were evoked with old M1 stimulation at least twice as often as new M1 were classified as originating from old M1, and vice versa. Axons that generated D-waves with both old M1 and new M1 stimuli at similar rates, or with neither stimulus, were classified as of unknown origin.

Peri-stimulus time histograms (PSTHs) were constructed for the responses to TMS and cTMS for all axons, and separately for non-lumbar old M1 and new M1 axons for TMS responses. There were not sufficient data to construct cTMS histograms by axon origin. To control against the PSTHs being dominated by a few highly responsive axons and for the unequal number of axons in which each stimulus was delivered, the number of the axons responding in a given window was calculated as a proportion of the total number of axons in which that stimulus was delivered. The depth of anaesthesia meant that spontaneous activity was too low to calculate a reliable baseline firing rate for each axon, above which responses could be assumed to be stimulus-driven. Therefore, the analysis was performed separately for axons in which only a single spike was observed in a given window, which may be due to spontaneous firing, and for axons in which more than one spike was observed in a given window, which were more likely to be stimulus-driven. For all subsequent analysis, only axons that responded more than once in a given window were included. Nonetheless, it is important to note that we do not dismiss all single spikes as

spontaneous activity due to the effects of deep anaesthesia on excitability; instead it is possible that these responses represent stimulation of axons at threshold intensities and are scientifically meaningful.

In addition to examining the proportion of axons in which each stimulus was effective, we also calculated the proportion of trials in which each stimulus evoked a response. Only axons which responded to the stimulus were included in this analysis. Thus the proportion does not represent the overall likelihood of a spike appearing in a given window for a given stimulus for all axons, but instead provides a measure of how reliably each stimulus could evoke a response in the responding axons.

To study the repetitive firing of individual axons, the following analysis was performed. The pattern of I-waves generated in each axon by each stimulus was determined by allocating a 0 to response windows in which no spikes were observed, and a 1 to response windows in which spikes were observed. The '0000' combination, indicating no I-waves, was excluded from the analysis. The observed patterns were compared against the null hypothesis that all I-waves are generated independently. The probability of each I-wave occurring, irrespective of I-waves in other windows, was calculated. Using these values, the predicted probability of each pattern was calculated by summing the response probabilities:

$$\prod_{i=1}^{n} (\text{Pi if Ii=1}) \text{ or } (\text{1-Pi if Ii=0})$$

To provide a statistical comparison of the predicted probabilities with the real data, the following Monte Carlo resampling method was performed. I-wave responses were simulated using the calculated probability of each I-wave and the assumption that each I-wave occurred independently. The probability of each pattern of I-waves being generated could then be calculated from this simulated data. Repetition of this process 1000 times generated distributions of the probability of each pattern of I-waves occurring if I-waves are assumed to be independent. The real data could then be compared to these distributions using a two-tailed test with p=0.05.

To compare the effects of PA and AP stimulation on individual axons, the number of axons in which both stimuli evoked a response was compared to the number of axons in which responses were observed with only one TMS coil orientation. This analysis was limited to axons in which both stimuli were delivered for at least 5 trials at a given intensity. For axons which responded to both stimuli, responses were classified as D- or I-waves and the probability of both PA and AP TMS generating I-waves (II), D-waves (DD) or a combination of the two (DI or ID) in the same axon was calculated. To test the statistical significance of the observed data relative to the null hypothesis that D- and I-waves were independently generated with each coil orientation, an additional Monte Carlo resampling method was performed. Data were simulated using the calculated probability of D- and I-waves for PA and AP TMS, under the assumption these responses were evoked independently. The number of times each D- and I-wave combination (DD, II, DI, ID) occurred was counted for the simulated data. Repetition of this process 1000 times generated distributions of the number of axons in which each combination of D- and I-waves was predicted to occur under the assumption that the two orientations were independent. The observed data were then compared to these distributions of predicted values using a two-tailed test with $p=0.05$.

Results

Epidural recordings

Epidural recordings were made from all six animals to determine the stimulation threshold for each orientation and pulse width of TMS. In all cases, the lowest threshold volley corresponded to a D-wave latency (i.e. <2.6ms). In agreement with the human literature (Day et al., 1989), significantly higher thresholds were observed with AP compared to PA TMS (Figure 2-3). It was not possible to make statistical comparisons with the AP30 and AP111 stimuli since these were only delivered in two monkeys.

Intensities series were performed with epidural recordings for each stimulus (Figure 2-4). Volleys occurring at D-wave latencies were reliably evoked with both PA and AP TMS and increased in amplitude with increasing stimulus intensity. I-waves were rarely seen, even with the highest stimulus intensities (Figure 2-4). This is in contrast to recordings made in conscious humans (Di Lazzaro et al., 2001), but shows similarities to human recordings made under anaesthesia

(Berardelli et al., 1990; Burke et al., 1993), presumably reflecting the reduction in cortical excitability associated with anaesthetic use.

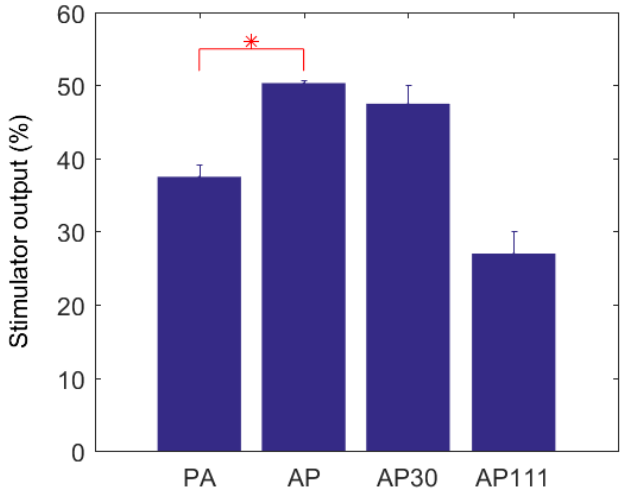

Figure 2-3. TMS thresholds

Mean epidural TMS thresholds measured for PA (n=6), AP (n=6), AP30 (n=2), and AP111 (n=2) stimulation. Error bars represent standard error and the red asterisk shows a statistically significant ($P<0.05$) difference between PA and AP thresholds.

Axonal responses to TMS

Individual corticospinal axons were successfully recorded in all animals except monkey K. In total, 264 corticospinal axons were identified, of which 154 responded to TMS and 106 responded to lumbar stimulation. Only 54 axons were identified which responded to TMS but not to lumbar stimulation, of which 29 were identified as originating from old M1 and 13 from new M1.

Both PA and AP TMS preferentially evoked D-waves in corticospinal axons (Figure 2-5*A*), although these were generated more frequently with PA than AP TMS (Figure 2-5*B*). Comparatively few I-waves were evoked with either orientation of stimulation, although both the number of spikes and axons was greater with AP TMS (Figure 2-5). In agreement with the human literature (Di Lazzaro et al., 1998b; Di Lazzaro et al., 2001), PA TMS did not reliable evoke I3-

waves with low intensity stimuli, and I1-waves were only clearly observed with AP TMS at the highest intensity.

AP TMS generated a short latency spike around 1.2ms that preceded the D-wave (see 2x threshold AP TMS panel on Figure 2-5). This shows similarities to the reduction in D-wave latency of 0.8-0.9ms with increasing TES intensity reported by Burke et al. (1993) and presumably reflects the site of activation of PTNs shifting deeper. The selectivity of this early D-wave for AP TMS may reflect an AP trajectory of axons in the brainstem. These short-latency spikes are likely unique to monkey recordings in which the comparatively small brain and large TMS coil allows current to spread deeper than observed in human studies.

Response probabilities

In addition to relatively few axons responding to each stimulus, of the axons in which responses were evoked, these rarely occurred on every trial (Figure 2-6). Fewer than 10% of stimuli delivered through the cortical electrodes in old and new M1 evoked a D-wave, and the probability of I-waves was even lower. Interestingly, a sequential reduction in response probability was observed with increasing latency for both old and new M1 stimulation. The same trend was not observed for either orientation of TMS. Instead, PA TMS showed a high probability of D-waves being evoked in a responding axon and whilst the I-wave probability was lower, it was similar across all I-waves. AP TMS showed similar probabilities of both D- and I-waves being evoked on each trial, particularly at high intensities. In both cases, the number of trials in which an axon responded to the stimulus was consistent with increasing intensity (Figure 2-6*C*), but the number of axons recruited increased (Figure 2-5*B*). Note that stimulation threshold was not determined for individual axons but instead was set for each monkey using epidural recordings.

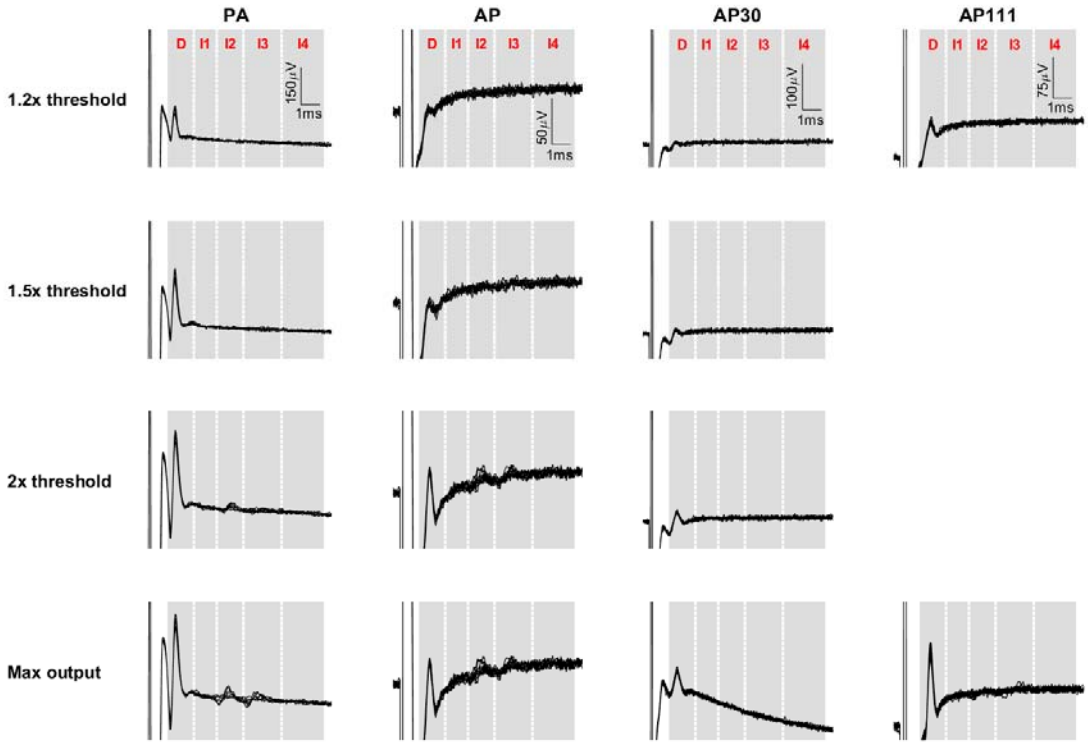

Figure 2-4. Epidural recordings

Example epidural recordings from monkey W. Each column represents the four different TMS stimuli delivered; each row is the intensity of this stimulus, relative to epidural threshold. Each sweep is an individual trial and the windows show the latencies representing D, I1, I2, I3 and I4 waves. There are no recordings at 1.5x and 2x threshold for AP111 since the maximum stimulator output with this pulse length was 44%, which was less than 1.5x threshold.

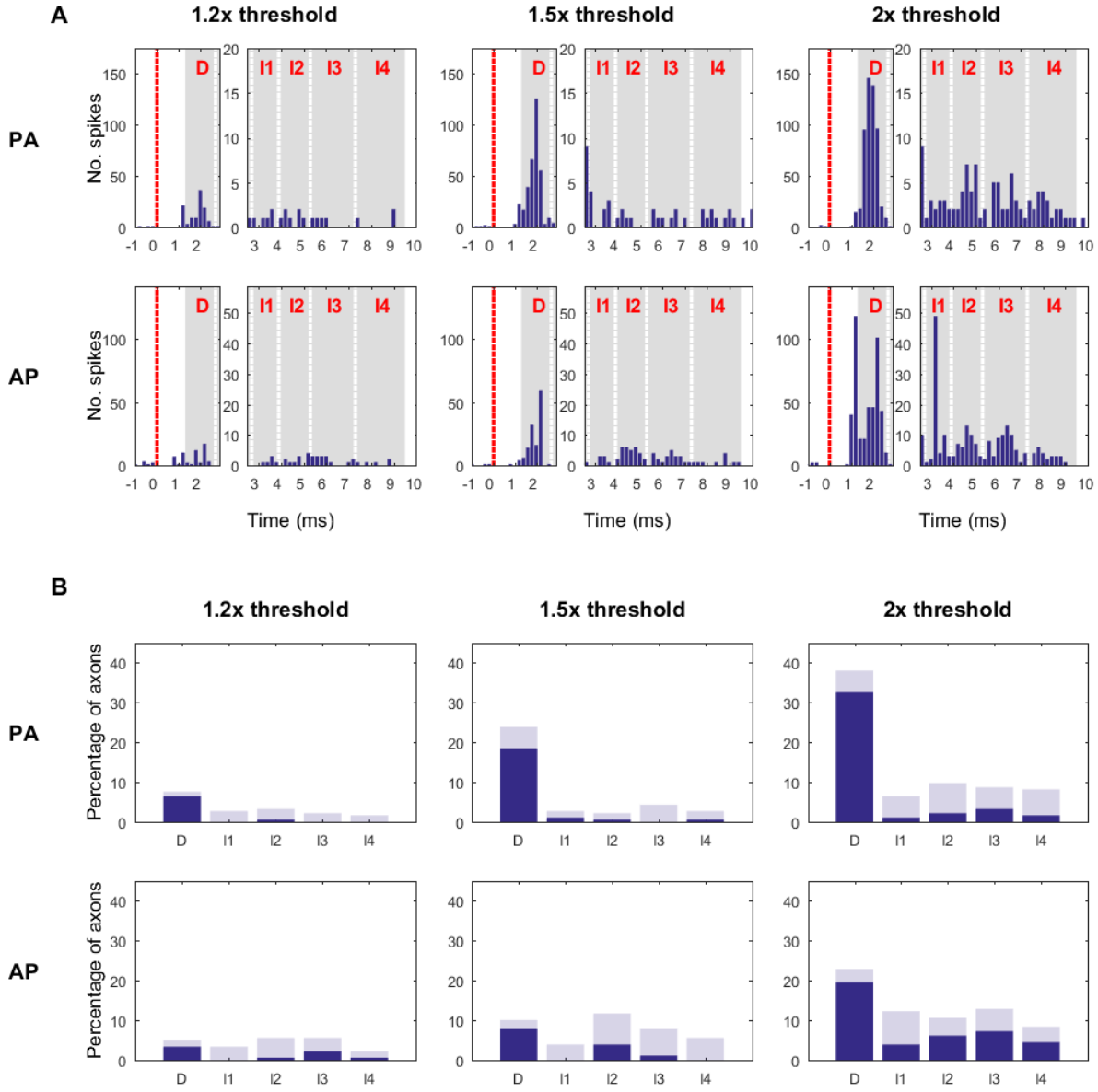

Figure 2-5. TMS responses

A. PSTHs for three intensities (columns) for PA and AP TMS (rows), summed across all corticospinal axons (n=264). The grey windows show the latencies representing D, I1, I2, I3 and I4 waves, relative to stimulus onset (red dotted line). The x axis has been split at 2.7ms to enable separate scales for the number of D- and I-wave spikes. ***B.*** Number of axons in which a spike was recorded during each wave, expressed as a percentage of the total number of axons in which PA (n=184) or AP (n=179) TMS was delivered. The lighter shade represents axons in which only one spike was recorded in the given window.

I-wave patterns

Examination of the patterns of responses generated in individual trials demonstrated that for both cortical stimulation and TMS, in less than 5% of trials was more than one spike at I-wave latency evoked. Compared to values predicted under the assumption that I-waves occurred independently, our results show that in individual trials, single I-waves were generated more often than expected and multiple I-waves were generated less often than expected (Figure 2-7*A*). In contrast, multiple I-waves were evoked in approximately 20% and 35% of axons responding to PA and AP TMS, respectively. The measured proportion of axons with each I-wave pattern were largely similar to the values predicted under the assumption that each I-wave occurred independently (Figure 2-7*B*). A notable difference between local stimulation through the cortical electrodes and gross stimulation with TMS is that whereas many axons responded to the former with four I-waves, no axons were identified which responded to TMS with more than three I-waves.

Activation of axons by both PA and AP TMS

At each stimulation intensity, four groups of axons were identified: those that didn't respond to TMS, those that responded to both PA and AP TMS, and those that only responded to one orientation of TMS (Figure 2-8*A*). With increasing stimulus intensity, a greater proportion of axons responded to both PA and AP stimulation. Analysis of the latencies of spikes evoked by PA and AP TMS in axons responding to both stimuli demonstrated that both coil orientations can directly activate the same axons, whereas indirect activation of individual axons with both PA and AP stimulation was less common (Figure 2-8*C*). There was no significant difference between the predicted and observed values for the number of axons in which PA and AP TMS could both generate I-waves, suggesting that I-waves with PA and AP TMS are independent. In contrast, D-waves were evoked with both PA and AP TMS by significantly more axons that predicted (Figure 2-8*B*).

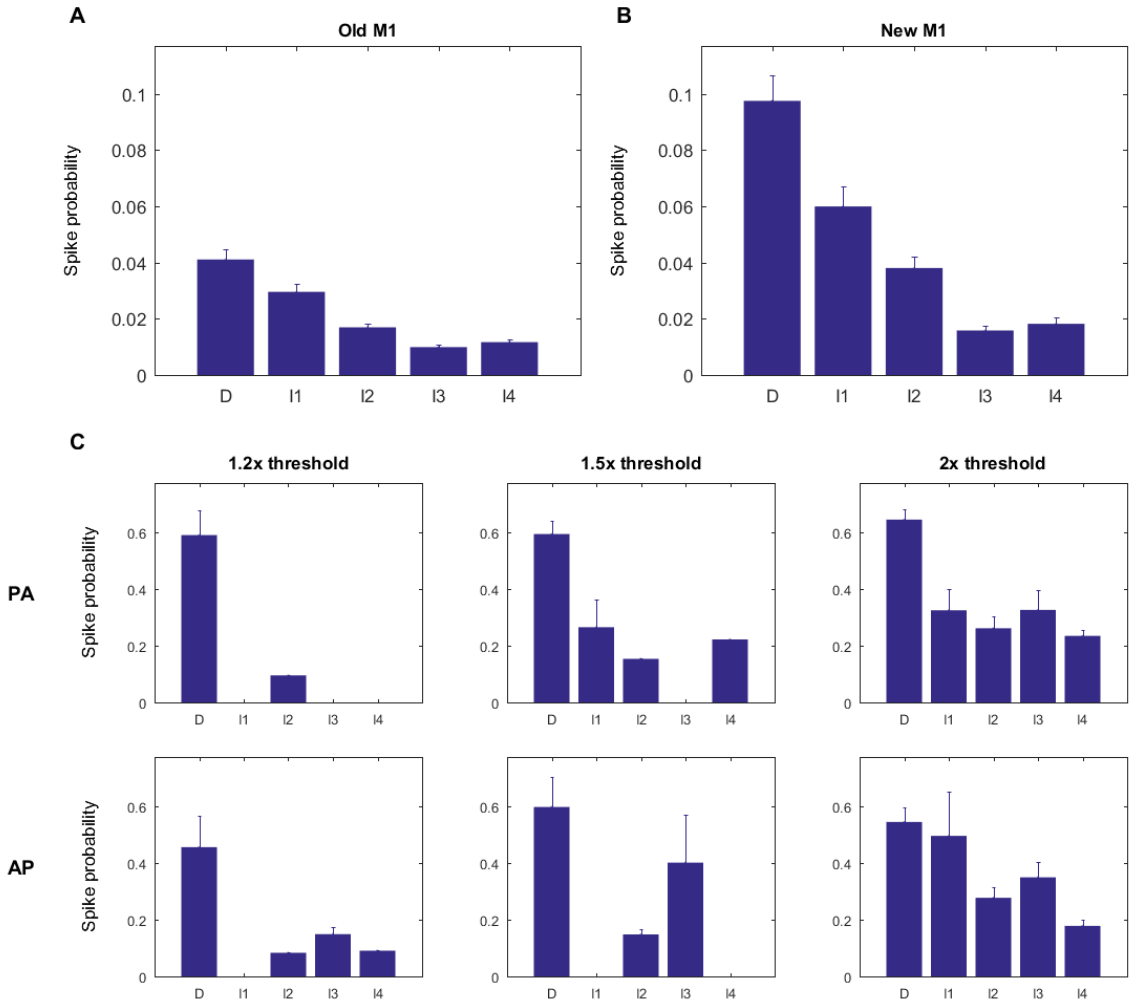

Figure 2-6. Wave probabilities

For axons which responded to a given stimulus in a given window, the mean proportion of trials in which the response was evoked in presented. These values equate to response probability and are presented for ***(A)*** old M1 stimuli, ***(B)*** new M1 stimuli and ***(C)*** three intensities of PA and AP TMS. Error bars represented standard error.

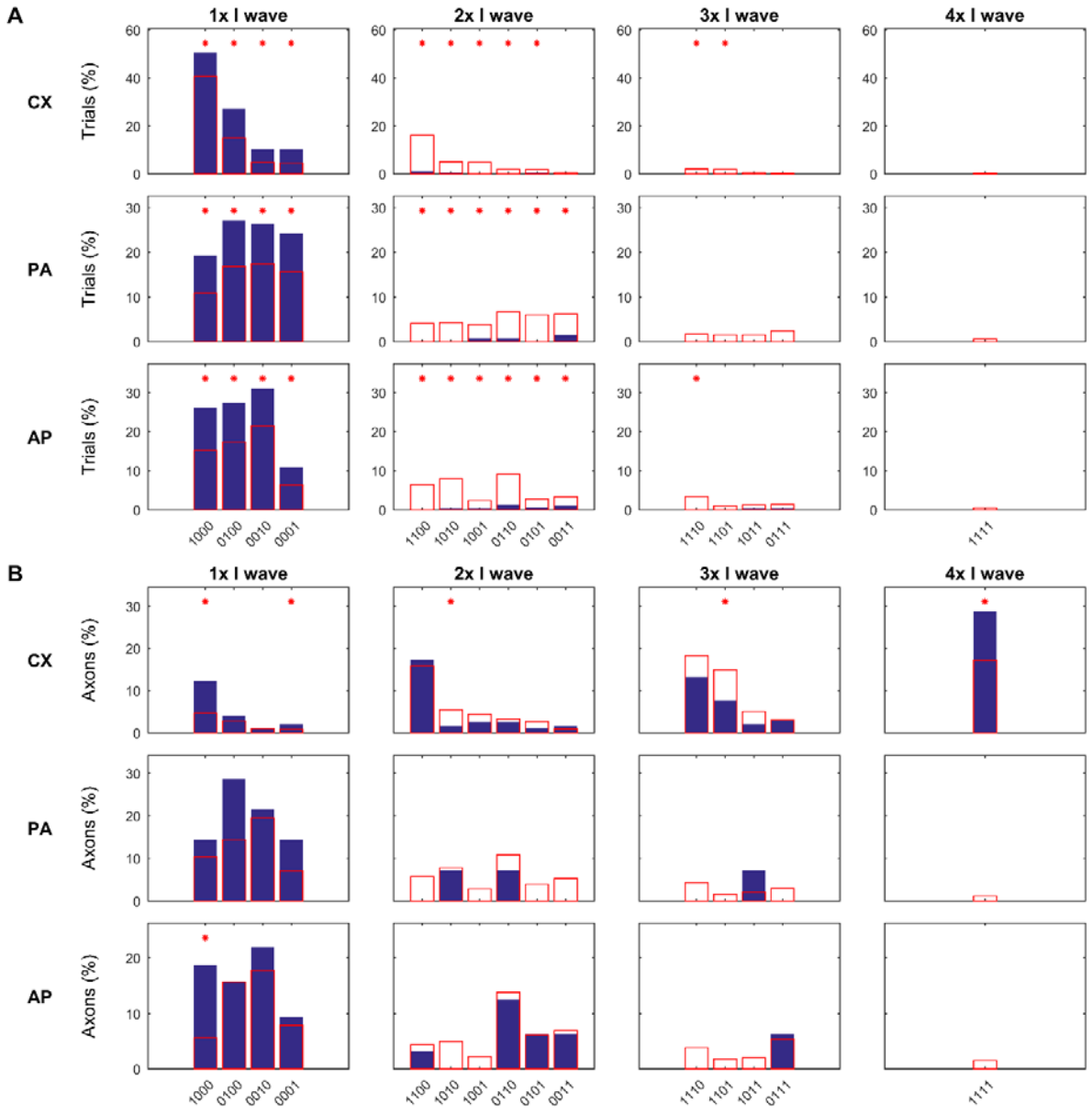

Figure 2-7. I-wave patterns

Patterns of I-waves recorded from *(A)* individual trials and *(B)* individual corticospinal axons, expressed as a percentage of the total number of trials or axons with I waves. Only axons which generated more than one spike in each window are presented. Blue bars represent recorded data, red lines show predicted results assuming all I waves to be independent. Red asterisks indicate a statistically significant (P<0.05) difference between actual and predicted data (see Methods). I wave patterns are shown as a 0s and 1s, representing the absence and presence of an I-wave in that window, respectively. The four digits represent the four I-wave windows: I1, I2, I3 and I4. For example, '1000' represents the stimulus evoking an I1-wave but no later I-waves.

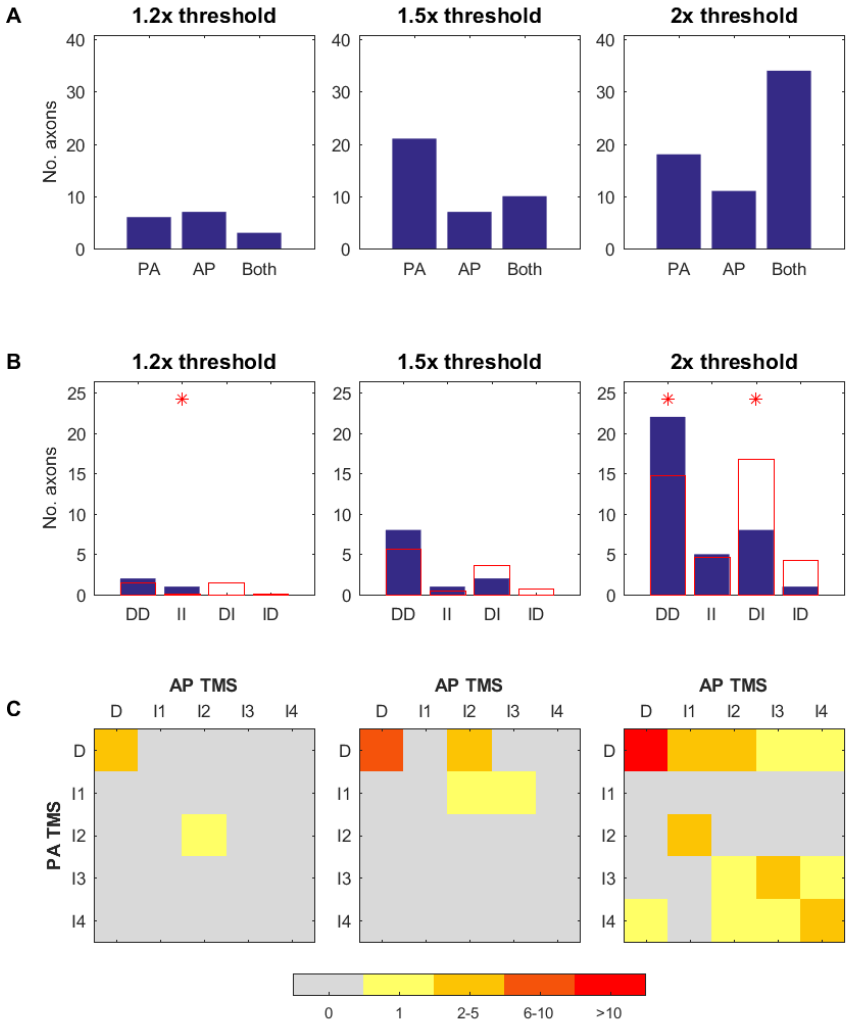

Figure 2-8. Activation of individual axons by both PA and AP TMS

A. The number of axons in which responses were evoked, at any latency, by PA TMS only, AP TMS only, or both PA and AP TMS. Axons were only included if more than 5 stimuli of each TMS orientation and intensity were delivered. ***B.*** Sub-analysis of the axons which responded to both PA and AP TMS. Blue bars show the number of axons which, in response to both PA and AP stimulation, evoked a D-wave (DD), an I-wave of any latency (II), or a D-wave with PA and I-wave with AP (DI) and vice versa (ID). Red outlines show the predicted number of axons for each of these combinations based on the assumption that D- and I-waves were independently evoked by PA and AP TMS in each axon. Red stars show a statistically significant ($P<0.05$) difference between predicted and observed values. ***C.*** The combination of D- and I-waves that can be evoked by PA and AP TMS in the same axon. The number of axons is represented with a colour scale. Only axons that responded with more than one spike in a given window were included.

Old and new M1

Both PA and AP TMS generated D- and I-waves from axons identified as originating from old and new M1 (Figure 2-9). D-waves were evoked from a greater proportion of new M1 axons, with PA being the more effective stimulus for this. Interestingly, with both coil orientations, I1-waves were only evoked from axons originating from old M1.

Axonal recordings with cTMS

AP TMS with different pulse widths was only tested in two animals (monkeys W and Y). Furthermore, in these two animals it was only delivered to 17 axons due to the difficulty in maintaining each axon recording for a sufficient time period. In total, AP30 and AP111 each evoked responses in 7 of these axons. The general trend observed was that AP30 preferentially evoked I3-waves, whilst AP111 has a less specific effect, predominantly evoking I2- and I3-waves (Figure 2-10).

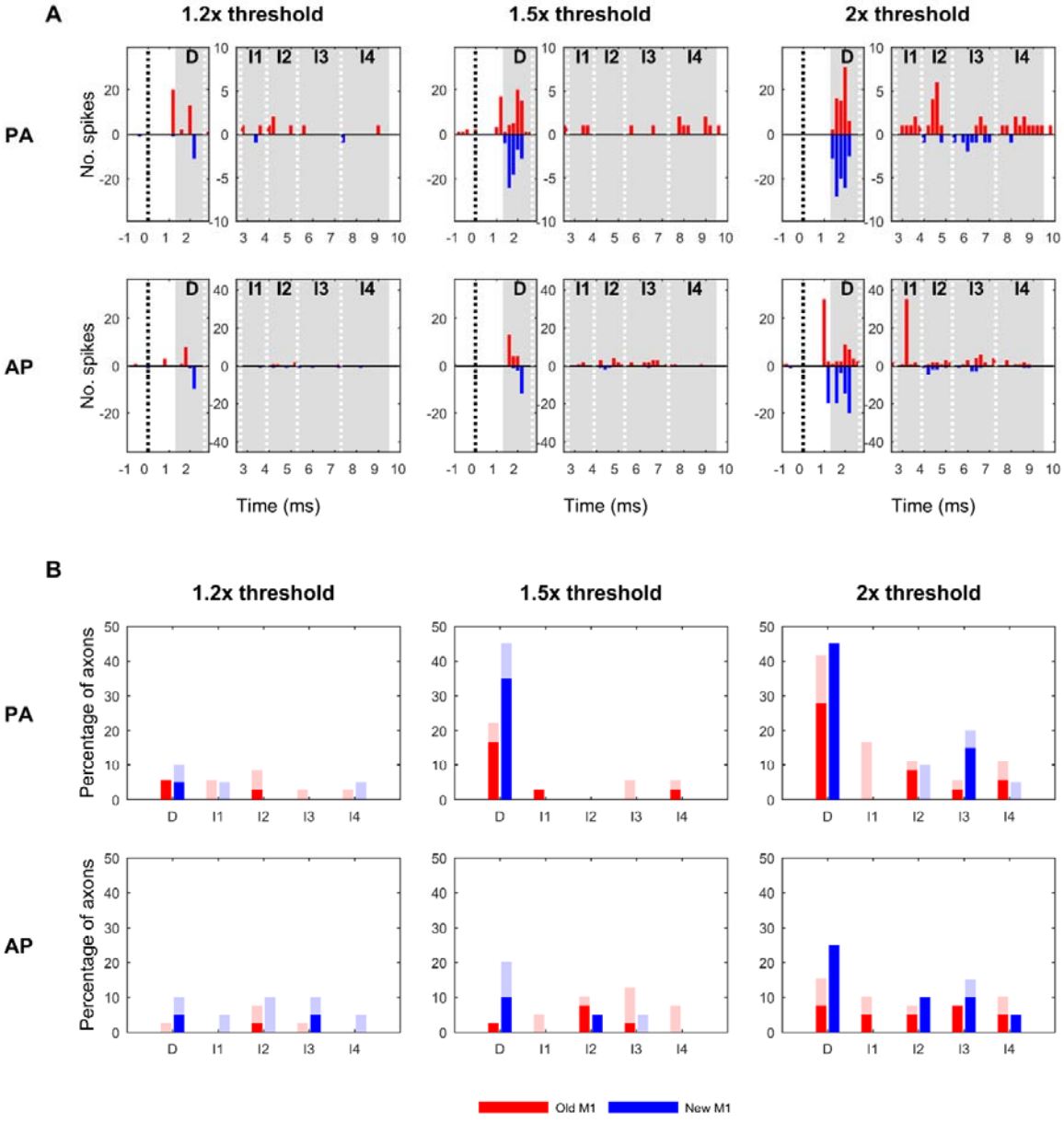

Figure 2-9. Old M1 vs New M1 TMS responses

A. PSTHs for three intensities (columns) for PA and AP TMS (rows), summed across non-lumbar corticospinal axons originating from old M1 (red, n=29) and new M1 (blue, inverted scale, n=13). The grey windows show the latencies representing D, I1, I2, I3 and I4 waves, relative to stimulus onset (black dotted line). The x axis has been split at 2.7ms to enable separate scales for the number of D- and I-wave spikes. ***B.*** Number of axons in which a spike was recorded during each wave, expressed as a percentage of the total number of old M1 axons (red) or new M1 axons (blue) in which PA or AP TMS were delivered. The lighter shade represents axons in which only one spike was recorded in the given window.

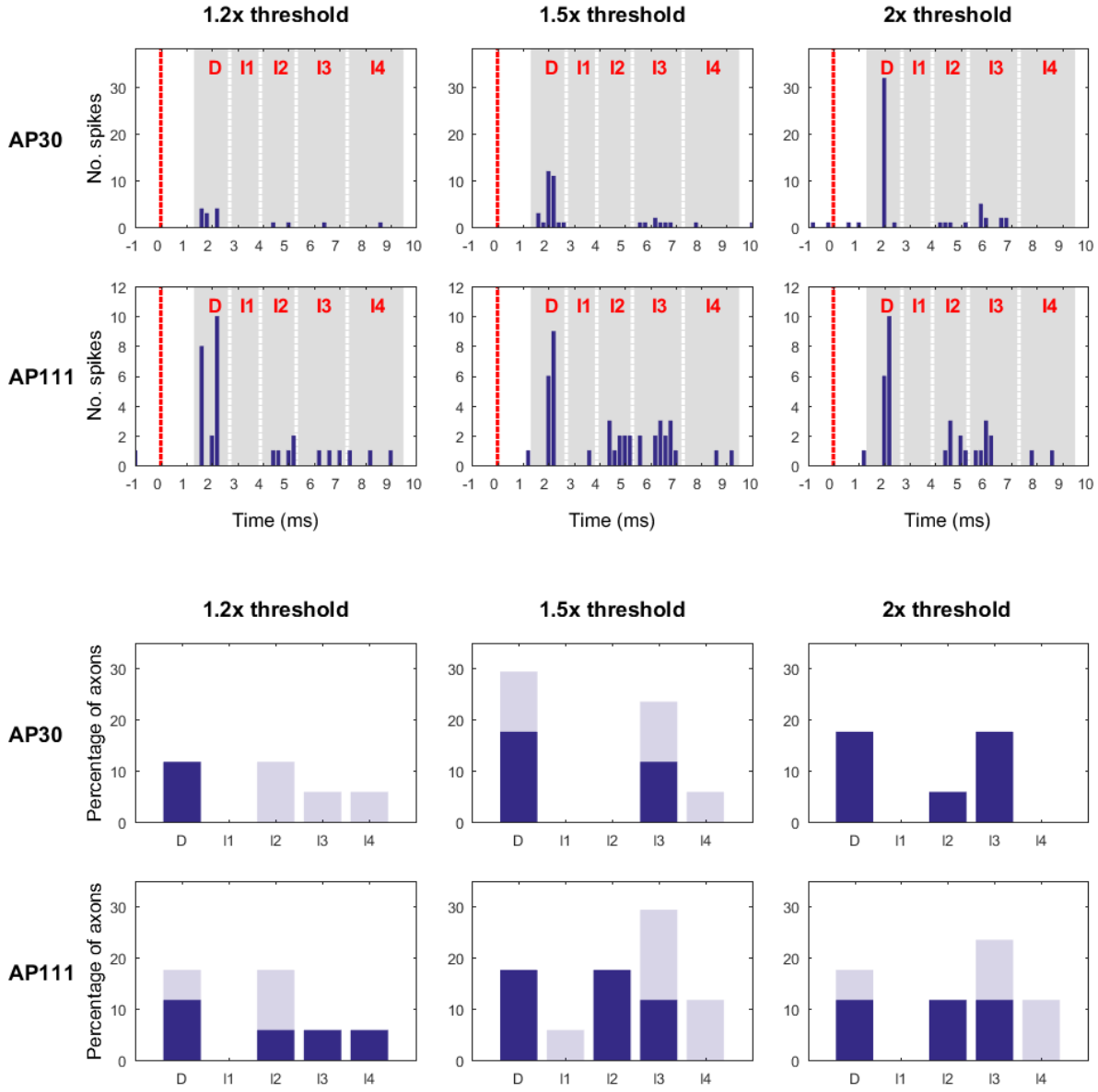

Figure 2-10. cTMS responses

A. PSTHs for three intensities (columns) for AP30 and AP111 cTMS (rows), summed across all corticospinal axons in which this stimulus was delivered (n=17). The grey windows show the latencies representing D, I1, I2, I3 and I4 waves, relative to stimulus onset (red dotted line). *B.* Number of axons in which a spike was recorded during each wave, expressed as a percentage of the total number of axons in which cTMS was delivered (n=17). The lighter shade represents axons in which only one spike was recorded in the given window.

Discussion

With few exceptions (Edgley et al., 1997), the study of TMS has focussed on epidural recordings from the spinal cord and recordings of muscle activity made from either EMG or single units. Valuable as these studies have been, neither method represents the activity of individual corticospinal axons (Edgley et al., 1997). Mechanistic understanding of the action of TMS requires the study of single cells since there is much heterogeneity in the origin, size and post-synaptic actions of corticospinal neurons (Lemon, 2008).

We report the first example of single corticospinal axon recordings with focal TMS. Despite the advantages of recording from individual corticospinal axons, it is important to note the limitations of this method, particularly when drawing comparisons to the human literature. Firstly, the small brain of the monkeys relative to the coil size makes it likely that we were able to stimulate deeper into the cortical and subcortical layers than is commonly achieved in humans. Secondly, the anaesthesia required for these experiments would have had a significant effect on cortical excitability, as has been reported in human studies (Berardelli et al., 1990; Burke et al., 1993), suppressing the generation of D- and I-waves (Baker et al., 1995; Di Lazzaro et al., 1998a). Thirdly, given that microelectrode recordings are more likely to be obtained from large diameter axons, and the inverse relationship between axon diameter and D-wave threshold (Edgley et al., 1997), it is likely that our recordings were biased to the large diameter, fast-conducting axons that represent only a minority of the corticospinal tract (Porter and Lemon, 1993; Firmin et al., 2014).

Nonetheless, our results show broadly similar patterns to those observed in previous studies, with higher threshold for AP than PA TMS (Sakai et al., 1997), I1-waves evoked more frequently with PA TMS, I3-waves evoked more frequently with AP TMS (Di Lazzaro et al., 2001), and shorter pulse widths of AP TMS selectively evoking later I-waves (D'Ostilio et al., 2016).

Early I waves

There is much evidence supporting the notion that I1-waves are generated by different circuits to the later I-waves. Primarily, unlike late I-waves, I1 is not affected by paired-pulse TMS techniques assessing cortical inhibition, such as short latency intracortical inhibition (Di Lazzaro et al., 1998c; Hanajima et al., 1998), long latency intracortical inhibition (Di Lazzaro et al., 2002),

interhemispheric inhibition (Di Lazzaro et al., 1999b) and short latency afferent inhibition (Tokimura et al., 2000). Further support for the involvement of inhibitory pathways in late I-wave but not I1 generation comes from the observation that allosteric modulators of the $GABA_A$ receptor only suppress late I-waves (Di Lazzaro et al., 2000).

Di Lazzaro and Ziemann (2013) recently proposed that I1-waves may be mediated by the monosynaptic projections of layer II and III pyramidal neurons to the large PTNs of layer V. These pyramidal neurons are easily excited by TMS due to their superficial location and in mouse, provide the main excitatory input to PTNs (Anderson et al., 2010). Our results are in agreement with this hypothesis, demonstrating that I1-waves are evoked in corticospinal axons originating from old M1, i.e. the convexity of the precentral gyrus, but not those originating from the deeper new M1. It is important to note that our methods did not permit assessment of whether the corticospinal axons formed mono- or disynaptic connections with motoneurons. However, given that large diameter, fast-conducting axons are likely to have lower activation thresholds (Edgley et al., 1997), responses evoked from old M1 likely reflect activation of fast PTNs that form disynaptic connections with motoneurons, whereas responses evoked from new M1 are presumably due to activation of fast CM cells (Rathelot and Strick, 2009; Witham et al., 2016). Thus, a D-wave evoked from new M1 will generate a response at D-wave latency in muscles whereas a D-wave evoked from old M1 will generate a response at I1 latency in muscles due to the additional synaptic delay.

We therefore propose that D-waves recorded from muscles represent activation of CM cells originating from new M1. In contrast, given that we did not observe the generation of I1-waves from new M1, responses at I1 latency in muscle likely represent the disynaptic transmission of D-waves in old M1 axons. Subsequent I-waves are a combination of disynaptic effects from old M1 and monosynaptic effects from new M1. Thus, these results suggest that it may be possible to selectively assess monosynaptic and disynaptic corticospinal pathways with TMS.

Late I waves

Since they were first described by Patton and Amassian (1954), several theories have been proposed to explain the periodicity of I-waves. It is well established that I-waves represent indirect

excitation of PTNs by cortical interneurons. However, the specific interneuron circuits involved have not been identified. The synaptic chain hypothesis originally suggested by Patton and Amassian (1954) proposed that sequential I-waves are generated by increasingly long chains of interneurons. Although this hypothesis accounts for the periodicity of I-waves, it has largely been disproven by the observation that I-waves can be evoked in a non-orderly sequence (Di Lazzaro et al., 2001). Our results show that with PA and AP TMS, the probability of evoking each I-wave does not decrease with latency, as could be expected by the increasing number of synapses. On this basis, our results provide further evidence for the rejection of the synaptic chain hypothesis. However, responses generated by stimulation of the cortical electrodes implanted into old and new M1 did show a progressive reduction in probability with increasing latency. In comparison to the gross stimulation provided by TMS, it is possible local stimulation through these implanted electrodes is able to activate chains of interneurons that terminate on PTNs. We propose that either TMS is unable to access these circuits, or that the responses generated by TMS are superimposed over these local circuits.

An alternative hypothesis is that I-waves are generated by independent circuits of interneurons (Day et al., 1989; Sakai et al., 1997). The non-orderly recruitment of I-waves is easily explained by this model. Under our experimental conditions, it was rare for a stimulus to generate more than one I-wave per trial, even though the axon may respond to the same stimulus with multiple different I-waves. Although this could be taken as evidence to suggest that I-wave circuits are not independent, a more likely explanation is that the relative refractory period of the PTNs reduced excitability and prevented multiple spikes in response to one stimulus. Therefore, although our results neither support nor reject the independent circuit hypothesis, they do suggest that the I-wave periodicity observed in epidural recordings represents a population effect and not repetitive discharge of individual neurons.

It has also been suggested that the late I-waves evoked with PA and AP TMS are mediated by different mechanisms. This hypothesis stems from the observation that short-latency afferent inhibition has a greater inhibitory effect on the I-waves evoked with PA TMS than the I-waves of AP TMS (Ni et al., 2011). Interestingly, although we found that both PA and AP TMS could excite the same axons, particularly when high intensity stimuli were delivered, it was rare for both coil orientations to evoke I-waves in the same axon. Our results suggest that in contrast to D-waves,

the generation of I-waves with PA and AP TMS is independent, thus providing indirect support for this hypothesis. It is perhaps logical that PA and AP I-waves are mediated by different mechanisms when considering the orientation of intracortical interneurons and PTNs, and the importance of axon orientation, axon bends, and the grey to white matter transition in determining the threshold for excitation (Rushton, 1927; Amassian et al., 1992; Maccabee et al., 1993; Salvador et al., 2011). One possibility is that the late I-waves of AP TMS are generated by excitation of long cortico-cortical fibres which originate from premotor areas (Dum and Strick, 2005) and project to M1 in an anterior to posterior direction. In support of this, stimulation of the ventral premotor cortex in both man (Cerri et al., 2003) and monkey (Shimazu et al., 2004) has been shown to evoke I-waves. Although we did not directly assess these projections, our observation that AP TMS was more effective in evoking I-waves provides some support for the involvement of cortico-cortical projections.

In addition to the differing responses evoked with PA and AP TMS, pulse duration may also play a significant role in selecting the I-waves generated. Although TMS is typically delivered with an 82μs pulse (Rothkegel et al., 2010), the recent development of cTMS (Peterchev et al., 2013) enables adjustment of this parameter. In accordance with previous work (D'Ostilio et al., 2016), our results suggest that I3-waves are preferentially generated by short AP pulses whereas longer AP pulses are less selective, evoking both I2- and I3-waves. Such findings add another level of complexity to I-waves.

Old M1 versus New M1

The extension of M1 into the central sulcus (Geyer et al., 1996) raises the question of which subdivisions of this structure (Rathelot and Strick, 2009; Witham et al., 2016) can be excited with TMS. In man, although there is a substantial degree of variation, the central sulcus is approximately 2cm deep (Cykowski et al., 2008). It has been estimated that the currents generated by TMS can penetrate 2-3cm deep in the brain (Maccabee et al., 1990) hence it is feasible that TMS can excite axons deep into the central sulcus, as has been demonstrated with imaging studies (Fox et al., 2004). We found that although TMS activated PTNs originating from both the anterior wall of the central sulcus (new M1) and the crown of the precentral gyrus (old M1), TMS responses were evoked in only 40.0% of new M1 axons compared to 71.4% of old M1 axons.

The most striking result from our comparison of old M1 and new M1 axons was the observation that I1-waves were only evoked in axons originating from old M1, as previously discussed. In addition, we found that with both PA and AP TMS, D-waves were evoked in a greater proportion of axons originating from new M1 than old M1. This may reflect the effect of axon bending on activation threshold (Rushton, 1927; Amassian et al., 1992; Maccabee et al., 1993; Salvador et al., 2011). Due to their relative locations, it is likely that the corticospinal axons projecting from new M1 have a sharper bend than those projecting from old M1 as they transition from the grey matter to the white matter, and so the new M1 axons could be expected to have lower activation thresholds.

Summary

In this study, we recorded the responses of individual corticospinal axons to PA and AP coil orientations of TMS, and identified a number of these axons as originating from either old M1 or new M1. Our results suggest that the earliest I-wave (I1) is evoked in axons originating from old M1 and we speculate that it may be possible to target selectively monosynaptic and disynaptic corticospinal pathways by measuring different latency components of MEPs. Limited recordings of axonal responses to different pulse durations of AP TMS support previous findings that short pulses evoke later I-waves than long pulses, thus providing another means to selectively activate different intracortical networks with TMS. Our data suggest that although local stimuli may activate chains of interneurons, these are not responsible for the I-waves evoked by TMS. Furthermore, we propose that the periodicity of I-waves recorded epidurally may be a population effect and does not represent repetitive discharge of individual neurons. Our findings largely support the model proposed by Di Lazzaro and Ziemann (2013) in which I-waves are generated by a combination of excitatory projections from superficial to deep pyramidal cells and local intracortical interneuron circuits, as well as longer cortico-cortical projections.

CHAPTER III

Modulation of rapid visual responses consistent with a putative tecto-reticulospinal pathway

The data described in this chapter were collected by myself and Thomas Tay, a summer student from NU Malaysia who I supervised for a two month project. I collected the data for Experiment 1 and Experiment 2b; Thomas Tay performed Experiment 2a, under my supervision. Stuart Baker devised the original experiments and programmed the task. I designed the plasticity protocol and performed all data analysis.

Introduction

Increasing evidence supports the role of reticulospinal pathways in upper limb function (Baker, 2011), from gross reaching (Schepens and Drew, 2004b, 2006a) to precise finger movements (Carlsen et al., 2009; Soteropoulos et al., 2012; Honeycutt et al., 2013). Accordingly, the reticulospinal tract (RST) has been shown to project to motoneurons innervating both distal and proximal muscles in primates (Davidson and Buford, 2004; Davidson and Buford, 2006; Riddle et al., 2009). However, in contrast to the corticospinal tract, there are limited methods available for the non-invasive assessment of reticulospinal excitability.

The tecto-reticulospinal pathway may provide a means of targeting the RST. It is well established that the reticular formation (RF) receives inputs from the deep layers of the superior colliculus (Illert et al., 1978; Grantyn and Grantyn, 1982). The firing of cells within the superior colliculus and the underlying RF has been shown to correlate with proximal arm movements (Werner, 1993; Stuphorn et al., 1999), and microstimulation of both these areas can evoke a range of arm movements (Philipp and Hoffmann, 2014), suggesting a role of tecto-reticulospinal pathways in upper limb function. These findings have been translated to human studies: fast reaching movements made towards visual targets evoke short-latency EMG activity that is similarly

proposed to be mediated by tecto-reticulospinal projections (Pruszynski et al., 2010). Thus choice reaction reaching tasks with visual targets may provide a means of non-invasively measuring reticulospinal excitability by delivering an input to this pathway via the superior colliculus, and an output measure in the form of short-latency EMG activity which can be recorded from proximal muscles. We refer to these responses as rapid visual reactions (RVRs).

Loud auditory stimuli may also provide a means of assessing reticulospinal activity. The auditory startle reflex, characterised by a stereotyped sequence of muscle contractions (Brown et al., 1991), is thought to be mediated by a circuit including the caudal pontine RF (Hammond, 1973; Leitner et al., 1980; Davis et al., 1982). If the RF acts as a site of multisensory integration, it is possible that visual and startling auditory stimuli (SAS) may interact to modulate reticulospinal output and thus RVRs.

In addition to the startle reflex, SAS can also reduce the reaction time for muscle responses (Valls-Sole et al., 1999). This phenomenon, termed StartReact, has similarly been proposed to involve the RF (Valls-Sole et al., 1999; Rothwell, 2006). The onset latency of EMG activity in response to SAS may thus provide a second measure of reticulospinal excitability which could be subject to modulation by the pairing of sensory inputs to the RF. The rationale for this comes from previous work suggesting that reticulospinal output can be modulated by pairing sensory inputs to the RF (Foysal et al., 2016), and that StartReact is modulated by the degree of reticulospinal involvement (Baker and Perez, 2017).

The aim of this study was to assess whether SAS with different latencies relative to visual target appearance are able to modulate RVRs and EMG onset latency in a fast reaching task, thereby providing support for the hypothesis that these responses reflect reticulospinal activity. Secondly, we investigated whether repeated pairing of SAS with visual target appearance can induce plasticity in these pathways. By measuring the size of RVRs and the onset of EMG activity, we propose that these experiments have enabled us to assess reticulospinal excitability non-invasively in man.

Methods

Subjects

Eight subjects participated in Experiment 1 (age: 22.7 ± 3.7 years; 4 female), 14 subjects participated in Experiment 2a (age: 23.1 ± 3.7 years; 10 female) and 15 subjects participated in Experiment 2b (age: 27.5 ± 8.8 years; 13 female). All subjects were right-handed, had no history of neurological disorders, and provided written informed consent to participate in the study. All procedures were approved by the local ethics committee and the study complied with the Declaration of Helsinki.

EMG recordings

Surface electromyography (EMG) recordings were made from the right medial deltoid and right pectoralis major (PM). Two silver/silver chloride electrodes (Kendall H59P, Medcat) were placed on the skin of each muscle along the direction of the muscle fibres. EMG signals were amplified (200-10,000 gain), filtered (30Hz to 2kHz bandpass) and digitised (5kHz) for off-line analysis (CED 1401 with Spike2 software, Cambridge Electronic Design).

Experimental sessions

Our experimental task was based upon that reported by Pruszynski et al. (2010). All experiments were performed using a control arm that consisted of two metal shafts connected to each other and a firm base by vertical revolving joints. A joystick mounted at the free end provided a grip for subjects to hold. The control arm allowed free movement in a horizontal plane and optical encoders tracked its position. Subjects sat on a chair in front of the control arm with a 90° bend at the elbow when holding the joystick in a central position with their right hand. Targets were projected from a screen onto the plane of movement using a half-silvered mirror. This mirror also acted to prevent subjects from seeing their own hand, and experiments were performed in the dark to increase this effect. A red LED on the top of the joystick indicated hand position at appropriate times during each trial.

The trial sequence is outlined in Figure 3-1.The appearance of a central marker (white circle, 1cm radius) indicated the start of each trial. Subjects moved the joystick to this marker at their own

pace. Successful positioning was indicated by the central marker changing colour from white to blue. Subjects were required to maintain this position for a randomised period of 1-2s after which the central marker disappeared for a gap period of 200ms, which has been shown to decrease reaction times (Fischer and Rogal, 1986; Gribble et al., 2002). A peripheral target (white circle, 1cm radius) then appeared in one of four directions (45°, 135°, 225° or 315° relative to the right horizontal axis) at a distance of 10cm from the central marker position. Subjects were instructed to make fast reaching movements to this new target. The red LED was turned off from the start of the gap period until the target was reached to encourage subjects to make ballistic rather than tracking movements. Auditory feedback was provided at the end of each trial to indicate whether the target was reached in less than 500ms.

Subjects performed blocks of 40 trials, separated by rest periods of 60s in which the mean reaction time for the preceding block was presented on the screen. For all experiments, subjects completed a total of 960 trials (24 blocks of 40 trials). During startle trials, SAS (~120dB, 20ms) were delivered during the gap period.

In Experiment 1, SAS was delivered 150ms, 100ms, 75ms, 50ms and 0ms before the appearance of the peripheral target. In combination with a control condition in which no SAS was delivered, this protocol gave a total of 6 stimulus conditions which were randomised across trials, resulting in 40 trials per stimulus per target direction. In Experiment 2a, subjects separately performed a plasticity protocol and control protocol spaced one week apart. The order of these two experimental sessions was randomised across subjects. During the plasticity protocol, subjects performed the first 4 blocks with no stimulus (pre-intervention: 4x40 trials), followed by 16 blocks with SAS delivered 100ms before peripheral target appearance (intervention, S1-4: 4x4x40 trials) and a final 4 blocks with no stimulus (post-intervention: 4x40 trials). This protocol is subsequently referred to as ‘Startle100’. In the control condition, subjects performed all 24 blocks without SAS to assess the effects of training and fatigue. In Experiment 2b, subjects performed the same plasticity protocol as Experiment 2a but SAS was delivered at the same time as peripheral target appearance (i.e. t=0). This protocol is subsequently referred to as ‘Startle0’. In all three plasticity protocols, target direction was randomised across each sequence of 160 trials so that targets appeared 40 times per target direction for the pre-intervention session, four intervention sessions (S1-4) and post-intervention session.

Each experiment lasted approximately one hour. Task parameters including joystick position, stimulus condition, target direction and reaction time were stored to disc along with EMG recordings. To prevent the processing and graphics delays of the computer generating timing errors, a photodiode on the screen detected target appearance and all recordings were aligned to this signal.

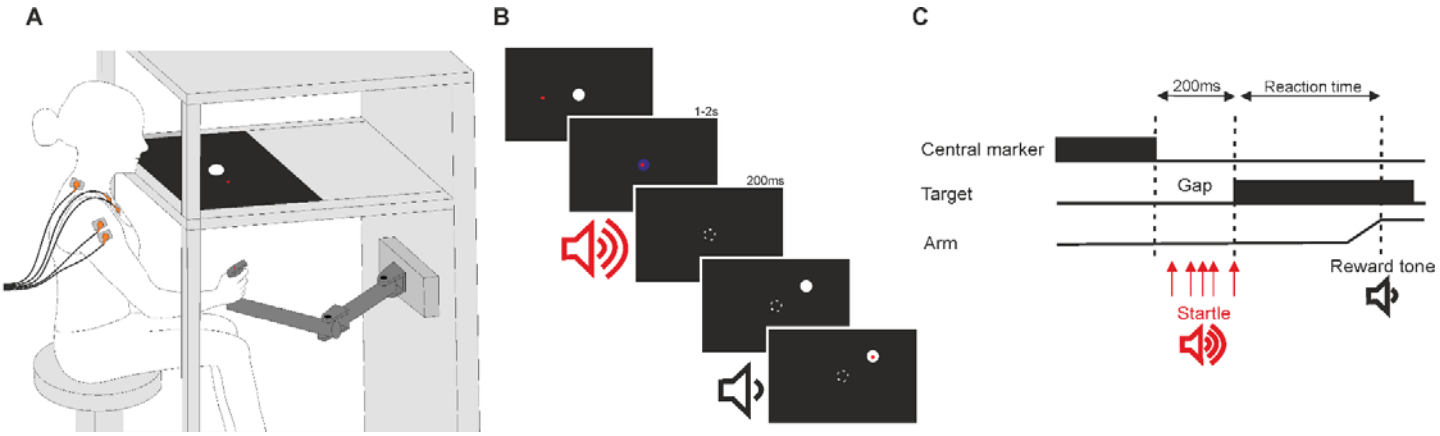

Figure 3-1. Experimental paradigm

Subjects made reaching movements in a horizontal plane by moving a control arm with their right hand. Targets were displayed on a screen and projected onto the plane of movement using a half silvered mirror that occluded view of the hand. A red LED on the handle of the control arm indicated position relative to the screen. Each trial began with the presentation of a central marker (white circle, 1cm radius). Subjects were required to align their hand with this. The central marker turned blue when the hand was correctly aligned. Subjects had to maintain this position for a randomised period of 1-2s. The central marker then disappeared for a fixed gap period of 200ms and the red LED was turned off. Following the gap period, a peripheral target (white circle, 1cm radius) appeared in one of four directions (45°, 135°, 225° or 315° relative to the right horizontal axis, 10cm from the central marker). Subjects were instructed to move to this target as quickly as possible. Once reached, the red LED turned on again, the target disappeared and the central marker reappeared indicating the start of the next trial. Subjects were provided with auditory feedback of task performance, with a high pitch tone indicating that the target was reached in less than 500ms, and a low pitch beep indicating a reaction time of more than 500ms. During the startle condition, SAS (~120dB, 20ms) were delivered at one of the following latencies relative to target appearance: -150ms, -100ms, -75ms, -50ms, 0ms. No startle was delivered during the control condition.

Data analysis

All data analysis was performed off-line using custom software written in MATLAB. EMG recordings were high pass filtered at 30Hz, full-wave rectified and smoothed over a 1ms window.

Only trials that did not meet the following exclusion criteria were included in the analysis. Firstly, trials were deemed anticipatory and excluded if the first 5mm of movement was not in the appropriate 90° arc for that target direction. Secondly, trials were excluded on the basis of reaction time. We did not assess this using the time taken to reach the target since it was common for subjects narrowly to miss the target and then spend considerable time searching for it, often quite ineffectively since they could not see their hand. Instead, for trials that were made in the correct direction, we measured the time taken to reach the target distance (10cm) since this provided a measure of reaction time independent of movement accuracy. Trials in which it took more than 500ms to reach target distance were excluded.

We observed two notable effects in our EMG traces. Firstly, SAS appeared to induce a latency shift (see bottom right panel of Figure 3-2) and so the data have been analysed as a StartReact paradigm. The latency of EMG onset for each muscle was defined as the time point at which EMG activity exceeded a threshold value of three standard deviations above mean baseline EMG activity for at least 20ms. Negative EMG latency values represented an increase in EMG activity during the gap period. Baseline EMG activity for each trial was measured in the 500ms preceding the gap period (i.e. 700 to 200ms before target appearance).

Secondly, the data demonstrated a band of short latency EMG activity (see top left panel of Figure 3-2) which resembled the visual response described by Pruszynski et al. (2010). We refer to this response as the rapid visual response (RVR) and defined it to occur in a window 75-125ms after target appearance since this encompasses the range of values reported in the literature (Pruszynski et al., 2010; Gu et al., 2016; Gu et al., 2018). RVR size was calculated by two methods. Firstly, we measured the area under the curve above baseline EMG between 75 and 125ms, expressed as a percentage of the mean total EMG activity for the control condition (trials without SAS in Experiment 1, the pre-intervention session in Experiment 2); this is subsequently referred to as RVRc. Secondly, we measured the area under the curve above baseline EMG between 75 and

125ms, expressed as a percentage of the mean total EMG activity for the same trial, since this isolated changes in RVR from changes in total EMG activity; this is subsequently referred to as RVRt. Total EMG activity for each trial was calculated as the area under the curve, above baseline EMG, measured from t=0 (peripheral target appearance) until the time at which target distance was reached.

The effect of stimulus and target direction on EMG latency, total EMG activity, RVR size, time to target and time to target distance in Experiment 1 was assessed using two-way repeated measures ANOVAs. The effect of session (pre-intervention, S1-4, post-intervention) and target direction was assessed for the plasticity protocols of Experiment 2. Post-hoc analysis was performed with t-tests. Significance was set at $P<0.05$.

To assess the effect of SAS throughout the time course of each trial, the following analysis was performed for Experiment 1. The mean EMG sweep for each target direction, stimulus and participant was divided into 10ms bins. The binned values for the control condition were subtracted from the binned values for each SAS condition, and this difference expressed as a percentage of the total EMG activity for the control condition (the sum of all bins from t=0 until the mean time taken to reach target distance). The same analysis was performed for the plasticity protocols using the pre-intervention session as the control condition against which each subsequent session was compared.

For all analyses except EMG onset latency in Experiment 1 (see Results), similar trends were observed for deltoid and PM recordings and so although both have been described in the text, only the deltoid analysis has been presented graphically.

Results

In Experiment 1, 75.1% of trials were made in the correct direction and so deemed not to be anticipatory; and in 97.8% of trials target distance was reached in less than 500ms, resulting in a total of 73.5% of trials being included in the analysis. In the control, Startle100 and Startle0 plasticity protocols, respectively, 88.8%, 83.4% and 81.3% trials were made in the correct direction, in 98.3%, 98.1% and 97.5% of trials target distance was reached in less than 500ms, resulting in 87.5%, 82.0%, and 79.9% of trials being included in the analysis.

Experiment 1: EMG latency

We observed a significant effect of SAS on the latency of EMG responses for deltoid (Figure 3-3*A*; F=24.2, P<0.001) and PM (F=5.25, P=0.001). Relative to the control condition, post-hoc analysis showed a significant reduction in EMG onset latency for all SAS latencies recorded in deltoid and all but the -75ms SAS latency recorded in PM. Across all SAS conditions, the mean latency reduction was 28.9 ± 21.7ms for deltoid and 25.7 ± 39.6ms for PM. The latency reduction was not uniform across all SAS conditions but instead demonstrated a negative correlation to SAS latency for deltoid (Figure 3-3*C*; r^2=0.92, P=0.010), with the earliest SAS condition (t=-150ms) evoking the shortest latency EMG response. Importantly, the reduction in EMG latency did not equal the relative SAS latency, i.e. SAS delivered 150ms before target appearance did not reduce EMG latency by 150ms. Instead, the slope of the linear regression (slope=-0.209) suggests an approximate ratio of 5:1 for the relationship between SAS latency and deltoid EMG latency. A similar correlation was not observed in PM recordings (r^2=0.43, P=0.232, slope=-0.083), possibly due to the difficulty we experienced in obtaining good quality EMG recordings from this muscle in females, who constituted half the subjects in Experiment 1.

The effect of SAS on EMG latency was consistent across subjects, with at least 6 out of 8 subjects showing a statistically significant reduction in EMG latency for each SAS condition for deltoid recordings (Figure 3-3*D*). Effects were more variable for PM. There was a significant effect of target direction on EMG latency for PM (F=3.56, P=0.03) but not deltoid (F=2.38, P=0.10).

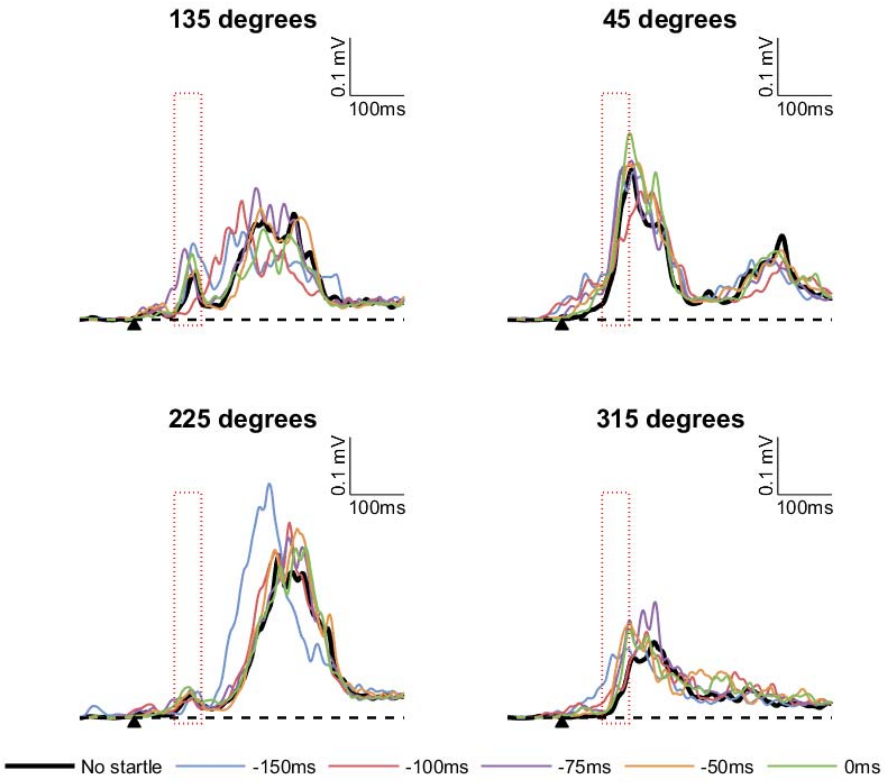

Figure 3-2. Example EMG recordings from a single subject

Mean rectified EMG traces from one subject showing deltoid activity during the choice reaction reaching task for targets appearing in each target directions (individual subplots) for each stimulus conditions (control; SAS at -150ms, -100ms, -75ms, -50ms, 0ms relative to target appearance). The black dotted line shows baseline muscle activity (mean EMG activity for all stimulus conditions measured for 500ms before the gap period). The black arrow indicates target appearance. The red box shows the RVR window (75-125ms).

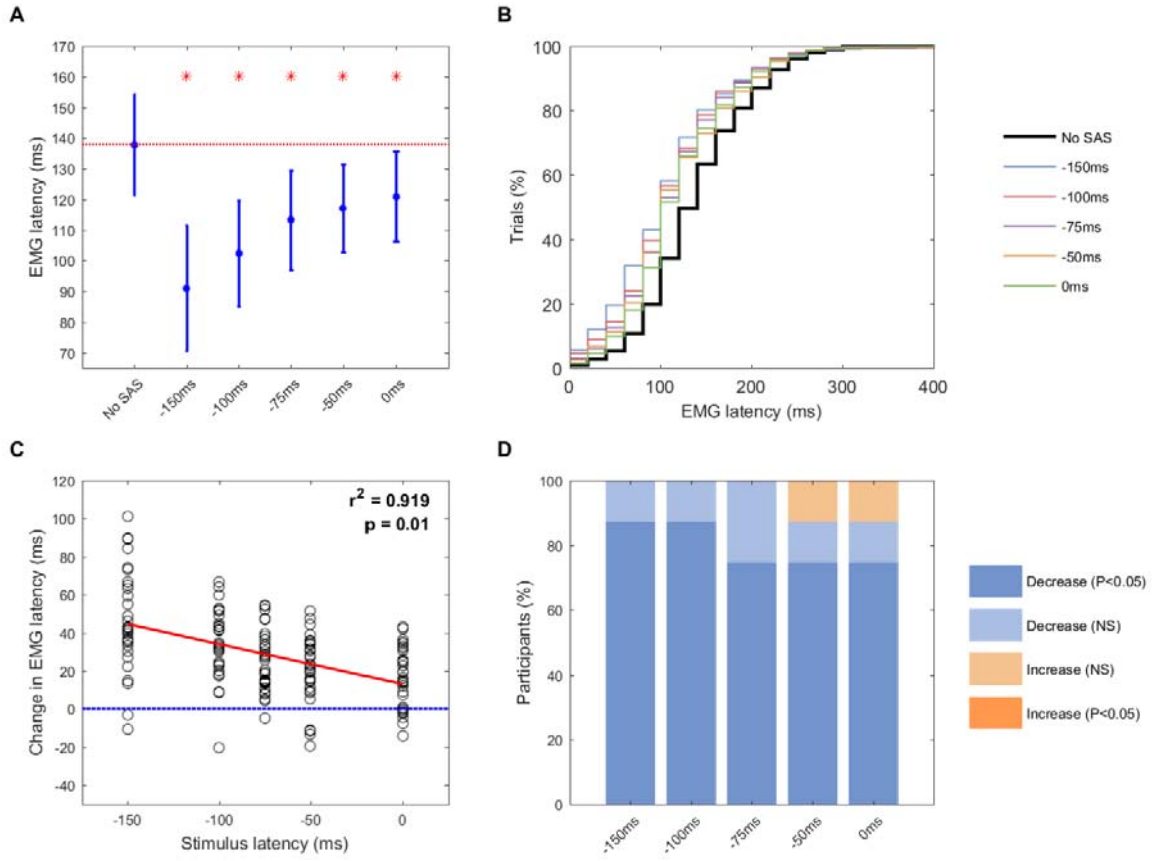

Figure 3-3. Effect of SAS on the onset of muscle activity

Response latency for each muscle was defined per trial as the time point at which EMG activity exceeded a threshold value of three standard deviations above the baseline mean EMG for at least 20ms. ***A.*** Mean EMG latency for deltoid averaged across all participants (n=8) and target directions for each stimulus. Error bars represent standard error. The red dotted line shows the EMG latency for the control condition, and the red asterisks represent a statistically significant (P<0.05) deviation from this for each SAS latency. ***B.*** Mean EMG latency for deltoid averaged across all participants (n=8) and target directions for each stimulus, presented as the cumulative percentage of trials. ***C.*** Correlation of deltoid EMG onset latency against SAS latency. Each point represents the mean change in EMG latency relative to the control condition for each subject and each direction. The red line shows the linear regression line, with the r^2 and p values for this presented on the plot. The blue line represents no change between SAS and control EMG latency. ***D.*** Percentage of participants (n=8) showing a statistically significant change in deltoid EMG latency for each SAS condition compared to the control condition.

Experiment 1: RVR

We measured the size of the EMG response 75-125ms after target appearance to quantify the RVR relative to the total EMG response (see Methods). We found a significant effect of SAS (Figure 3-4*A*; deltoid: F=9.26, P=0.005; PM: F=15.0, P<0.001) and target direction (deltoid: F=5.65, P=0.005; PM: F=3.57, P=0.031) on RVRc size. The general trend of an increase in RVRc size with SAS was observed across all SAS conditions and target directions (Figure 3-4*A*) but post-hoc analysis did not identify a specific SAS latency that was most effective. Similarly, although the majority of subjects showed an increase in RVRc size with SAS, this was only significant in approximately half of subjects with either deltoid (Figure 3-4*B*) or PM recordings.

To examine the RVR in isolation from overall changes in EMG activity, we calculated RVR as a percentage of the total EMG activity of the same trial, rather than the control condition. We found a significant effect of SAS (deltoid: F=4.16, P=0.005; PM: F=14.9, P<0.001) and target direction (deltoid: F=6.19, P=0.004; PM: F=3.51, P=0.033) on RVRt size.

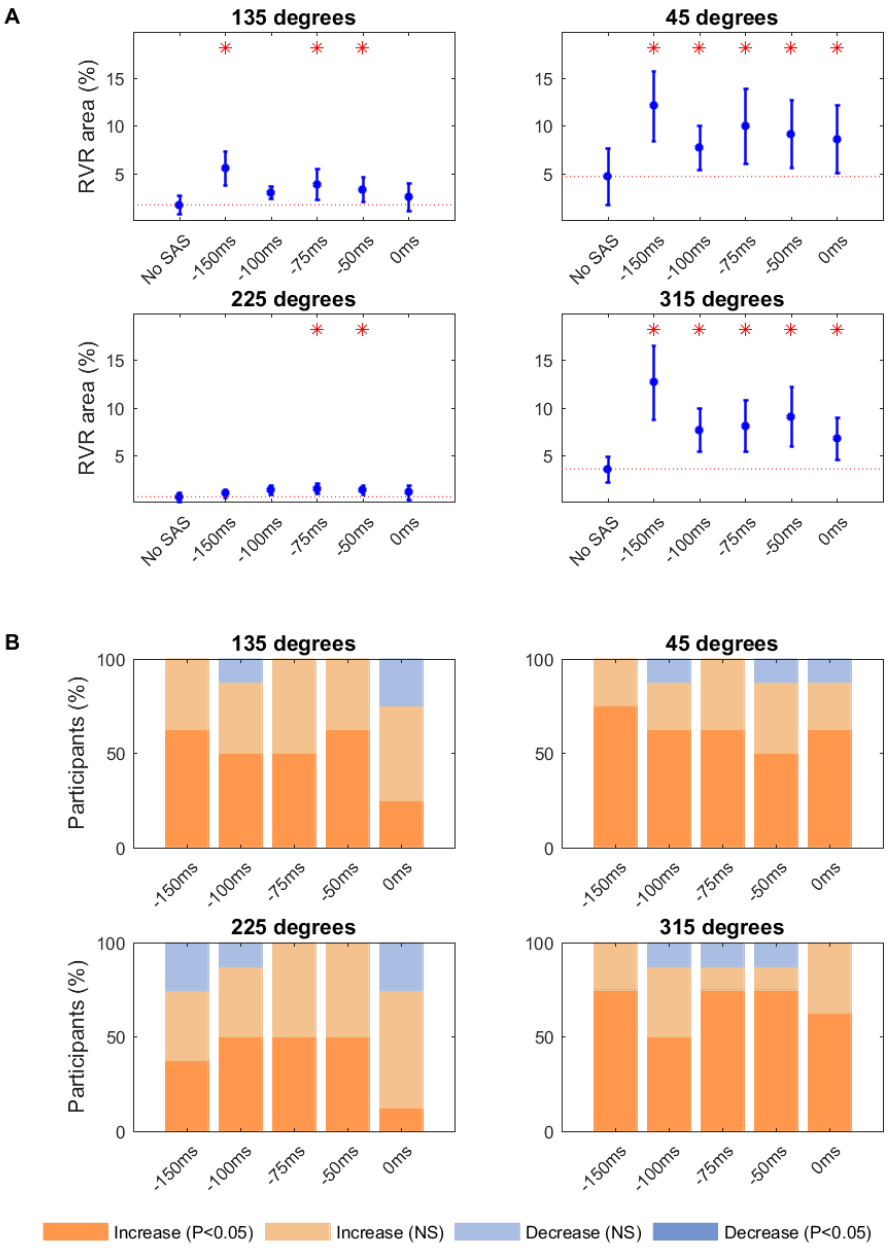

Figure 3-4. Effect of SAS on RVRc magnitude

RVRs were measured as EMG activity above baseline 75-125ms after target appearance, and are expressed as a percentage of the mean total EMG activity for the control trial (EMG activity above baseline from target appearance until target distance reached, see Methods). ***A.*** Mean deltoid RVRc size for all participants (n=8), displayed for each SAS condition and target direction. Error bars represent standard error. The red line shows the control condition RVRc, and red asterisks represent a statistically significant (P<0.05) deviation from this. ***B.*** Percentage of participants showing a statistically significant change in deltoid RVRc size with SAS, displayed for each SAS latency and target direction.

Experiment 1: Total EMG activity

Although the data can be analysed as a RVR or StartReact effect, the overall effect of SAS on EMG activity appears more complex. There was a significant effect of SAS on the total EMG activity generated in each trial (deltoid: F=8.11, P<0.001; PM: F=11.4, P<0.001). Post-hoc analysis showed that all SAS latencies significantly increased total EMG relative to the control condition for both muscles, except the -50ms SAS in deltoid recordings (Figure 3-5*A*). This is particularly interesting given that although SAS did not affect the time taken to reach the target on each trial (Figure 3-7*A*; F=1.701, P=0.159), there was a significant effect on time to reach target distance (Figure 3-7*B*; F=15.8, P<0.001). Post-hoc analysis showed a significant reduction in time to reach target distance for all SAS latencies, thereby reducing the length of the window over which EMG activity was assessed. It should be noted that although the effect of SAS on target performance was consistent across subjects (Figure 3-7*B*), there was considerable inter-subject variability in the total EMG activity produced during each trial, with 0-4 and 2-6 out of 8 subjects showing statistically significant increases in this value for deltoid (Figure 3-5*B*) and PM, respectively. There was no effect of target direction on either total EMG activity (deltoid: F=1.77, P=0.184; PM: F=0.928, P=0.445) or task performance (time to target: F=1.63, P=0.213; time to target distance: F=1.54, P=0.234).

Comparison of each 10ms window of a trial with SAS to the control condition showed that SAS facilitated the response across at least the first 200ms (Figure 3-6). In the case of 135 and 225° targets for deltoid (Figure 3-6), and 45° and 315° targets for PM, SAS increased the EMG activity for all except the final stages of the trial.

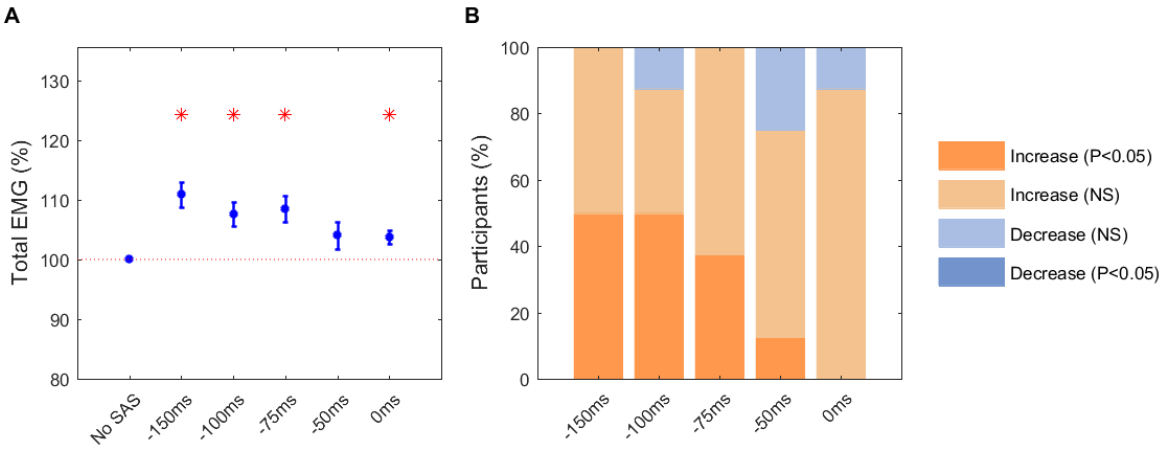

Figure 3-5. Effect of SAS on total EMG activity

Total EMG activity for each trial was measured as EMG activity above baseline from target appearance until target distance reached (see Methods), and expressed as a percentage of total EMG activity for the control condition. ***A.*** Mean total deltoid response for all participants (n=8) and target directions, for each SAS condition. Error bars represent standard error. The red line shows the total EMG activity for the control condition, and red asterisks represent a statistically significant (P<0.05) deviation from this. ***B.*** Percentage of participants showing a statistically significant change in total deltoid EMG with SAS, averaged across target directions and displayed for each SAS latency.

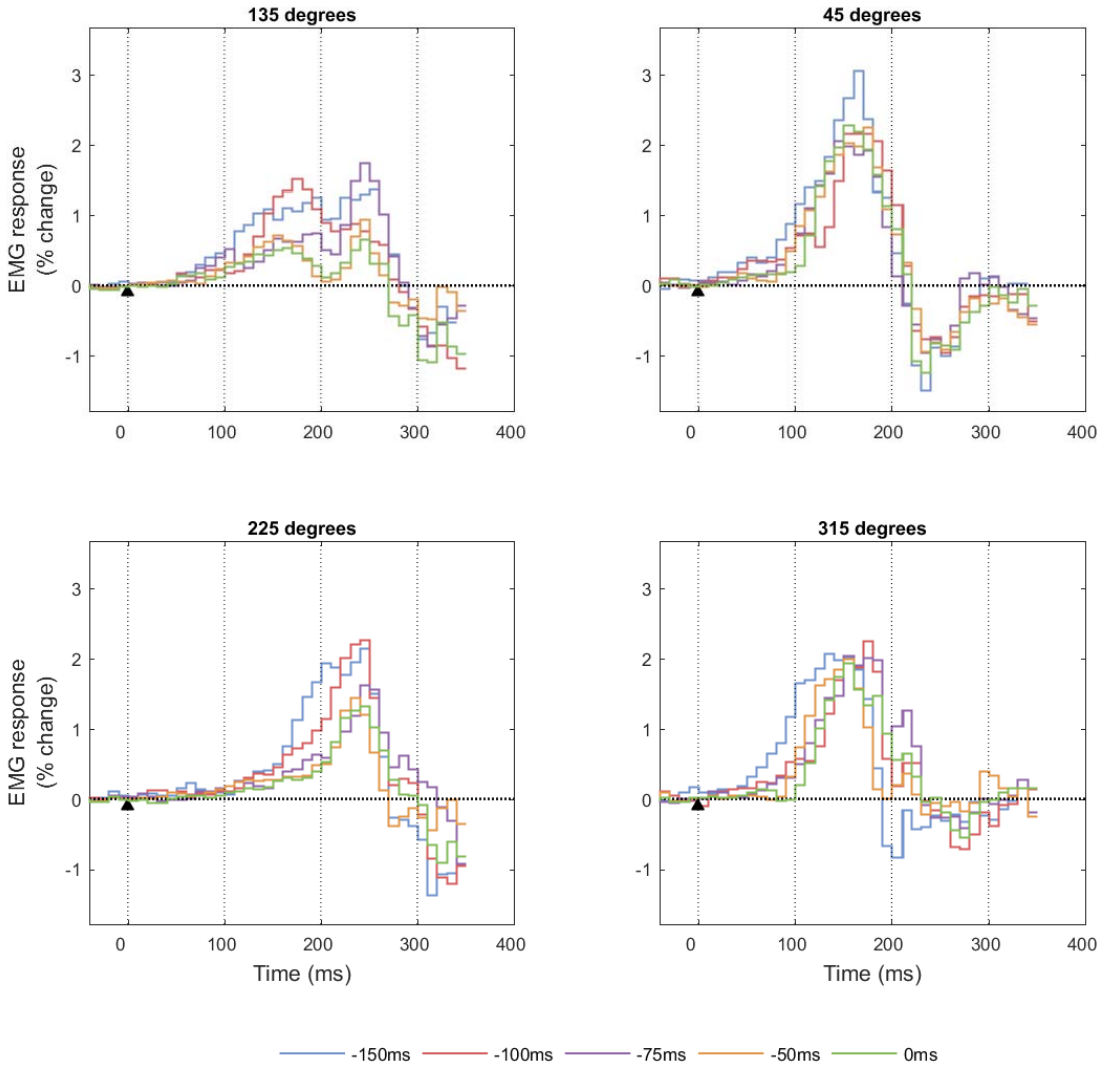

Figure 3-6. Effect of SAS throughout the time course of each trial

Deltoid EMG activity during SAS trials was compared to the control condition by dividing the mean EMG sweeps for each target direction and stimulus latency into 10ms bins, subtracting the equivalent values for the control condition from these and expressing this difference as a percentage of the total EMG activity for the control condition (the sum of all the bins up until the mean time taken to reach target distance). Percentage change values, averaged across all subjects (n=8) are presented for each target direction and SAS latency. The black arrow indicates target appearance, the horizontal black dotted line shows no change compared to the control condition, and the vertical black dotted lines show 100ms intervals. The traces are truncated at the mean trial duration (time taken to reach target distance).

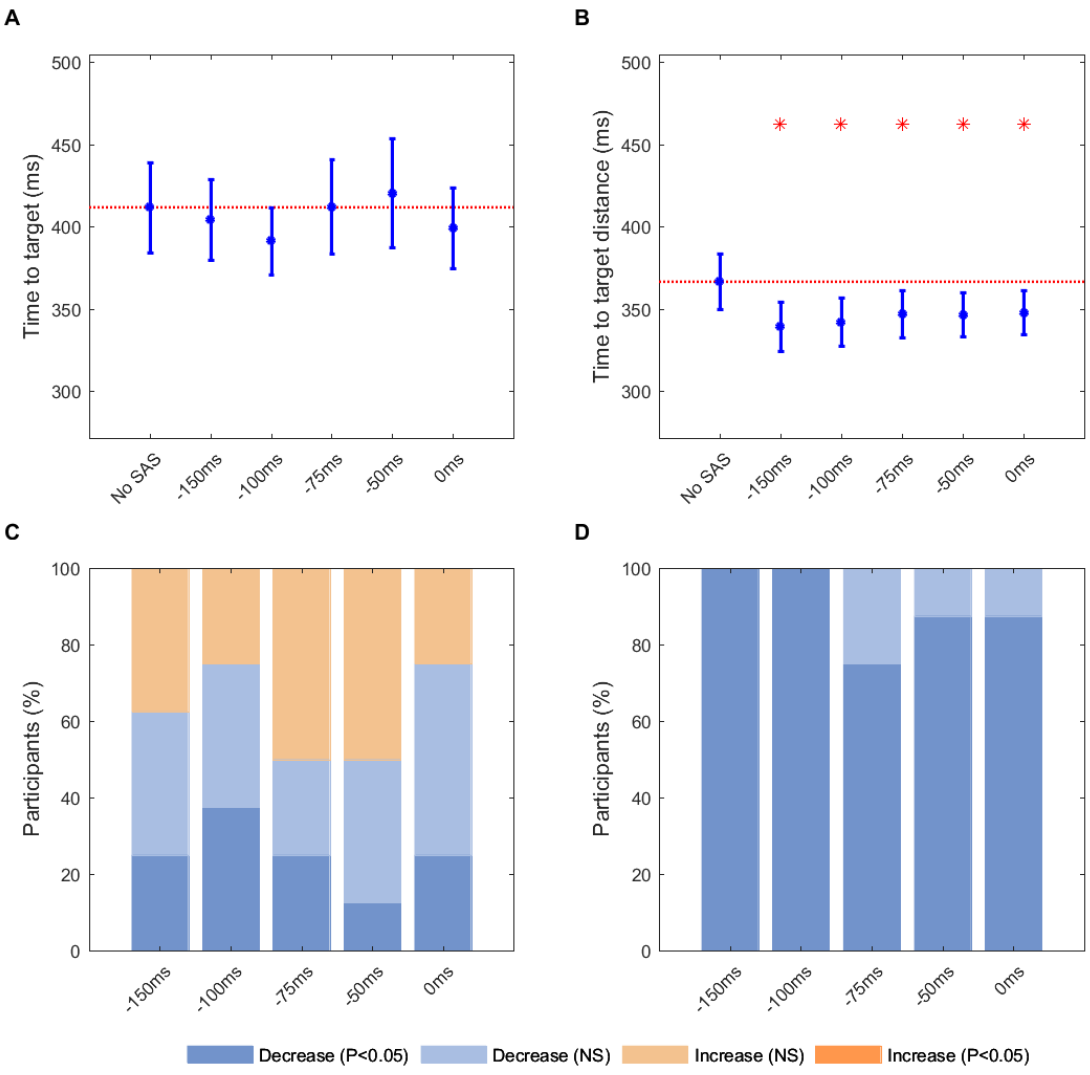

Figure 3-7. Effect of SAS on task performance

Task performance was assessed by measurement of time to reach target (***A,C***) and time to reach target distance (***B,D;*** see Methods). ***A,B.*** Mean values for all participants (n=8) and target directions relative to the control condition (red dotted line), with red asterisks representing a statistically significant (P<0.05) deviation from this. Error bars represent standard error. ***C,D.*** Percentage of participants showing a statistically significant change in reaction time with SAS, displayed for each SAS latency.

Experiment 2: EMG latency

In the plasticity experiments, a significant effect of session number on EMG latency was observed for both SAS protocols but not the control protocol (Figure 3-8*A*; Control deltoid: F=1.38, P=0.245; Control PM: F=2.35, P=0.050; Startle100 deltoid: F=8.56, P<0.001; Startle100 PM: F=4.98, P<0.001; Startle0 deltoid: F=14.0, P<0.001; Startle0 PM: F=9.50, P<0.001). Post-hoc analysis showed that only in the Startle0 condition was there a significant reduction in EMG latency from the pre- to post-intervention session. This was observed in both muscles and was statistically significant in 8 and 7 out of 15 subjects for deltoid and PM recordings, respectively.

In contrast to the results of Experiment 1, target direction had a significant effect on EMG latency for all protocols (Control deltoid: F=57.4, P<0.001; Control PM: F=49.2, P<0.001; Startle100 deltoid: F=41.6, P<0.001; Startle100 PM: F=40.6, P<0.001; Startle0 deltoid: F=40.8, P<0.001; Startle0 PM: F=84.5, P<0.001).

Experiment 2: RVR

There was a significant effect of session on RVRc size for all deltoid recordings (Figure 3-9*A*; Control: F=3.53, P=0.007; Startle100: F=5.60, P<0.001; Startle0: F=8.68, P<0.001) and all except the control protocol for PM recordings (Control: F=1.62, P=0.168; Startle100: F=5.30, P<0.001; Startle0: F=2.83, P=0.022). Only the Startle0 protocol generated a statistically significant difference in RVRc size between the pre- and post-intervention sessions, with this being observed in both deltoid and PM recordings. Although the trend of the Startle0 intervention increasing RVR size was present in the majority of subjects, it was significant in less than half of subjects in either muscle (deltoid: Figure 3-9*B*). Similarly to Experiment 1, there was a significant effect of target direction on RVRc size for all plasticity protocols (Control deltoid: F=10.6, P<0.001; Control PM: F=12.2, P<0.001; Startle100 deltoid: F=6.26, P=0.001; Startle100 PM: F=4.70, P=0.007; Startle0 deltoid: F=17.2, P<0.001; Startle0 PM: F=15.4, P<0.001).

To isolate changes in RVR from changes in total EMG activity, we also measured RVR size as a percentage of the total EMG activity for the same trial (RVRt). This method demonstrated a significant effect of session on RVRt size for deltoid (Control: F=2.95, P=0.019; Startle100: F=2.90, P=0.020; Startle0: F=3.34, P=0.009) but not PM recordings (Control: F=0.47, P=0.794;

Startle100: F=0.81, P=0.559; Startle0: F=0.29, P=0.919). Significant increases in RVRt size between the pre- and post-intervention sessions were observed in three target directions with the Startle0 protocol (45°, 135°, 225°) and one target direction with the control protocol (315°). No significant changes in RVRt size were observed been the pre- and post-intervention sessions with PM recordings.

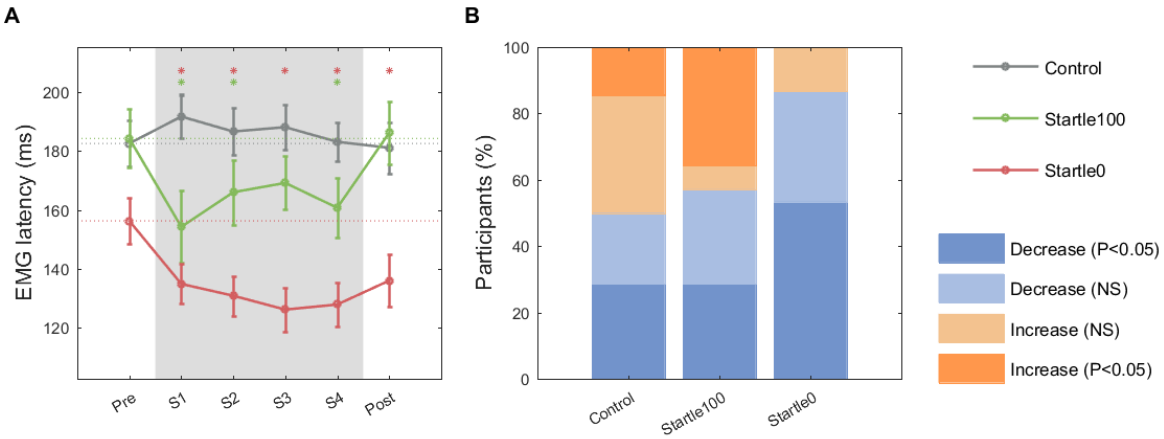

Figure 3-8. Effect of plasticity protocol on onset of muscle activity

Response latency for each muscle was defined per trial as the time point at which EMG activity exceeded a threshold value of three standard deviations above the baseline mean EMG for at least 20ms. ***A.*** Mean EMG latency for deltoid averaged across all participants (Control: n=14; Startle100: n=14; Startle0: n=15) and target directions for each plasticity intervention (Control: no SAS; Startle100: SAS 100ms before target appearance; Startle0: SAS with target appearance). Error bars represent standard error. S1-S4 are the four intervention sessions (see Methods). The dotted lines show the EMG latency in the pre-intervention session, and the asterisks represent a statistically significant (P<0.05) deviation from this during or after each intervention. ***B.*** Percentage of participants (Control: n=14; Startle100: n=14; Startle0: n=15) showing statistically significant changes in deltoid EMG latency between the pre- and post-intervention sessions.

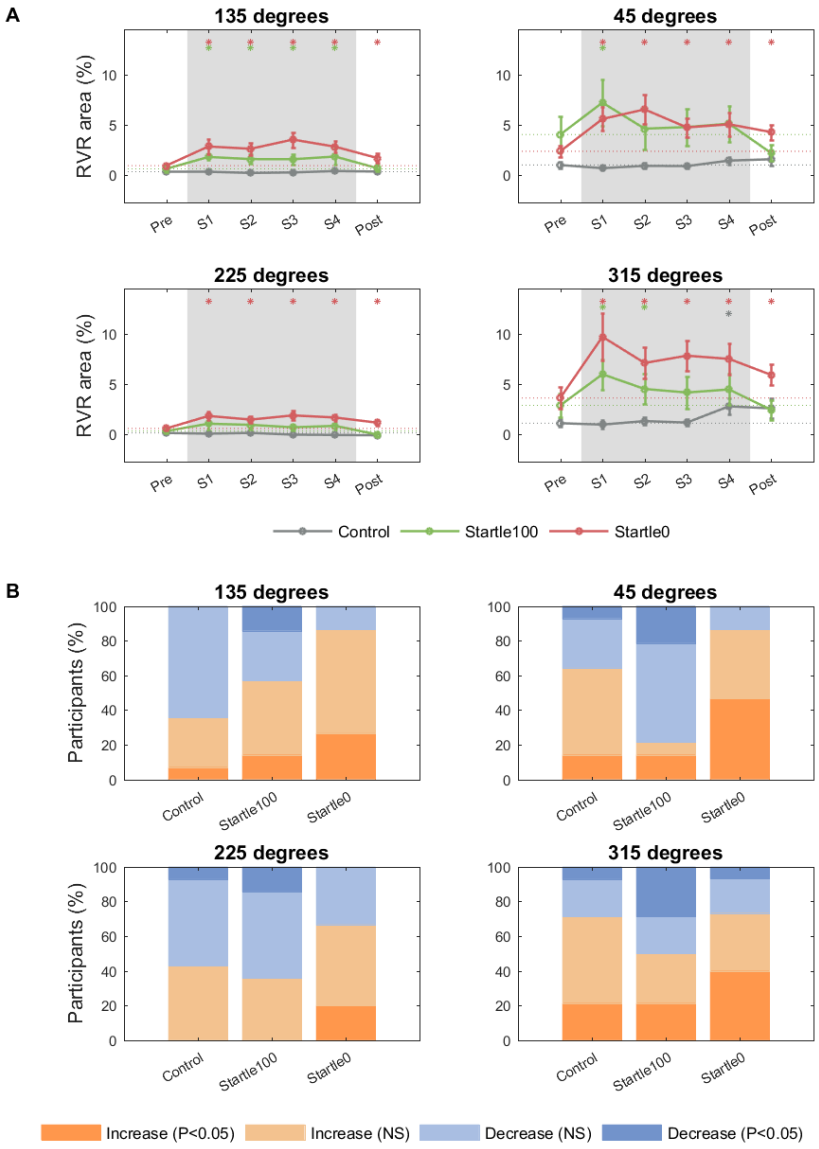

Figure 3-9. Effect of plasticity protocol on RVR magnitude

RVRs were measured as EMG activity above baseline 75-125ms after target appearance, and are expressed as a percentage of the mean total EMG activity for the pre-intervention session (EMG activity above baseline from target appearance until target distance reached, see Methods). ***A.*** Mean deltoid RVRc size for all participants (Control: n=14; Startle100: n=14; Startle0: n=15), for each plasticity intervention (Control: no SAS; Startle100: SAS 100ms before target appearance; Startle0: SAS with target appearance), displayed for each target direction. Error bars represent standard error. The dotted lines show the RVRc size before the intervention, and asterisks represent a statistically significant (P<0.05) deviation from this during or after the intervention. ***B.*** Percentage of participants (Control: n=14; Startle100: n=14; Startle0: n=15) showing a statistically significant change in deltoid RVRc size between the pre- and post-intervention sessions.

Experiment 2: Total EMG activity

Similarly to Experiment 1, there was no effect of target direction on total EMG activity (Control deltoid: F=1.16, P=0.335; Control PM: F=1.06, P=0.379; Startle100 deltoid: F=0.41, P=0.745; Startle100 PM: F=1.08, P=0.368; Startle0 deltoid: F=0.63, P=0.602; Startle0 PM: F=1.14, P=0.341). The effect of session was more varied, with only the Startle100 protocol having a significant effect on total deltoid EMG activity (Figure 3-10*A*; Control: F=0.85, P=0.516; Startle100: F=7.43, P<0.001; Startle0: F=1.74, P=0.138), whilst both Startle0 and Startle100 had a significant effect on total PM EMG activity (Control: F=1.17, P=0.335; Startle100: F=3.57, P=0.007; Startle0: F=4.42, P=0.002). The only significant change in total EMG activity between the pre- and post-intervention sessions was a decrease in deltoid activity with the Startle100 protocol (Figure 3-10*A*) and an increase in PM activity with the Startle0 protocol. Although the former effect was significant in 9 out of 14 subjects (Figure 3-10*B*), the latter was significant in only 7 out of 15 subjects.

In contrast to Experiment 1, there was a significant effect of target direction on task performance for all protocols (Control time to target: F=4.44, P=0.009; Startle100 time to target: F=3.49, P=0.025; Startle0 time to target: F=10.4, P<0.001; Control time to target distance: F=9.01, P<0.001; Startle0 time to target distance: F=4.14, P=0.012; Startle100 time to target distance: F=4.43, P=0.009). Similarly, there was a significant effect of session on task performance for all protocols except the time to target distance recorded with the control protocol (Figure 3-12 *A*,*B*; Control time to target: F=2.94, P=0.019; Startle100 time to target: F=2.60, P=0.033; Startle0 time to target: F=5.41, P<0.001; Control time to target distance: F=2.04, P=0.085; Startle0 time to target distance: F=6.00, P<0.001; Startle100 time to target distance: F=5.37, P<0.001). Only with the Startle0 protocol was the reduction in time to target and time to target distance significant between the pre- and post-intervention sessions (Figure 3-12*A*,*B*); this effect was observed in over 60% of subjects (Figure 3-12*C*,*D*).

Figure 3-12 shows the size of the EMG response for each session relative to the pre-intervention session in 10ms intervals for each plasticity protocol. Note that even with the control protocol there was a change in EMG activity over the sessions but only with the Startle0 protocol did this amount to a clear facilitation during that intervention that persisted in the post-intervention session.

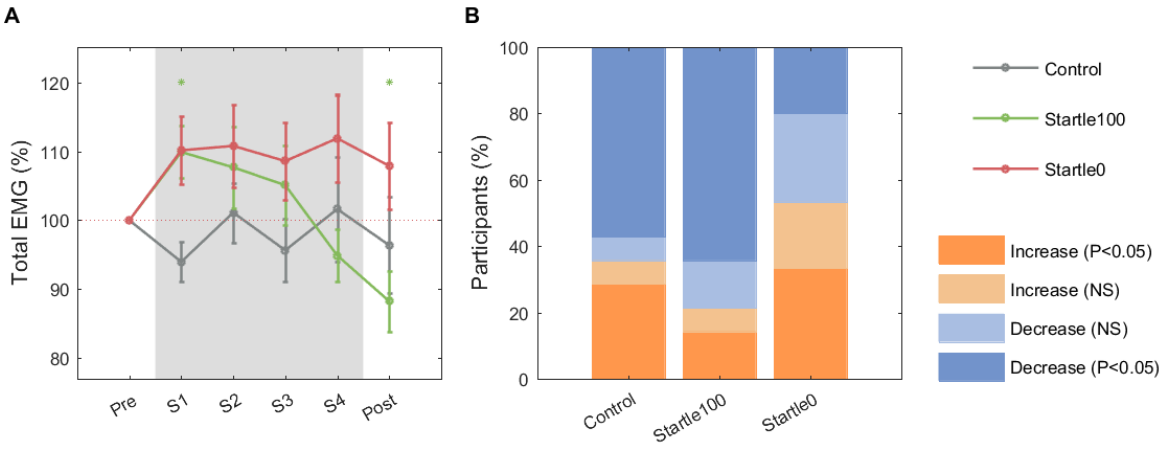

Figure 3-10. Effect of plasticity protocol on total EMG activity

Total EMG activity for each trial was measured as EMG activity above baseline from target appearance until target distance reached (see Methods), and expressed as a percentage of total EMG activity for each trial, measured during the pre-intervention session. ***A.*** Mean total deltoid response for all participants (Control: n=14; Startle100: n=14; Startle0: n=15) and target directions, for each plasticity intervention (Control: no SAS; Startle100: SAS 100ms before target appearance; Startle0: SAS with target appearance). Error bars represent standard error. The dotted lines show the total EMG activity in the pre-intervention session, and asterisks represent a statistically significant (P<0.05) deviation from this during or after intervention. ***B.*** Percentage of participants (Control: n=14; Startle100: n=14; Startle0: n=15) showing a statistically significant change in total deltoid EMG between the pre- and post-intervention sessions.

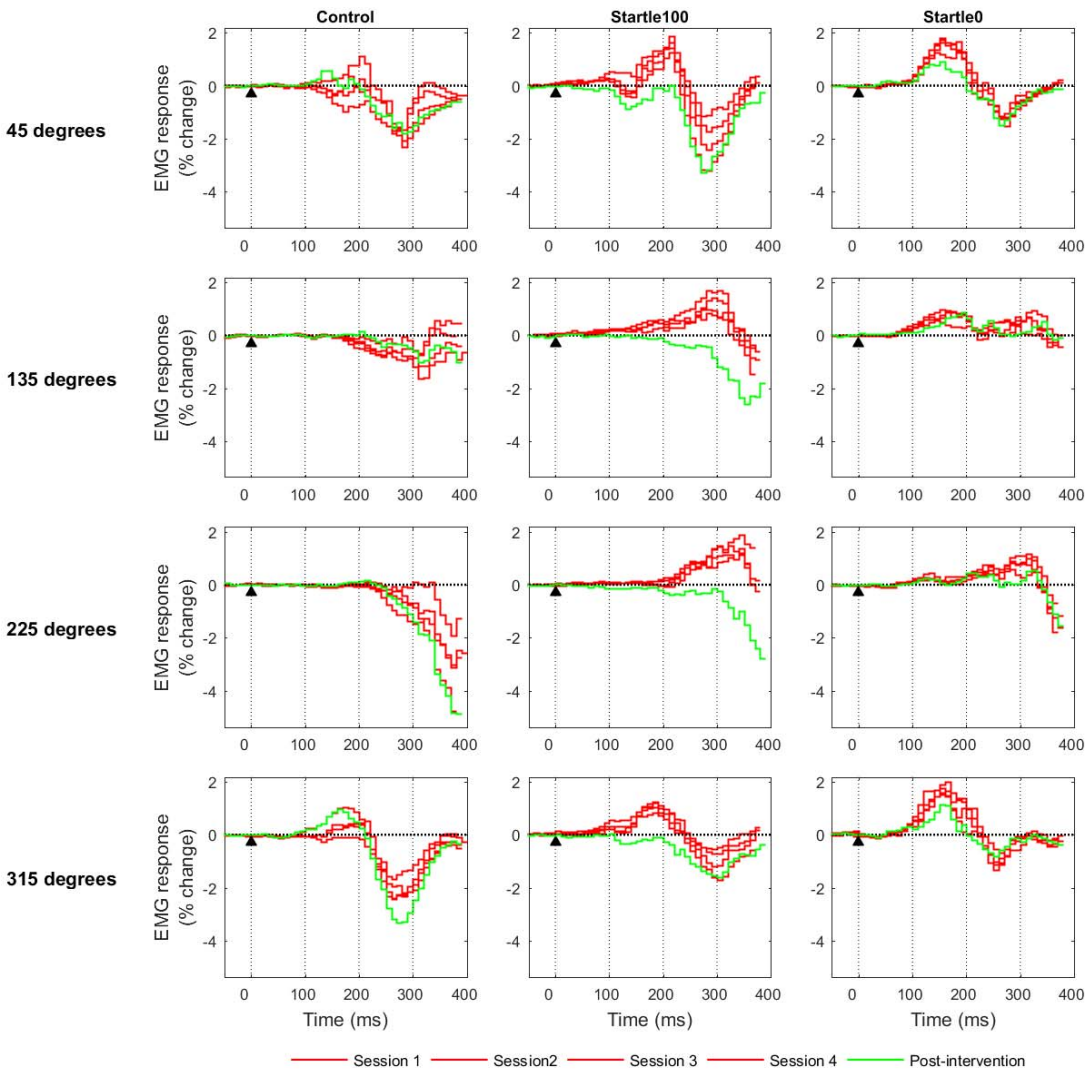

Figure 3-11. Effect of plasticity protocols throughout the time course of each trial

Changes in deltoid EMG activity during and after each intervention (Control: no SAS; Startle100: SAS 100ms before target appearance; Startle0: SAS with target appearance) were calculated as followed. The mean EMG sweep for each target direction, block and participant was divided into 10ms bins. The binned values in the pre-intervention session were subtracted from the binned values during or after the intervention. This difference was expressed as a percentage of the total EMG activity for the pre-intervention (the sum of all the bins until the mean time taken to reach target distance). Percentage change values, averaged across all subjects (Control: n=14; Startle100: n=14; Startle0: n=15), are presented for each target direction and intervention. The black arrow indicates target appearance, the horizontal black dotted line shows no change compared to the pre-intervention session, and the vertical black dotted lines show 100ms intervals. The traces are shown for the mean trial duration (time taken to reach target distance).

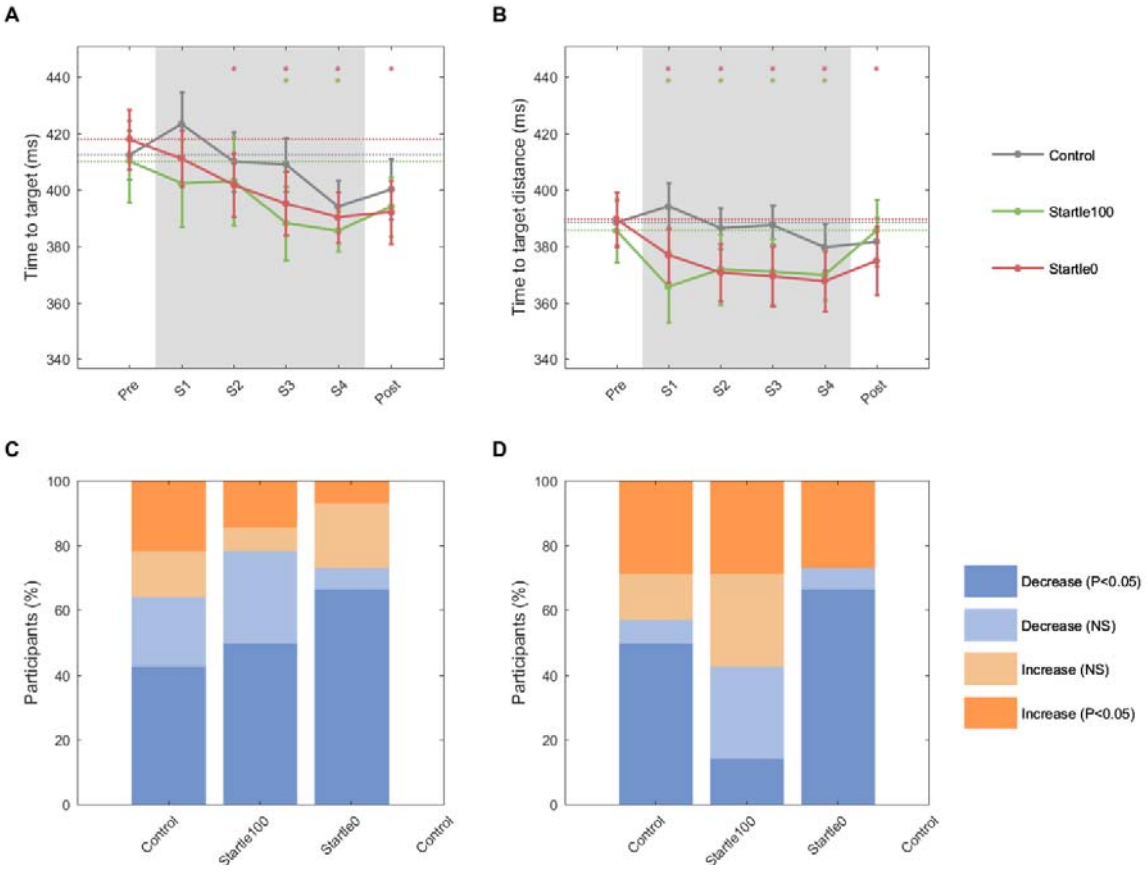

Figure 3-12. Effect of plasticity protocols on task performance

Task performance was assessed by measurement of time to reach target (***A,C***) and time to reach target distance (***B,D***; see Methods). ***A,B.*** Mean values for all participants (Control: n=14; Startle100: n=14; Startle0: n=15) and target directions for each intervention (Control: no SAS; Startle100: SAS 100ms before target appearance; Startle0: SAS with target appearance). Dotted lines show the values recorded during the pre-intervention session, with asterisks showing a statistically significant (P<0.05) deviation from this. Error bars represent standard error. ***C,D.*** Percentage of participants (Control: n=14; Startle100: n=14; Startle0: n=15) showing a statistically significant change in reaction time between the pre- and post-intervention sessions.

Discussion

In this study we paired SAS with visually-evoked fast reaching movements to show that a range of SAS latencies can facilitate the first 75-125ms of responses and reduce the onset latency of activity in two shoulder muscles. Furthermore, our results show that repeated pairing of SAS with the appearance of the visual stimulus can induce plastic changes in both of these outcome measures. These results can be considered in the context of StartReact, stimulus-locked short-latency responses, which we refer to as rapid visual responses (RVRs), or as part of a more integrated approach encompassing several ideas about reticulospinal pathways.

StartReact

StartReact is the phenomenon whereby SAS, typically delivered as a "go" cue, can drastically reduce voluntary reaction times (Valls-Sole et al., 1999). Our results show such an effect with the majority of SAS conditions significantly reducing the latency of EMG onset in deltoid and PM. Furthermore, repeated delivery of SAS synchronously with the appearance of the visual target (Startle0) induced a plasticity effect in which EMG responses continued to appear at a reduced latency in the absence of further auditory stimuli. Although we did not record the sternocleidomastoid response, a measure often used to demonstrate an overt startle response (Carlsen et al., 2011), Reynolds and Day (2007) showed that the latency shift associated with SAS can be observed in a choice reaction task in the absence of a startle reflex.

Rapid visual reactions

Originally described by Pruszynski et al. (2010), RVRs are short-latency, stimulus-locked responses evoked during reaching movements to visual targets and are proposed to be mediated by a tecto-reticulospinal pathway. This hypothesis originates from primate data showing that cells in the superior colliculus and RF fire during proximal arm movements (Werner, 1993; Stuphorn et al., 1999), as well as the recent observation that arm movements can be evoked by electrical stimulation of these regions (Philipp and Hoffmann, 2014). Our results support a reticulospinal involvement by demonstrating that RVRs can be facilitated by SAS (Figure 3-4), and that this facilitation persists when responses are normalised to the total EMG response, suggesting that it is independent of the general increase in EMG activity we observed with SAS. Similarly to the

StartReact effect, we were able to induce plasticity in RVRs through repeated pairing of SAS with the appearance of the visual target.

We propose that the increase in short-latency EMG activity observed is not simply a consequence of StartReact reducing response latency and thereby increasing the proportion of the response that appears within our 75-125ms window for several reasons. Firstly, visual inspection of the data reveals a short-latency component of the response that qualitatively appears to increase in size rather than shift in latency (see top left panel of Figure 3-2). Secondly, in accordance with previous reports (Pruszynski et al., 2010), we found this short-latency window of EMG activity to be spatially tuned, whereas there was no effect of target direction on EMG onset latency recorded from deltoid. Finally, it is important to note that we do not claim to have captured the RVR either exclusively or in its entirety with the chosen 75-125ms window. However, by encompassing the latencies reported in the literature (Pruszynski et al., 2010; Gu et al., 2016; Gu et al., 2018), we aimed to provide a comparable measure and to isolate a region of the EMG response that is likely to be largely devoid of cortical input. Nonetheless, given that both the latency reduction and RVRs are proposed to act via the RF, it is likely that these two effects are not entirely separable and perhaps it is debatable whether this distinction is important if the conclusion can be drawn that both measures imply an increase in reticulospinal output.

An integrated approach

Valls-Sole et al. (1999) proposed that the latency shift observed with StartReact may relate to storage of pre-planned movements in brainstem or spinal structures, with SAS triggering their release. An important feature of StartReact is therefore that the required movement is known in advance such that it can be prepared and stored, this is supported by studies showing the absence of a latency reduction in choice reaction tasks (Carlsen et al., 2004b). However, modest reductions in EMG onset latency have been reported with SAS in a choice reaction task in which subjects made stepping movements towards visual targets that shifted position mid-step (Reynolds and Day, 2007). The authors propose that this choice reaction task is theoretically distinct from the simple reaction tasks that have dominated the StartReact literature since it is not possible for subjects to predict the upcoming movement and thus store an appropriate blueprint. Instead, they suggest that the reduction in reaction time, which at 18-31ms is modest compared to the ~100ms

values reported by Valls-Solé et al. (1995), represents a reduction in visuo-motor processing time, which could possibly occur through an interaction of visual and auditory stimuli at the caudal pontine RF (Reynolds and Day, 2007).

Although the task described by Reynolds and Day (2007) constitutes a lower-limb perturbation protocol, it shows many similarities to the choice reaction upper-limb reaching task used in our study. For example, they report reaction times of around 100ms in the absence of SAS, a similar finding to the 100-150ms reaction times reported with upper-limb perturbation (Carlton, 1981; Soechting and Lacquaniti, 1983; Day and Lyon, 2000), as well as the 75-100ms response latency reported by Pruszynski et al. (2010). We recorded mean reaction times of 135.5ms and 128.7ms for deltoid and PM, respectively, in trials without the SAS stimulus. These values are all considerably lower than typical reaction times for visual stimuli, which have been reported to be around 180ms (Brebner and Welford, 1980), and so may reflect a subcortical involvement, as has been demonstrated for reaching movements (Day and Brown, 2001). Furthermore, Reynolds and Day (2007) argue that the nature of their task, in which movements were made in the same reference frame as the visual stimuli, crucially differs from classical StartReact protocols (e.g. Carlsen et al., 2004b) in which the visual target and reaching endpoint are spatially separated. They propose that the transformation of arbitrary visual stimuli into appropriate movement likely requires considerable cortical processing, whereas more natural movements may not have the same cortical dependence. This sentiment has been echoed by Perfiliev et al. (2010), who showed that reaching movements towards physical target have reaction times in the range of 90-110ms and suggest that in a natural environment, reaching movements may be controlled reflexively. Given the demonstration that microstimulation of the superior colliculus can evoke reaching-like arm movements (Philipp and Hoffmann, 2014), the tecto-reticulospinal pathway is one possible candidate that could mediate such reflexes. Although our task did not involve physical stimuli, the projection of visual targets into the plane of movement, similarly to Reynolds and Day (2007), may have reduced the requirement for cortical processing and therefore evoked reflexive reaching likely to involve subcortical pathways and largely bypass the cortex, at least in their initial stages.

Further evidence that our task evoked reticulospinal responses comes from examination of the strength of contractions produced. In classical StartReact studies, the pattern of EMG activity generated is unaltered except for its onset latency (Valls-Sole et al., 1999; Carlsen et al., 2004a;

Dean and Baker, 2017). However, in accordance with our results (Figure 3-5), there are several reports of SAS facilitating EMG responses (Siegmund et al., 2001; Carlsen et al., 2003; Kumru et al., 2006; Kumru and Valls-Sole, 2006). Given that auditory stimuli have been shown to excite reticular neurons (Irvine and Jackson, 1983; Fisher et al., 2012), and the number of neurons recruited is positively correlated with stimulus intensity (Yeomans and Frankland, 1995), Carlsen et al. (2003) proposed that this increase in EMG activity with SAS may represent facilitation of a reticulospinal contribution to the movement. In turn, this reticulospinal activity is likely to increase motoneuron excitability, thereby increasing the efficacy of the later descending corticospinal commands. This hypothesis matches with our proposal that in addition to facilitating the early component of responses, SAS affects the full time course of each trial, perhaps through an initial reticulospinal input which primes the system for subsequent corticospinal modulation. It is also possible that SAS affects the corticospinal response via ascending projections from the RF to the cortex (see Carlsen et al., 2012).

We observed relatively consistent results with SAS delivered up to 150ms prior to visual target appearance. Simple reaction tasks have shown that SAS delivered up to 1.4s before the “go” cue can reduce reaction times, although on a trial by trial basis, early stimuli were less likely to evoke a latency shift (MacKinnon et al., 2007). This effect may reflect the progressive preparation of movement in anticipation of an imperative stimulus (MacKinnon et al., 2007). However, as discussed above, it is unlikely that specific movements were prepared in our choice reaction task. Instead, the efficacy of the different SAS latencies used in our experiment could suggests that SAS produces relatively long-lasting changes in reticular excitability. This is supported by RF recordings in primates which show that even under deep anaesthesia, reticular neurons can continue to fire for up to 25ms after a (non-startling) auditory stimulus (Fisher et al., 2012). However, our data show a general trend of the earliest latency SAS (t=-150ms) having the greatest effect on response latency and RVR size, suggesting that SAS are not simply increasing reticular excitability for a fixed period but instead may somehow be non-specifically preparing the system for movement.

Reticulospinal plasticity

It is well established that pairing of inputs can induce plasticity in the corticospinal tract (Stefan et al., 2000). However, until recently, such effects were unexplored in reticulospinal pathways. Foysal et al. (2016) provided the first demonstration that the long-latency stretch reflex (LLSR) can be modulated by paired delivery of auditory clicks and electrical stimulation of the biceps. Given the evidence supporting a reticular involvement in the LLSR (Soteropoulos et al., 2012; Kurtzer, 2014), this study may reflect the induction of plasticity in reticulospinal pathways. On this basis we paired SAS with the appearance of the visual target over 640 trials and observed that enduring changes in RVR size and EMG onset latency could be induced. This was not simply a training effect since a control protocol in which no SAS was delivered did not evoke the same effects. Furthermore, in contrast to our facilitation findings, the latency was important, with simultaneous SAS and visual target appearance inducing plasticity whilst SAS delivered 100ms prior to visual target appearance had no such effect.

Summary

In conclusion, we have used a choice reaction reaching task to show that loud auditory stimuli delivered across a range of latencies can significantly reduce reaction times in proximal muscles and facilitate short-latency responses. We propose that this reflects modulation of reticulospinal excitability. Furthermore, we have shown that repeated pairing of SAS with the presentation of the visual target can induce plasticity in these outcome measures, which may reflect enduring changes in the excitability of reticulospinal pathways. Given the wealth of sensory information received by the RF, it is possible that this structure acts as a site of multisensory integration and thus that appropriate pairing of inputs may provide a means of modulating its output. In the context of accumulating evidence supporting a role of the RST in functional recovery after corticospinal lesions (Dewald et al., 1995; Baker, 2011; Zaaimi et al., 2012), we tentatively suggest that the ability to influence reticulospinal excitability non-invasively with such techniques may be of clinical significance.

CHAPTER IV

Cortical, corticospinal and reticulospinal contributions to strength training

The experiments described in this chapter were supported by Norman Charlton, who designed and manufactured the apparatus for the behavioural task, and designed the headpieces; Terri Jackson, who undertook the initial behavioural training of the monkeys, assisted in the training sessions throughout the study and managed post-operative care; and Stuart Baker who performed the surgeries, contributed to the experimental design and set up the spinal recordings. I trained the monkeys on the task, manufactured the EMG implants and cortical electrodes, assisted in the surgeries, ran the recording sessions, recorded the spinal data and performed all data analyses.

Introduction

It is well established that the initial stages of strength training are dominated by neural adaptations rather than intramuscular mechanisms (Moritani and deVries, 1979; Sale, 1988; Folland and Williams, 2007). There are several arguments supporting this, including the absence of hypertrophy in the first few weeks of a strength training programme (Komi, 1986; Jones and Rutherford, 1987; Akima et al., 1999), and the effect of cross-education in which unilateral training elicits bilateral gains (Enoka, 1988; Zhou, 2000; Lee and Carroll, 2007).

Over the last few decades, attempts have been made to characterise the neural adaptations associated with strength training by examining elements of the corticospinal tract (CST), the dominant descending pathway in primates (Lemon, 2008). A recent meta-analysis proposed that strength training is characterised by changes in intracortical and corticospinal inhibitory networks, rather than corticospinal excitability (Kidgell et al., 2017). Adaptations may also occur at the level of the motoneuron, although there are technical limitations associated with these studies (Carroll et al., 2011).

An alternative pathway in primate motor control has been overlooked in the strength training literature. Increasing evidence suggests that the reticulospinal tract (RST) plays an important role in upper limb function in primates (Baker, 2011). In addition to its established role in postural control (Prentice and Drew, 2001; Schepens and Drew, 2004b, 2006a), the RST has been shown to project to motoneurons innervating both distal and proximal muscles (Davidson and Buford, 2004; Davidson and Buford, 2006; Riddle et al., 2009), and contributes to motor control throughout the upper limb, including hand function in humans (Carlsen et al., 2009; Honeycutt et al., 2013; Dean and Baker, 2017) and non-human primates (Soteropoulos et al., 2012). We therefore propose that reticulospinal pathways may contribute to strength training.

In support of this hypothesis, Lawrence and Kuypers (1968b) reported an increase in strength 4-6 weeks after bilateral pyramidal tract lesions in monkeys suggesting that strength adaptations can be achieved in the absence of the CST. Similarly, the human literature suggests that the RST may mediate recovery of strength after stroke (Xu et al., 2017). Given the adaptive changes that occur in the RST after corticospinal lesions (Zaaimi et al., 2012), reticulospinal pathways are a likely candidate in mediating strength adaptations.

The aim of this study was to compare the relative contributions of intracortical, corticospinal and reticulospinal networks to the neural adaptations associated with strength training. We undertook two sets of experiments in rhesus macaques that were trained to perform a weight lifting task. Firstly, we measured motor-evoked potentials (MEPs) in response to M1, pyramidal tract (PT) and medial longitudinal fasciculus (MLF) stimulation to assess adaptations in the cortex, CST and RST, respectively. Secondly, after completion of the strength training protocol, we measured spinal field potentials elicited with PT and reticular formation (RF) stimulation to assess spinal adaptations. To our knowledge, this is the first attempt to perform a strength training study in non-human primates and to investigate specifically strength-induced changes in reticulospinal function. Our results suggest that both intracortical and reticulospinal mechanisms contribute to the neural adaptations associated with strength training.

Methods

All animal procedures were performed under UK Home Office regulations in accordance with the Animals (Scientific Procedures) Act (1986) and were approved by the Local Research Ethics Committee of Newcastle University. Recordings were made from two chronically implanted rhesus macaques (monkeys N and L; both female). Both animals were intact prior to the study, with the exception of monkey N who had lost fingers on the right hand in an unrelated incident.

Behavioural Task

Both monkeys were trained to pull a loaded handle towards the body using their right hand. After each trial the handle returned to its original position by the action of the load. Using a pulley system, weights could be attached to the handle so that the force required to pull it ranged from <5N in the unloaded control condition to 65N in the maximally loaded condition (Figure 4-1). The task was self-paced, with the only time constraint being a minimum inter-trial interval of 1s. Trials were identified as successful if the handle was moved at least 4cm; these were rewarded with food, and in the case of monkey L, stimulation of the nucleus accumbens as described below.

Surgical Preparation

Following successful training on the behavioural task, each animal underwent two surgeries, the first to implant a headpiece, electromyography (EMG) recording electrodes and cortical wires; and the second to implant chronic PT and MLF stimulating electrodes. Both surgeries were performed under general anaesthesia with full aseptic techniques.

The animals were initially sedated with an intramuscular injection of ketamine. Intubation and insertion of a central venous line enabled anaesthesia to then be maintained through inhalation of sevoflurane and continuous intravenous infusion of alfentanil. During surgery, hydration levels were maintained with a Hartmann's solution infusion, a thermostatically controlled heating blanket maintained body temperature, and a positive pressure ventilator ensured adequate ventilation. Pulse oximetry, heart rate, blood pressure, core and peripheral temperature, and end-tidal CO_2 were monitored throughout surgery, and anaesthetic doses adjusted as necessary. A full program of post-operative analgesia and antibiotic care followed surgery.

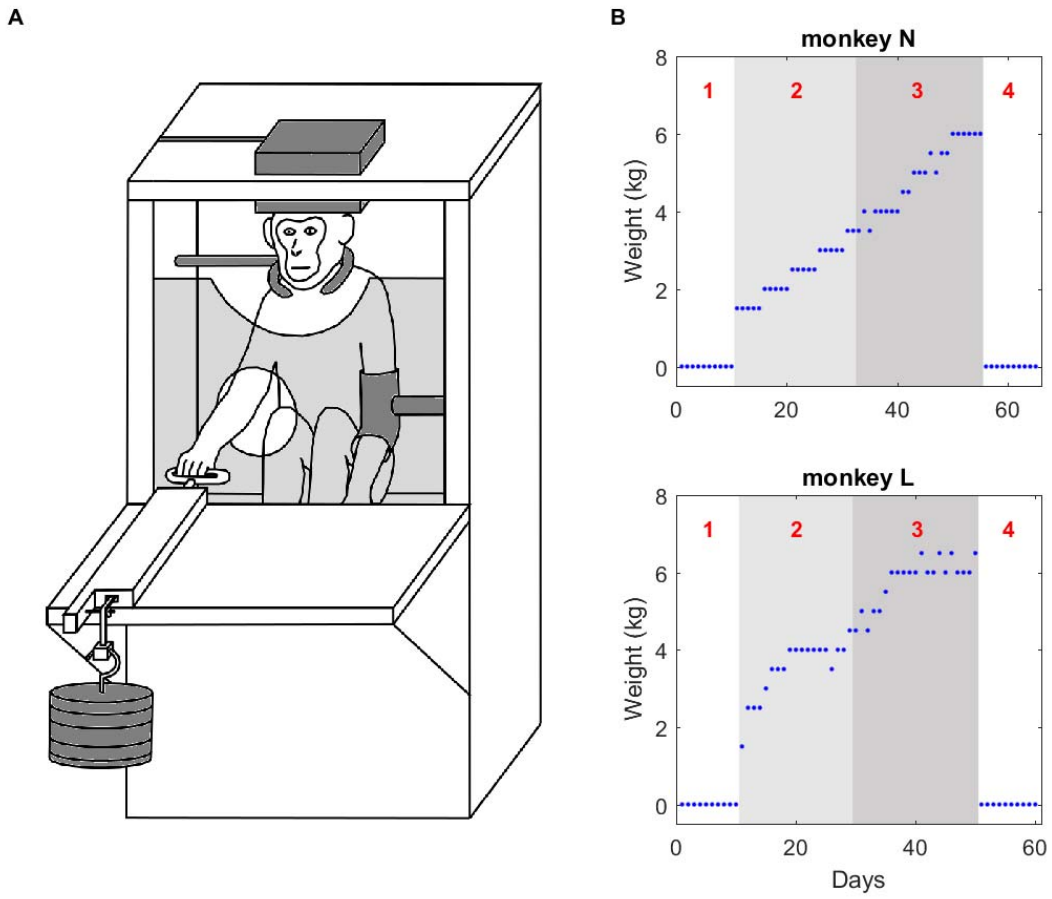

Figure 4-1. Strength training task

A. Schematic of the experimental set-up. The animal was atraumatically head-fixed, and wore a neck collar and a restraint on the left (untrained) arm. The right (trained) arm was free to reach through a hole in the front of the cage to pull a handle. The load was adjusted by adding weights to the other end of the handle. EMG activity was recorded and stimulation was delivered via connectors on the headpiece. *B.* Daily weight progression for each animal. The intervention consisted of four stages: an initial assessment period with no added load (1), strength training with low loads (2), strength training with high loads (3), and a washout period with no added load (4).

In the first surgery, a headpiece was implanted to enable atraumatic head fixation during the behavioural task and to provide a mount for the electrode connectors. The headpieces were designed using a structural MRI scan, 3D printed with titanium powder, coated with hydroxyapatite and surgically attached to the skull using the expanding bolt assemblies described by Lemon (1984). During the same surgery, electrodes for EMG recording were implanted into the first dorsal interosseous (IDI), flexor digitorum superficialis (FDS), flexor carpi radialis (FCR), extensor digitorum communis (EDC), biceps brachii (BB), triceps brachii, pectoralis major (PM) and posterior deltoid (PD). Electrodes were placed bilaterally with the exception of the FCR, which was implanted on the left side of monkey L and right side of monkey N. Each EMG electrode was custom made and consisted of a pair of insulated steel wires, bared for 1-2mm at their tips, which were sewn into the muscles using silk sutures. The wires were tunnelled subcutaneously to the headpiece upon which their connectors were mounted. To facilitate stimulation of the motor cortex, two custom made wires were implanted onto the surface of each M1 and their connectors cemented onto the headpiece using dental acrylic.

In a second surgery, performed three weeks later, four parylene-insulated tungsten electrodes (LF501G, Microprobe Inc, Gaithersburg, MD, USA) were chronically implanted bilaterally into the medullary PT and MLF, rostral to the decussation, to allow stimulation of the CST and RST, respectively. The double angle stereotaxic technique, described by Soteropoulos and Baker (2006), was used to aim each electrode at the desired target, from a craniotomy placed at an arbitrary convenient location on the headpiece. The optimal position for the PT electrodes was defined as the site with the lowest threshold for generating an antidromic cortical volley in ipsilateral M1, without eliciting a contralateral M1 volley at 300µA. The optimal MLF electrode position was defined as the site approximately 6mm above the PT electrode, which had the lowest threshold for generating a spinal volley without an antidromic cortical volley. All electrodes targeted an antero-posterior coordinate at the inter-aural line (AP0). The estimated medio-lateral coordinate for PT electrodes was 0.5-3.1, and for MLF electrodes 0.5-1.4 relative to the midline. The dorso-ventral location of the electrodes was estimated as 6.5-9.3 for PT, and 0.1-5.5 for MLF. Threshold for evoking a spinal volley was 10-20µA for PT, and 20-100µA for MLF. Cortical volleys were obtained by recording from the cortical wires implanted in the previous surgery. Spinal volleys

were recorded using a wire temporarily positioned in the paraspinal muscle near the cord with a needle; this was removed at the end of surgery.

Monkey L underwent an additional surgery prior to the start of the strength training protocol chronically to implant a parylene-insulated tungsten electrode (LF501G, Microprobe Inc, Gaithersburg, MD, USA) into the nucleus accumbens, stimulation of which has been shown to be an effective behavioural reward (Bichot et al., 2011). Following sedation with ketamine, a burr hole was drilled above the target penetration site and sealed with acrylic. The following day, in the awake animal, the acrylic was removed and an insulated tungsten electrode was driven towards the nucleus accumbens target location. To optimise its position, stimulus trains were delivered through the electrode (1.0mA biphasic pulses, 0.2ms per phase, 200Hz frequency, 200ms train duration) and the facial expressions and vocalisations of the animal monitored until an optimal response was observed. Typically, we found a sequence as the electrode was advanced: the animal first showed a mild orienting reaction following the stimulus, with characteristic retraction of the ears. Further electrode advancement produced vocalisation (typically grunting), which became stronger at deeper sites. At the optimal site, vocalisation could be produced at a threshold of 100µA. The electrode was then fixed in place and a connector cemented onto the headpiece with dental acrylic. During subsequent training sessions, monkey L received nucleus accumbens stimulation every 1-3 successful trials at random, with the stimulation intensity increased as necessary to maintain motivation (1.0-2.5mA biphasic pulses, 0.2ms per phase, 200Hz frequency, 200ms train duration).

Experiment 1: EMG recordings

Following recovery from surgery and retraining on the task, the animals underwent 12- (monkey L) and 13-week (monkey N) strength training protocols. The following sessions were performed 5 days per week. Each day began with an initial stimulation session in which the animals performed 50 unloaded trials whilst receiving stimulation of the four brainstem electrodes (bilateral PT and MLF: 500µA biphasic pulses, 0.2ms per phase, 2Hz repetition rate) and four cortical electrodes (bilateral medial and lateral M1: 3mA biphasic pulses, 0.2ms per phase, 2Hz repetition rate) in pseudo-random order. The unloaded task served to generate low-level background EMG activity upon which MEPs could be recorded. The animals then performed the strength training session

consisting of 50 loaded trials (1.5-6.5 kg); no stimulation was delivered during this session. Finally, to assess short-term adaptations, a second stimulation session was performed with the same format as the first. These three daily sessions will subsequently be referred to as the 'pre-training', 'strength training' and 'post-training' sessions (Figure 4-2).

Figure 4-2. Overview of daily training sessions

Training was performed 5 times per week. Each day began with a pre-training stimulation session in which the animals performed 50 unloaded trials whilst receiving PT, MLF and cortical stimulation. This was followed by 50 loaded trials without stimulation for the strength training session. Finally, a second stimulation session was performed.

During all of these sessions the task was performed with the right arm whilst the left arm was held in a restraint, a collar placed around the neck, and the head atraumatically fixed by the headpiece to allow connection to the EMGs and stimulating electrodes (Figure 4-1*A*). EMG (5kHz sampling rate, 200-1000 gain, 0.1 Hz to 10 kHz band-pass) and task parameters, such as lever position and stimulus times, were stored to disc. The total training each day took approximately 20 minutes.

The first two weeks (initial assessment period) and last two weeks (washout period) of the training protocol were performed without weights during the strength training session in order to establish an unloaded baseline measure and to assess post-training washout effects. During the remaining 7-8 weeks, the weights were gradually increased day by day, as tolerated by the animals (Figure 4-1*B*).

All analysis of EMG data were performed off-line using custom software written in MATLAB. EMG recordings were high pass filtered at 30Hz and then full-wave rectified. Visual inspection of mean traces identified stimulus-muscle combinations with reliable MEPs and only these were included in subsequent analyses. Background EMG activity was measured over a 40ms window

(from 50ms to 10ms before each stimulus). MEPs were measured as the area under the curve above background EMG between cursors that were manually positioned for each included stimulus-muscle combination. Due to the variation in background EMG activity, and the known effect of this on MEP amplitude (Hess et al., 1987), MEPs were normalised by dividing by their corresponding background EMG measure. The human TMS and TES literature suggests that a linear relationship does not exist between background EMG level and MEP size (Kischka et al., 1993; Taylor et al., 1997), but can instead plateau above a certain background EMG, depending upon the muscle. Nonetheless, we have persisted with this normalisation method because although it may attenuate our effects by over-compensating for background EMG activity, it reduces the likelihood that any trends observed are simply due to changes in background EMG activity.

To assess short-term effects of individual strength training sessions, the daily recording sessions were grouped into four weight ranges for each monkey: no weight (0kg, unloaded task), light (0.5-3.5kg), moderate (4.0-5.0kg) and heavy (5.5-6.5kg). Before and after effects were expressed as a percentage change in normalised MEP size from the pre-training session to the post-training session. Similar percentages were obtained for the different muscles and so the results were grouped simply by averaging the percentage change values for all of the included muscles for each stimulus and day. Statistically significant ($p<0.05$) changes in MEP size were identified with a one-sample t-test and multiple comparisons were corrected within each monkey using a Benjamini-Hochberg correction with a false discovery rate of 5%. This analysis was repeated for background EMG measures.

To assess long-term adaptations to strength training, the pre-training daily sessions were grouped into four stages for each monkey: initial assessment, strength training 1, strength training 2 and a washout period (Figure 4-1*B*). Note that these sessions are time-based in contrast to the sessions used for assessment of short-term training adaptation, which are weight-based. For single muscles, mean MEP size for each stage was expressed as a percentage of the mean initial assessment period MEP. This analysis was performed for both the original MEP values and those normalised to background EMG, as described above. To combine the responses across muscles in order to provide a single measure for each stimulus, the daily MEP size for each muscle was Z-score transformed by subtracting the mean initial assessment period MEP and then dividing by the standard deviation of the initial assessment period MEP. These values were summed across

muscles and divided by the square root of the number of muscles to give a single daily measure across muscles, and averaged across days to give a single measure of MEP magnitude per stimulus per stage. Independent t-tests were performed relative to the initial assessment period and multiple comparisons were corrected within each monkey using a Benjamini-Hochberg correction with a false discovery rate of 5%. This analysis was repeated for background EMG measures. No long-term analysis was performed on the post-training sessions.

Experiment 2: Spinal recordings

Following completion of the 12-13 week strength training protocol, each animal continued with a daily strength training regimen as part of a separate study in which single unit recordings were made from M1 and the reticular formation (RF). Over a 3 month period, 20-50 trials were performed approximately 5 days per week with each of the following weights: 0.5kg, 1kg, 1.5kg, 2kg, 3kg, 4kg and 6kg; hence the animals received as least as much strength training as in the main intervention. An experiment under terminal anaesthesia was then performed in which recordings were made from the spinal cord to assess changes in synaptic efficacy.

Initial sedation was achieved with an intramuscular injection of ketamine. Anaesthesia was then induced with intravenous propofol and maintained through intravenous alfentanil and inhalation of sevoflurane. Pulse oximetry, heart rate, blood pressure, core and peripheral temperature, and end-tidal CO_2 were monitored throughout surgery, and anaesthetic doses adjusted as necessary to ensure deep general anaesthesia was maintained.

A craniotomy and laminectomy were performed to expose the right motor cortex and cervical spinal cord, respectively. The vertebral column was clamped at the high thoracic and mid-lumbar levels and the head fixed in a stereotaxic frame. The anaesthetic regimen was then switched to an intravenous infusion of alfentanil, ketamine and midazolam.

Using the methods described above, parylene-insulated tungsten electrodes (LF501G, Microprobe Inc, Gaithersburg, MD, USA) were inserted bilaterally into the PT and RF via a craniotomy adjacent to the foramen magnum, with their placement optimised using cortical and spinal volleys recorded from epidural ball electrodes. All electrodes targeted an antero-posterior coordinate at the inter-aural line (AP0) at an angle 30 degrees anterior. The estimated medio-lateral coordinate

for PT electrodes was 1.0, and for RF electrodes 2.0 relative to the midline. The dorso-ventral location of the electrodes was estimated as 7.7-9.4 for PT, and 4.3-5.5 for RF.

Although chronic electrodes were already implanted into the PT and MLF, the decision was made to implant new electrodes for the spinal recordings due to gliosis likely reducing the efficacy of the chronic electrodes. Furthermore, reticular activity was assessed using electrodes implanted into the RF for the spinal recordings, in contrast to the MLF stimulation site used for the EMG recordings. This difference reflects the importance of laterality and symmetrically positioned electrodes in the spinal recordings, which was best achieved by targeting the RF via the obex, compared to the importance of evoking responses in a large number of muscles in the EMG recordings, which is most likely when targeting an axon bundle such as the MLF.

To record the spinal field potentials, the dura was opened at a rostral (C5-C6) and caudal (C6-C7) site on the cord. Recordings were made using a single 16-channel electrode (LMA, 50µm contacts spaced 240µm apart, Microprobe Inc, Gaithersburg, MD, USA) per site. A series of 10 penetrations was made, progressing from lateral to medial in 500µm increments. Successive recordings alternated from the left to the right side of the cord, minimising the likelihood of differences being observed between the two sides due to changes in excitability with time, as may occur with changes in anaesthetic dose. The 500µm spacing of penetrations and 240µm spacing between electrode contacts produced a grid of recording sites across a cross-section of the cord (Figure 4-3). For each penetration, an intensity series was delivered through each of the newly implanted PT and RF electrodes for both single stimuli (50-500µA biphasic pulses in 50µA increments, 0.2ms per phase, 4Hz repetition rate) and trains of three stimuli (50-500µA biphasic pulses in 50µA increments, 0.2ms per phase, 4Hz repetition rate, 333Hz train frequency). In monkey N, spinal field potential recordings were made under neuromuscular blockade (atracurium); no neuromuscular block was used in monkey L. The spinal recordings (25 kHz sampling rate) and stimulation parameters were stored to disc.

The aim of these recordings was to assess whether there were changes in the spinal field potentials on one side of the cord relative to the other as a result of strength training the right arm. We did not directly compare the spinal field potentials on the two sides since it was likely that slight differences in stimulus electrode location would have led to different volley output for a given

intensity (see Figure 4-6*B*). Instead our analysis focussed on the relationship between the volley and field across different stimulation intensities to give an indication of the relative strength of the synapses on either side of the cord. All analysis of spinal data were performed off-line using custom software written in MATLAB.

Field and volley measurements were made between manually positioned cursors, with amplitude being defined as the maximum value between the cursors relative to the reference cursor (Figure 4-4*C,D*). Cursor positions were fixed for all recordings made at a given site (rostral and caudal) in each monkey, in response to each stimulus.

We rarely observed field potentials in response to a single stimulus. However, they were reliably evoked with trains of three stimuli (see Results and Figure 4-4*A*). We therefore measured field potentials after the third stimulus of a train. To prevent contamination of the field potentials with the decay of the volley, the data were post-processed as follows. For each recording, the volley evoked by a single stimulus, in which no field was present, was subtracted from the volley of the third stimulus in a train to produce an isolated field (Figure 4-4*B*).

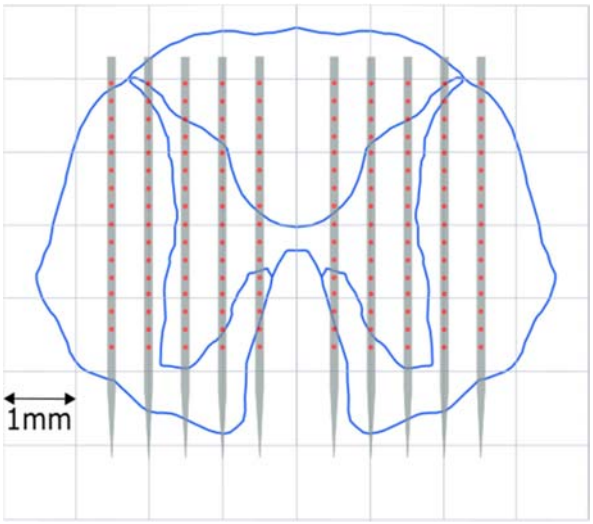

Figure 4-3. Electrode positions for spinal recordings

A single electrode was inserted into the spinal cord at 500µm intervals relative to the midline and at a constant depth. The electrode consisted of 16 contacts (red dots) spaced 240µm apart, with the first contact 1.5mm from the tip.

The volley measurements for each penetration and electrode contact were used to generate surface plots representing cross-sections of the spinal cord (Figure 4-5). This enabled identification of the dorsolateral funiculus (DLF) for the PT stimuli, and the ventrolateral funiculus (VLF) and ventromedial funiculus (VMF) for the RF stimuli. The locations corresponding to these regions were manually selected for each monkey and each electrode (Figure 4-5) and the volley amplitudes across them averaged to give a measure of the mean input to the cord by that stimulus for each stimulus intensity. It was thus possible to plot an input-output curve for each location on the cord where the input values were the summed volley amplitudes for each region (DLF, VLF and VMF) at each intensity and the output values were the individual field amplitudes for that location at each intensity. The slope of this line (Figure 4-6*C*) represents the gain of the system and thus provides a measure of synaptic efficacy. Comparing the slopes of the lines for corresponding locations mirrored across the midline thus gives a measure of changes in synaptic efficacy on one side of the cord compared to the other. The difference between the two gradients was calculated and an ANCOVA performed to test the significance of this. Positions with a negative gradient or an insignificant regression ($p>0.05$) were excluded from subsequent analysis.

To summarise the results across the four equivalent recordings (a caudal and rostral recording site per monkey), an average of the gradient differences was calculated once the gradient differences for each stimulus were normalised to scale between 0 and 1. The significance of these group changes was assessed by assigning each of the original gradient differences 0 for an insignificant change, +1 for a significantly steeper gradient on the right cord compared to the left, and -1 for a significantly shallower gradient on the right cord compared to the left. Summing these values across the four equivalent recordings gave a score from -4 (all recordings showed a significantly steeper gradient on the right side of the cord) to +4 (all recordings showed a significantly shallower gradient on the right side of the cord). By simulating all possible combinations of scores across the 5 (penetrations) x 16 (electrode contacts) recording grid, we found that a score of +2 or higher, or -2 or lower, could be considered significant at $p<0.05$.

After completion of the study, electrolytic lesions were made by passing current through the chronic PT and MLF electrodes (100 µA for 20 s) and the newly implanted PT and RF electrodes. Anaesthesia was then increased to a lethal level and animals were perfused through the heart with phosphate buffered saline followed by formal saline.

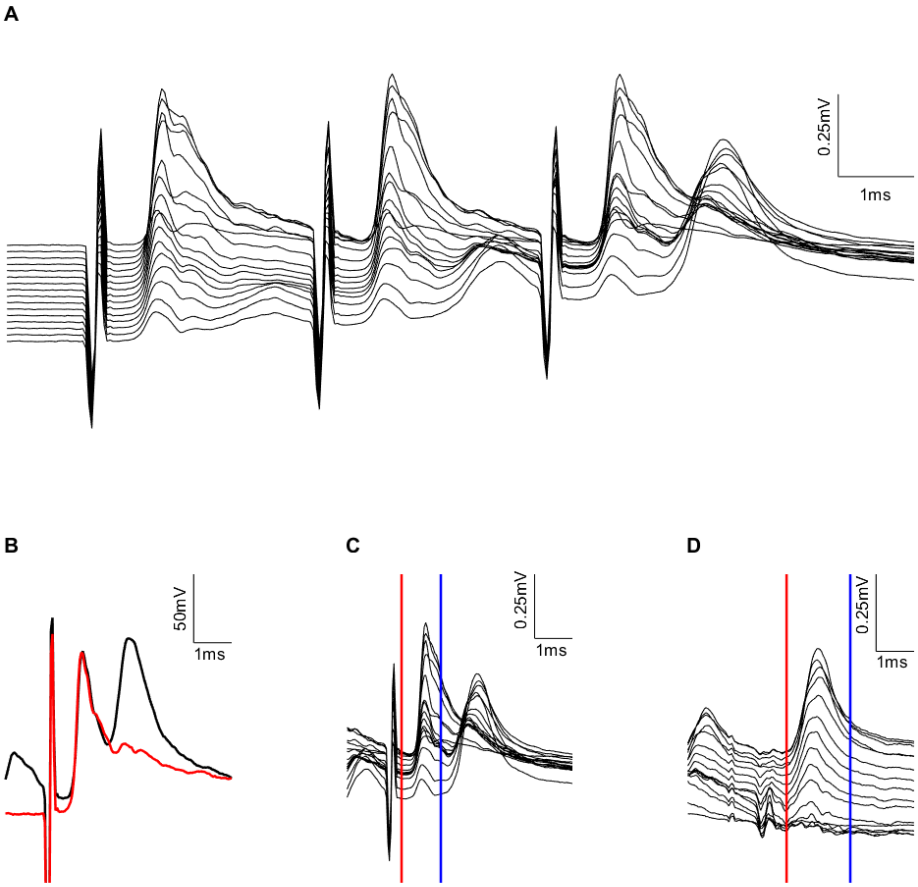

Figure 4-4. Example spinal traces and amplitude measurements

Example spinal traces recorded from all contacts of a single electrode positioned 2mm left of the midline at the caudal site of monkey N in response to a 300µA left PT stimulus. ***A.*** Recording of train of three stimuli. Note the constant size of the volley in contrast to the growing field. ***B.*** Example application of field isolation. The response to a single stimulus (red) was subtracted from the response to the last stimulus in a train of three (black), to isolate the field from the decay of the volley. The amplitude of the volley (***C.*** Original recording) and field (***D.*** Isolated field data) were measured as the maximum value between the cursors relative to the reference cursor (red).

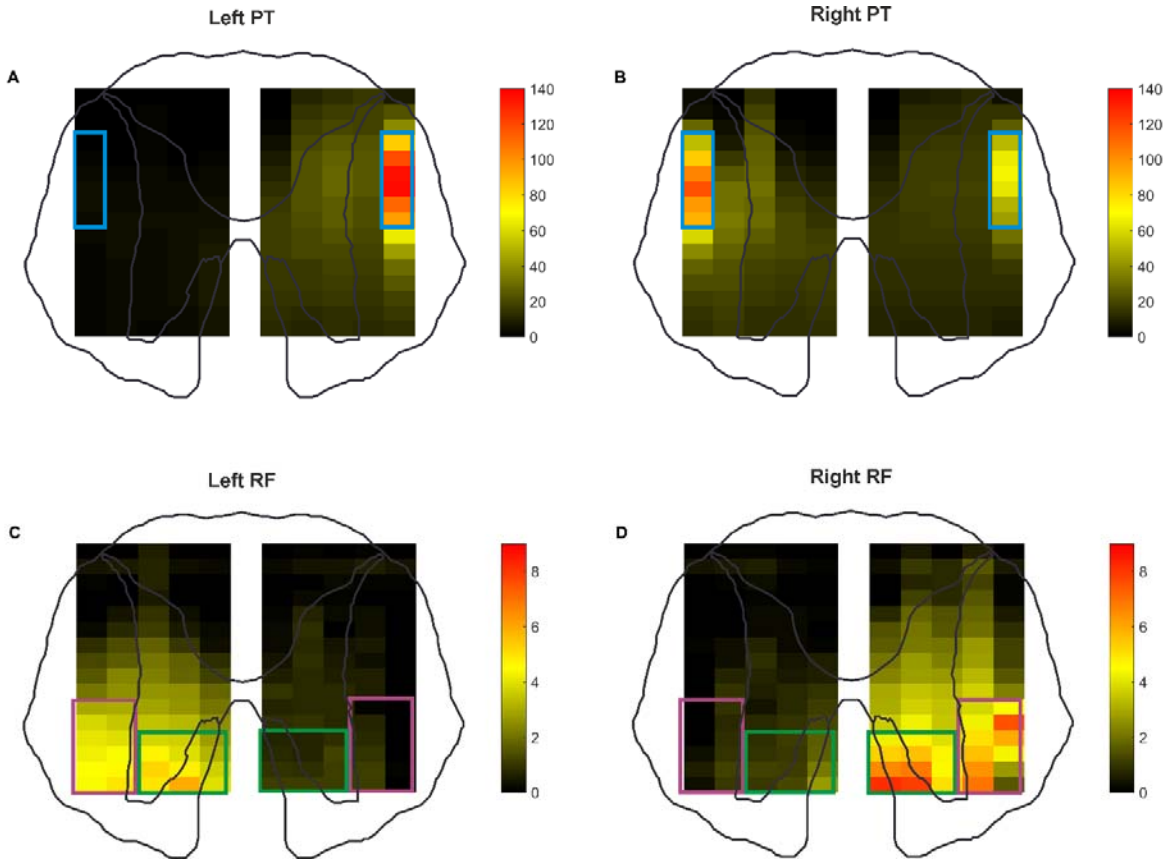

Figure 4-5. Coordinates of volley recordings

Spinal volley amplitudes recorded with ***(A)*** left PT, ***(B)*** right PT, ***(C)*** left RF and ***(D)*** right RF stimulation were used to define the DLF (blue squares), VLF (purple squares) and VMF (green squares) for their respective stimuli. The shown recordings are from the rostral site of monkey L with a 200µA stimulus intensity.

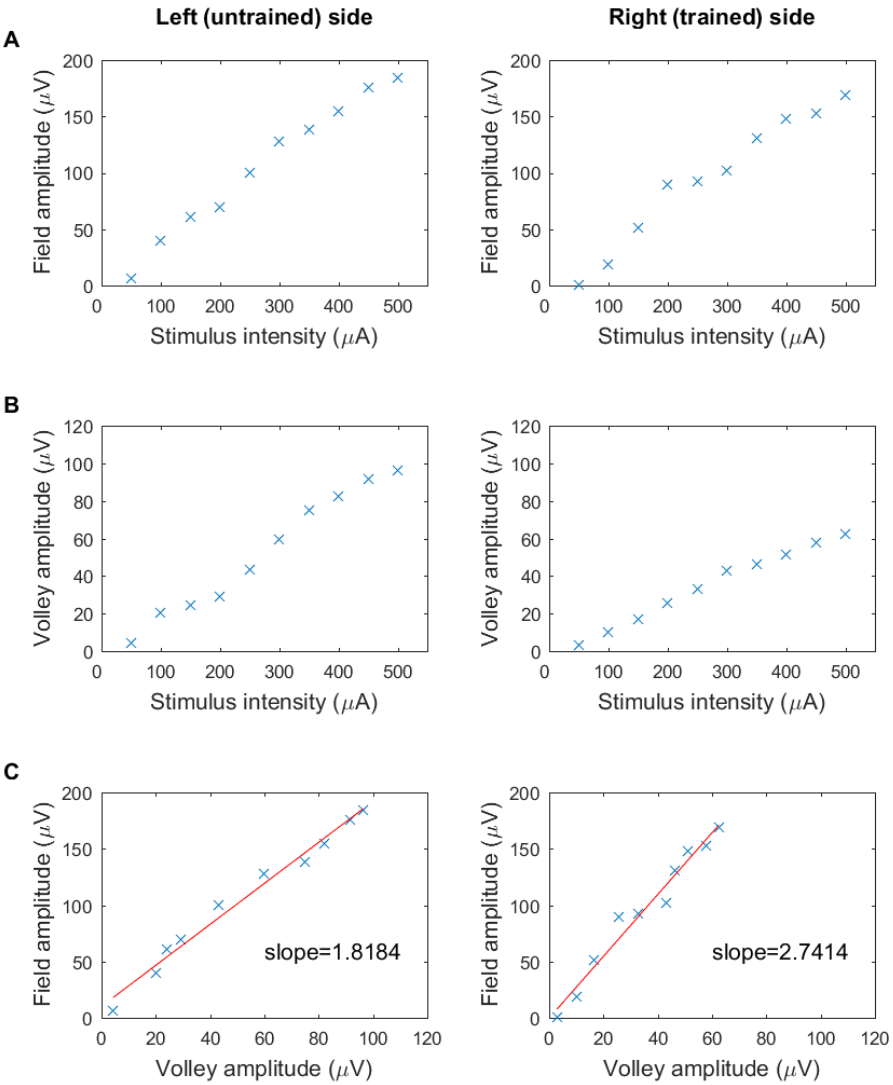

Figure 4-6. Example of gradient calculation for field and volley relationship

The data presented were recorded from the deepest contact of the caudal electrode of monkey N, 0.5mm to the left (first column) and right (second column) of the midline, in response to contralateral PT stimulation with the volley assessed at the DLF. Volley (***A***) and field (***B***) amplitude were measured (see Figure 4-4 and Figure 4-5) for a range of stimulus intensities. ***C.*** For each stimulus intensity, field amplitude was plotted against volley amplitude. A linear regression was performed to calculate the gradient of this volley-field relationship, which gave a measure of the synaptic efficacy of the stimulus at that site in the cord. The difference between gradients for mirrored locations on the cord was calculated (e.g. 2.7414-1.8184=0.9230) to compare the effects of the unilateral strength training intervention. The significance of this difference was assessed with an ANCOVA (e.g. P=0.000125). This analysis was repeated for each position on the recording grid (see Figure 4-3), for each recording site (rostral or caudal) and each monkey.

Results

Task performance

Both animals complied well with the task, completing the required 150 trials on all but a few days. The progression of weight added to the task during the strength training session differed between the two animals and it is likely that the first few weeks of this ('Training 1') constituted familiarisation with lifting weight rather than intensive strength training. It was not possible to perform measures of maximum voluntary contraction (MVC) and so unlike in human strength training experiments, we were unable to fix the load to generate a certain percentage of MVC. Instead, subjective assessments were made of each animal's capability, in terms of both strength and motivation, and the weights increased accordingly. Although we cannot definitively prove that the animals found the weights heavy and thus that this constituted a weight training programme (see Discussion), it should be noted that by the end of the intervention each was performing 50 consecutive trials with at least 6kg, which was approximately equivalent to their body weight.

The task was found to activate all recorded muscles on the right (trained) arm (Figure 4-7*A*), with increasing muscle activation with weight. Although designed to be unilateral, the task generated some bilateral activation, particularly in proximal muscles and with heavier loads (Figure 4-7*B*). Since the left (untrained) arm was held in a restraint, this activation does not represent bimanual task performance but instead may result from mirror activation (Armatas et al., 1994; Mayston et al., 1999) or postural bracing for the heavier loads.

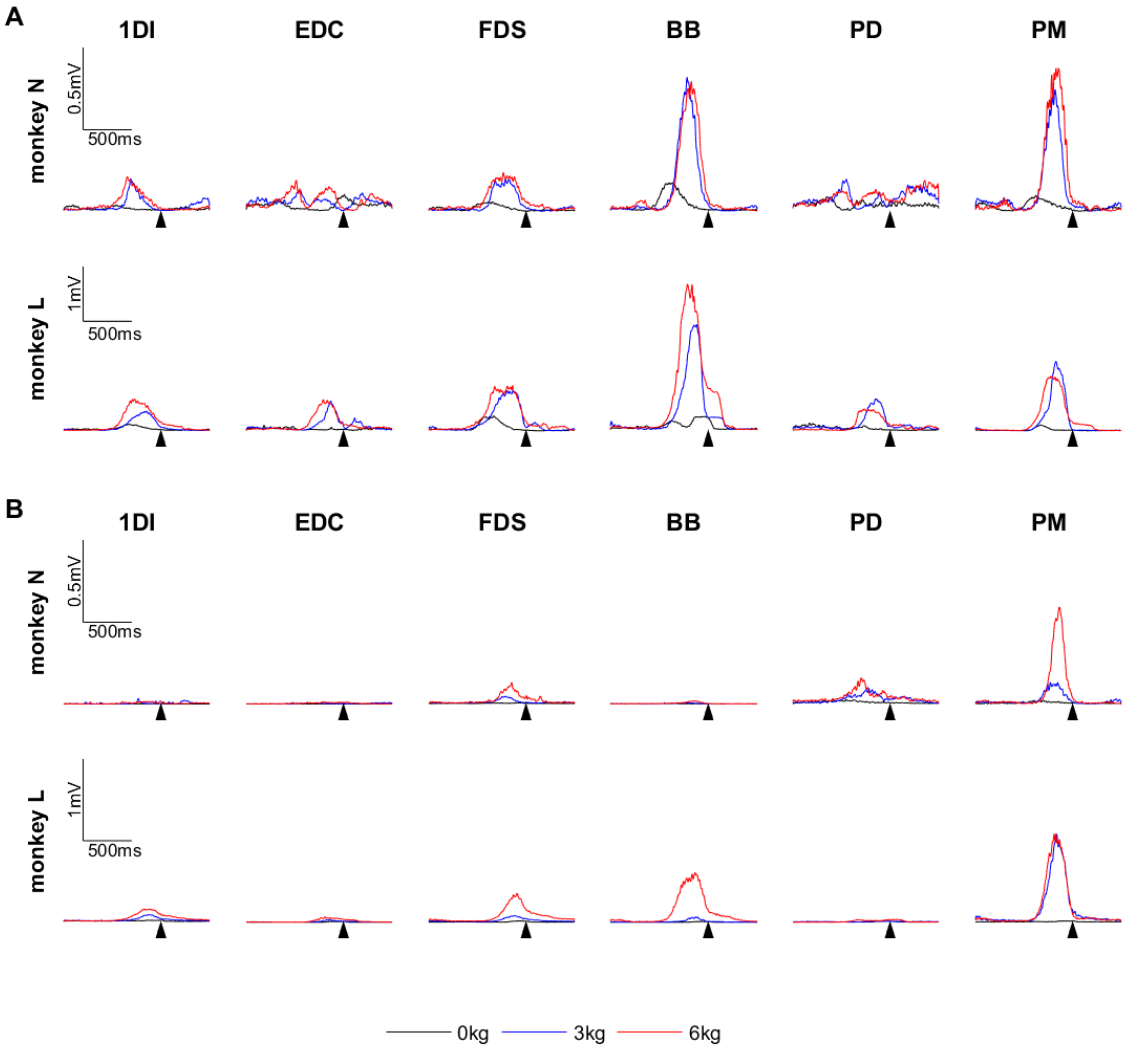

Figure 4-7. Example EMG activity during task with different loads

Mean rectified EMG activity for all trials (n=50) on a given day recorded from muscles on the ***(A)*** right (trained) arm and ***(B)*** left (untrained) arm. Recordings are from the strength training sessions of day 2 (0kg), day 26 (3kg) and day 50 (6kg) for monkey N; and day 2 (0kg), day 15 (3kg) and day 36 (6kg) for monkey L. Sweeps are aligned to maximum lever displacement (arrow). Note that the left arm was held in a restraint during these recordings.

MEP recordings

MEPs were consistently observed in most muscles in response to contralateral PT and cortical stimulation. FCR and triceps brachii were excluded from the analysis since the former was only implanted unilaterally and the EMG recordings from the latter were unreliable. The medial and lateral cortical wires generated similar MEPs and so only responses to the lateral cortical wires have been presented. Although implanted bilaterally, the left MLF electrode elicited no MEPs in monkey L and few in monkey N so has been excluded from the analysis. In contrast, the right MLF electrode elicited clear MEPs bilaterally in both monkeys and so for the purposes of this analysis has been used to assess reticulospinal output in a non-lateralised manner. It is likely that the bilateral effect of this electrode relates both to current spread across the midline and the established bilateral effects of the RST, particularly in terms of facilitation of upper limb flexors (Davidson and Buford, 2006). The inefficacy of the left MLF electrode in both animals may simply relate to the tip being dislodged as the electrode was fixed in place, an outcome that is more likely with a small target such as the MLF.

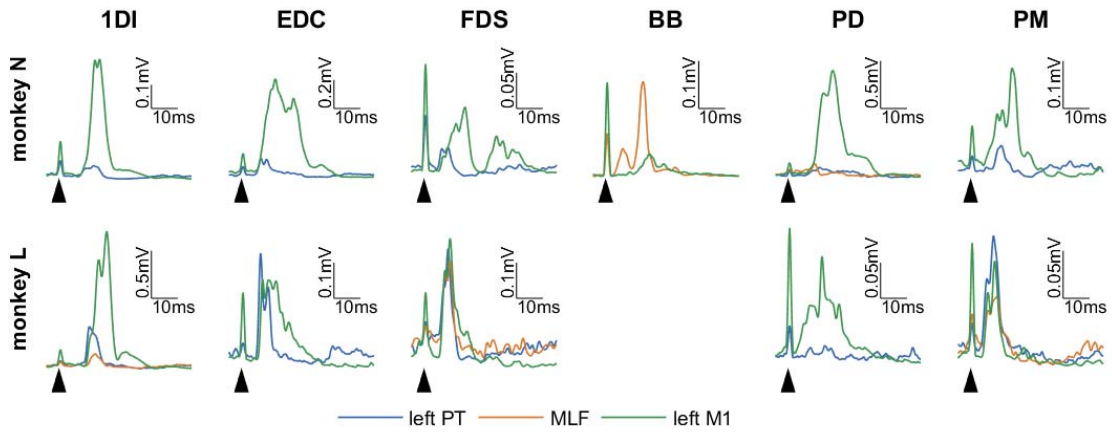

Figure 4-8. Example MEP recordings

Mean rectified EMG traces showing MEPs recorded from the muscles of the right (trained) arm during the pre-strength training stimulation session of day 47 (monkey N) and day 31 (monkey L). Only stimuli giving a clear MEP in the specified muscle are shown. Sweeps are aligned to the stimuli (arrows).

Epidural electrical stimulation over the motor cortex generates D- and I-waves (Rosenthal et al., 1967; Di Lazzaro et al., 2004) implying that it can activate corticospinal cells directly and also via intracortical circuits. We therefore propose that our M1 stimulation can be considered comparable to TMS. In contrast, our chronically implanted PT electrodes were positioned to stimulate the descending corticospinal fibres distant to the cortex, so that the volley evoked should be independent of cortical excitability. This stimulus can be considered comparable to cervicomedullary (or transmastoid) stimulation in humans, and to a lesser extend transcranial electrical stimulation (TES), both of which are thought to stimulate corticospinal axons directly (Rothwell et al., 1994; Taylor and Gandevia, 2004). Importantly, comparisons between M1 and PT MEPs can give an indication of whether adaptations are occurring within the cortex or subcortical levels, similarly to the comparison in the human literature between TMS and TES or transmastoid stimulation (Rothwell et al., 1994; Taylor and Gandevia, 2004). Finally, in addition to reticulospinal fibres (Jankowska et al., 2003; Edgley et al., 2004), the MLF contains vestibulospinal (Nyberg-Hansen, 1964b; Wilson et al., 1968) and tectospinal fibres (Nyberg-Hansen, 1964a). However, we propose that MLF stimulation used in these experiments provided a generalised activation of reticulospinal fibres for reasons discussed elsewhere (Riddle et al., 2009; Riddle and Baker, 2010).

Short-term training adaptations

Increasing load in the strength training sessions was associated with a progressive reduction in background EMG activity in monkey N but had no such effects in monkey L, as measured in the post-training session (Figure 4-9). This variation in background EMG activity provides justification for the MEP normalisation method previously described.

From the pre-training to the post-training session, the normalised MEPs evoked by PT stimulation showed a consistent trend of increasing in size with low loads and decreasing in size with higher loads in both monkeys (Figure 4-10). However, the only statistically significant difference between the pre-training and post-training sessions was the facilitation of M1 MEPs in monkey L in the unloaded condition.

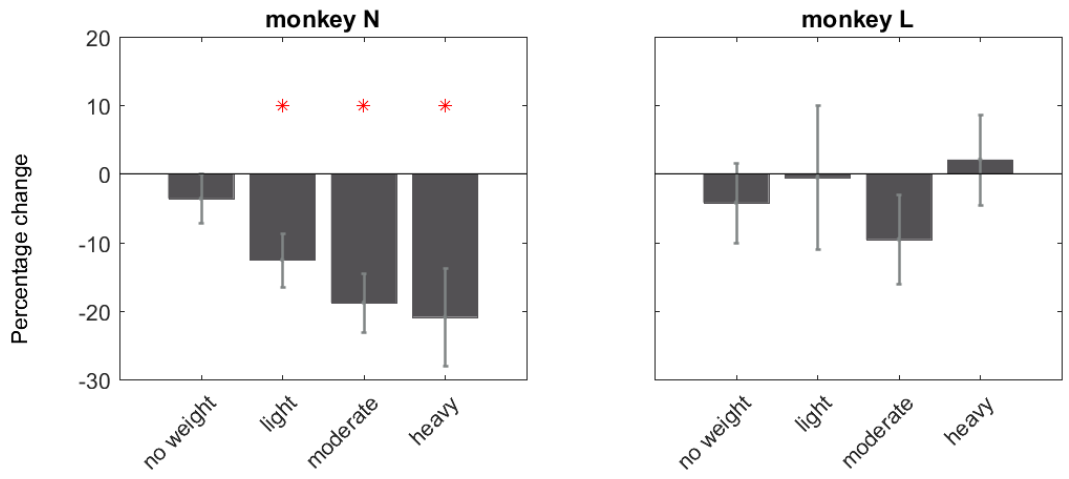

Figure 4-9. Short-term changes in background EMG activity in the right (trained) arm

Percentage change in background EMG activity from the pre-training to the post-training stimulation session. Background EMG was calculated as mean rectified EMG activity measured over a 40ms window (-50 to -10ms) prior to each stimulus. Results have been combined across muscles (1DI, EDC, FDS, BB, PD, PM) on the right (trained) arm and stimulus type, and grouped into weight ranges (no weight: 0kg; moderate: 0.5-4.0kg; heavy: 4.5-6.5kg). Asterisks represent a statistically significant change ($p<0.05$) in background EMG from the pre-strength training to the post-strength training stimulation session.

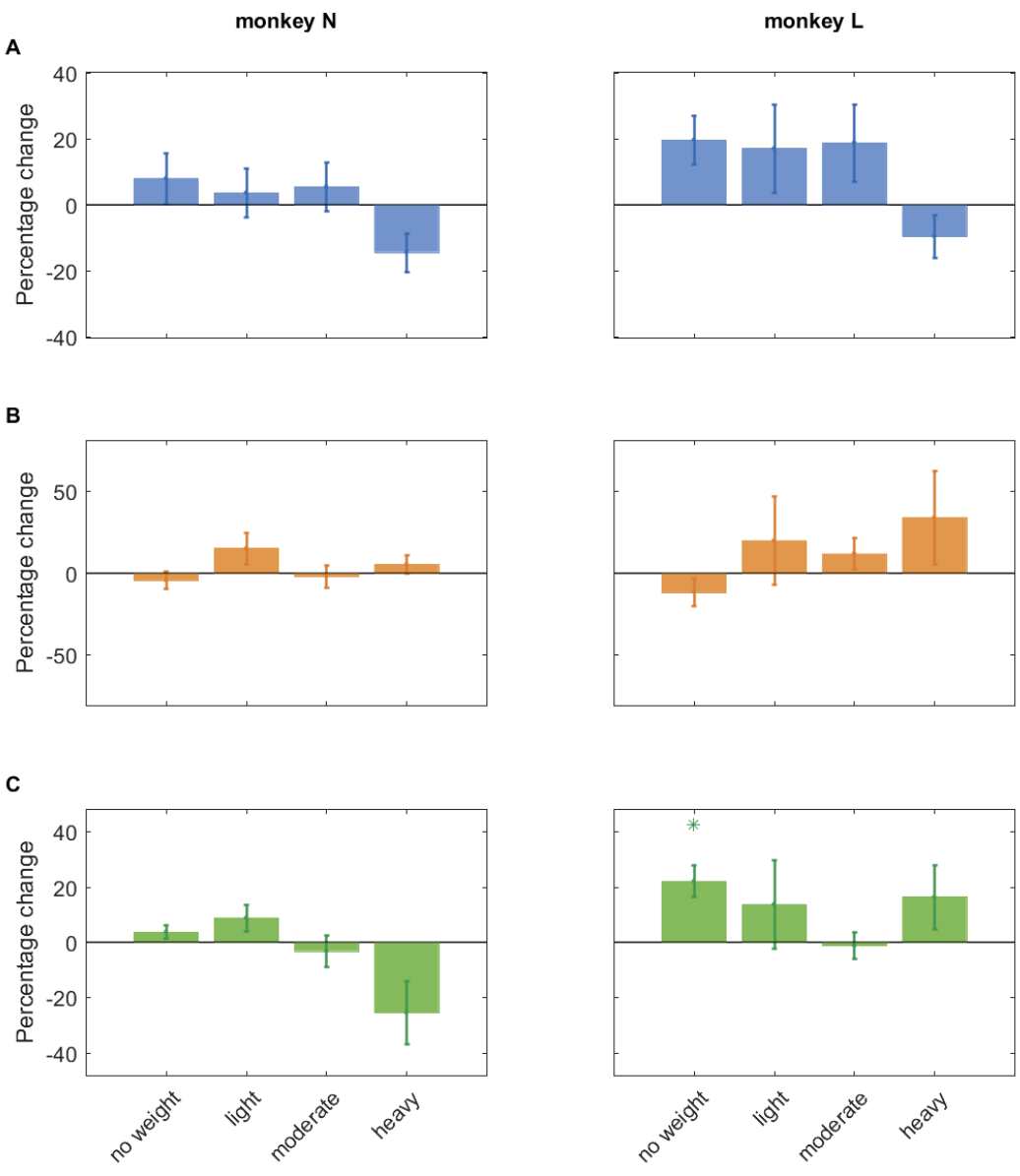

Figure 4-10. Short-term adaptations to strength training in the right (trained) arm

Percentage change in MEP area from the pre-strength training to the post-strength training stimulation session for ***(A)*** PT, ***(B)*** MLF and ***(C)*** M1 stimulation. MEP area was calculated as the area above background EMG, divided by background EMG, for a custom window for each muscle-stimulus combination. Results have been combined across all muscles on the right (trained) arm that showed a clear MEP for the given stimulus (see Figure 4-8), and grouped into weight ranges (no weight: 0kg; light: 0.5-3.5kg; moderate: 4.0-5.0kg; heavy: 5.5-6.5kg). Asterisks indicate statistically significant changes ($p<0.05$) in MEP size from the pre-training to the post-training stimulation session.

Long-term training adaptations

Comparison of the pre-training stimulation sessions showed that during the strength training programme, there was a significant increase in background EMG levels in monkey N and decrease in background EMG levels in monkey L in the right (trained) arm (Figure 4-11*A*). This was largely consistent across all muscles recorded (Figure 4-11*B*). To account for these changes, MEP values were normalised to background EMG activity - both original and normalised values are presented in Figure 4-12, with similar trends being observed in both datasets. Focussing on the normalised data, both monkeys showed a significant facilitation of M1 MEPs. MLF MEPs were facilitated in both monkeys but this was only significant in monkey N. The PT MEPs show an inconsistent trend, with a significant suppression in monkey N and no change in monkey L (Figure 4-12*B*).

Similarly, in the left (untrained) arm, significant increases in background EMG levels were observed in most muscles in monkey L, and although an upwards trend was observed at the group level for monkey N, the changes in individual muscles were more variable (Figure 4-13). It should be noted that the left (untrained) arm was held in a restraint during these recordings and so with the exception of bilateral activation during the task and movements unrelated to the task, background EMG levels here were expected to be low.

Interestingly, despite no strength training in the left arm and the lack of substantial background EMG activity, the changes in MEP size in the left (untrained) arm were similar to those observed in the right (trained) arm. In both monkeys there was a significant increase in M1 MEPs whereas PT MEPs showed a significant reduction in monkey N and a significant increase in monkey L. MLF MEPs were facilitated in monkey L and showed no overall change in monkey N (Figure 4-14).

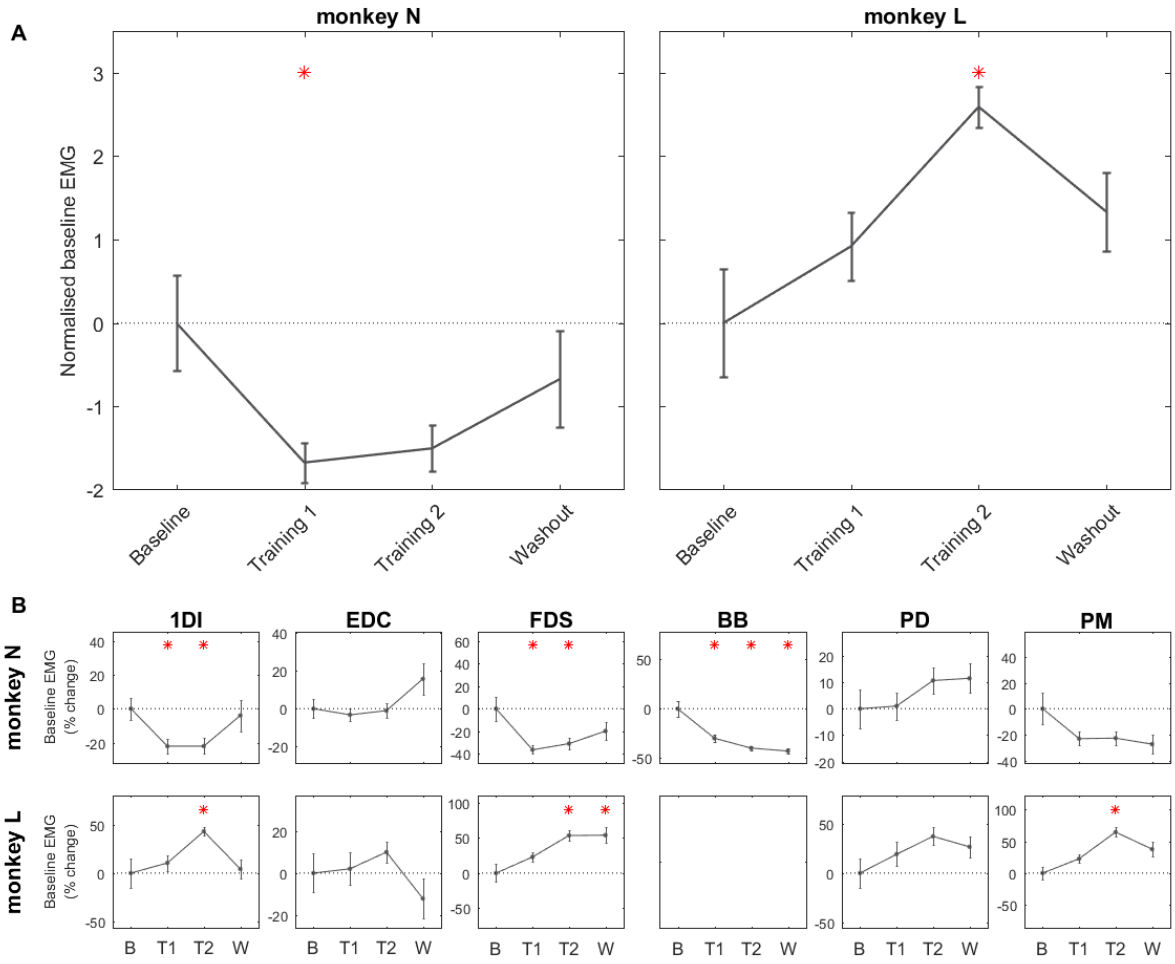

Figure 4-11. Long-term changes in background EMG activity in the right (trained) arm

Change in background EMG activity recorded from muscles on the right (trained) arm relative to the initial assessment period. Background EMG was calculated as mean rectified EMG activity measured over a 40ms window (-50 to -10ms) prior to each stimulus. Asterisks represent a statistically significant change ($p<0.05$) in background EMG relative to the initial assessment stage. ***A.*** Changes in background EMG activity averaged across all muscles (1DI, EDC, FDS, BB, PD, PM) following Z-score transformation of individual muscle percentages. ***B.*** Percentage change in background EMG activity for individual muscles across the four training stages: initial assessment (IA), training 1 (T1), training (T2) and washout (W). See Figure 4-1 for training stage details.

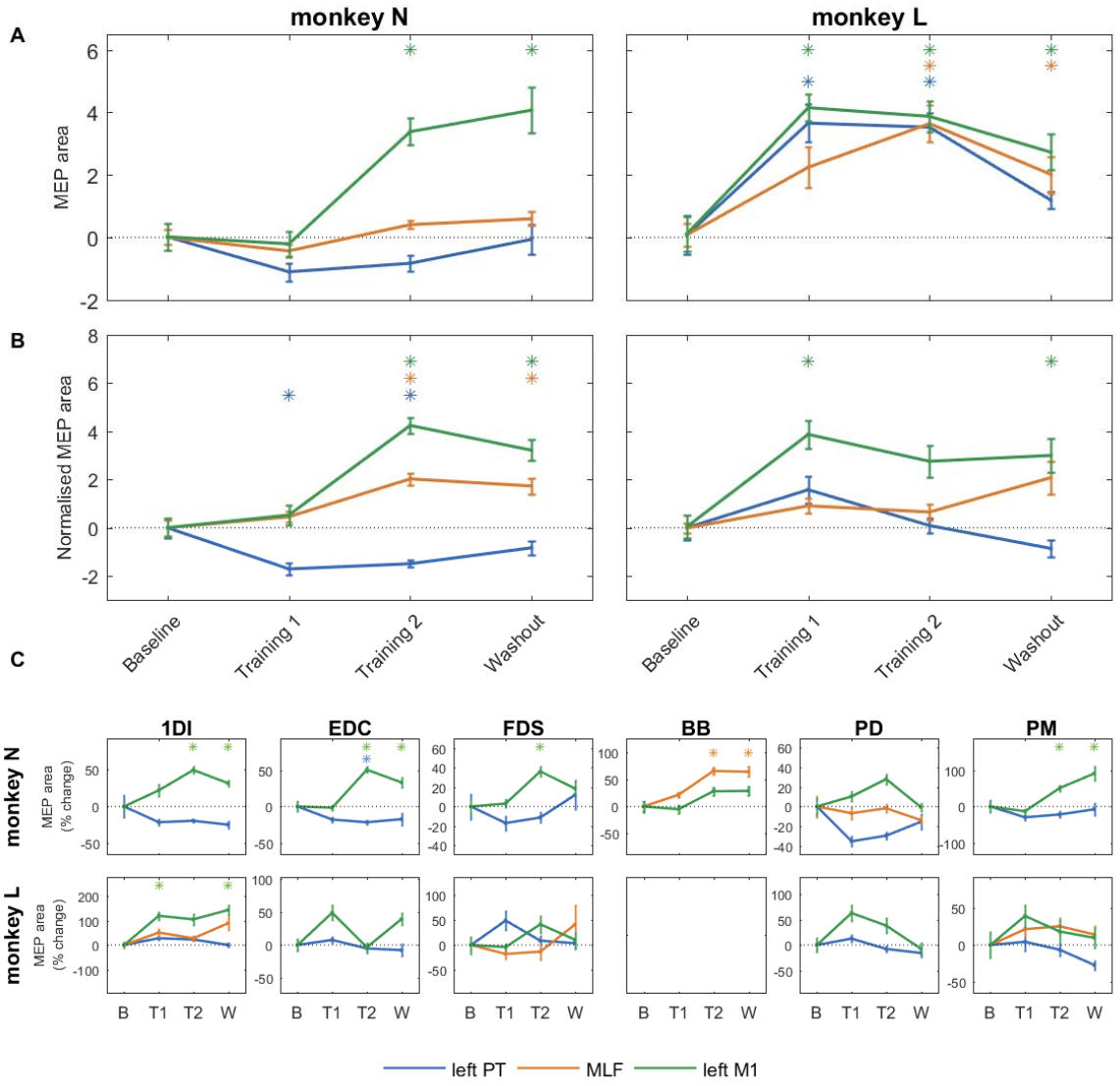

Figure 4-12. Long-term adaptations to strength training in the right (trained) arm

Change in MEP size recorded from muscles on the right (trained) arm relative to the initial assessment period. MEP area was calculated as the area under the curve above background EMG activity for a custom window for each muscle-stimulus combination. Asterisks represent a statistically significant change ($p<0.05$) in MEP size relative to the initial assessment stage. ***A.*** Changes in MEP size averaged across all muscles (1DI, EDC, FDS, BB, PD, PM) following Z-score transformation of individual muscle percentages. ***B.*** Same, but with normalisation of values relative to background EMG. ***C.*** Percentage change in MEP size for individual muscles normalised relative to background EMG across the four training stages: initial assessment (IA), training 1 (T1), training (T2) and washout (W). See Figure 4-1 for training stage details.

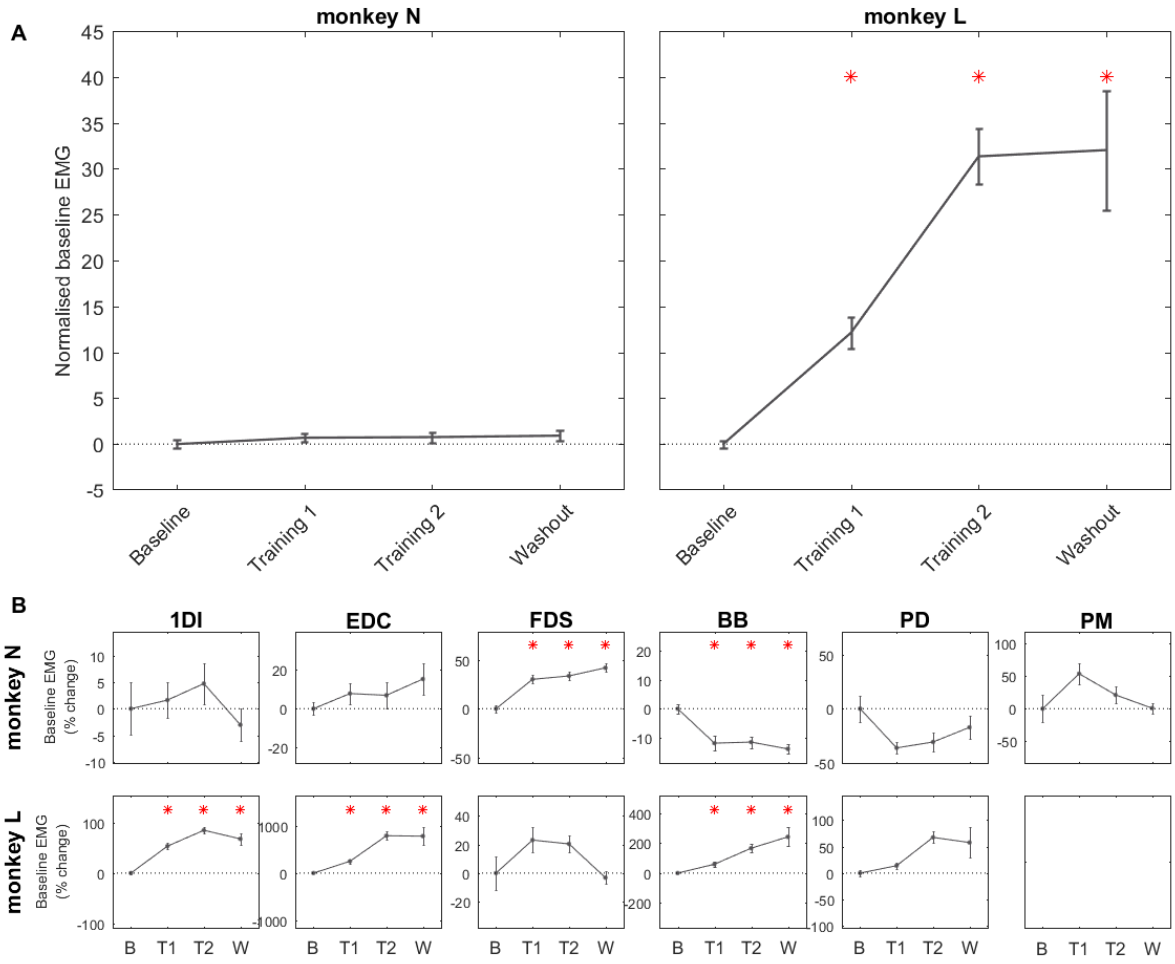

Figure 4-13. Long-term changes in background EMG activity in the left (untrained) arm

Change in background EMG activity recorded from muscles on the left (untrained) arm relative to the initial assessment period. Background EMG was calculated as mean rectified EMG activity measured over a 40ms window (-50 to -10ms) prior to each stimulus. Asterisks represent a statistically significant change ($p<0.05$) in background EMG relative to the initial assessment stage. ***A.*** Changes in background EMG activity averaged across all muscles (1DI, EDC, FDS, BB, PD, PM) following Z-score transformation of individual muscle percentages. ***B.*** Percentage change in background EMG activity for individual muscles across the four training stages: initial assessment (IA), training 1 (T1), training (T2) and washout (W). See Figure 4-1 for training stage details. Note that the arm was held in a restraint during these recordings.

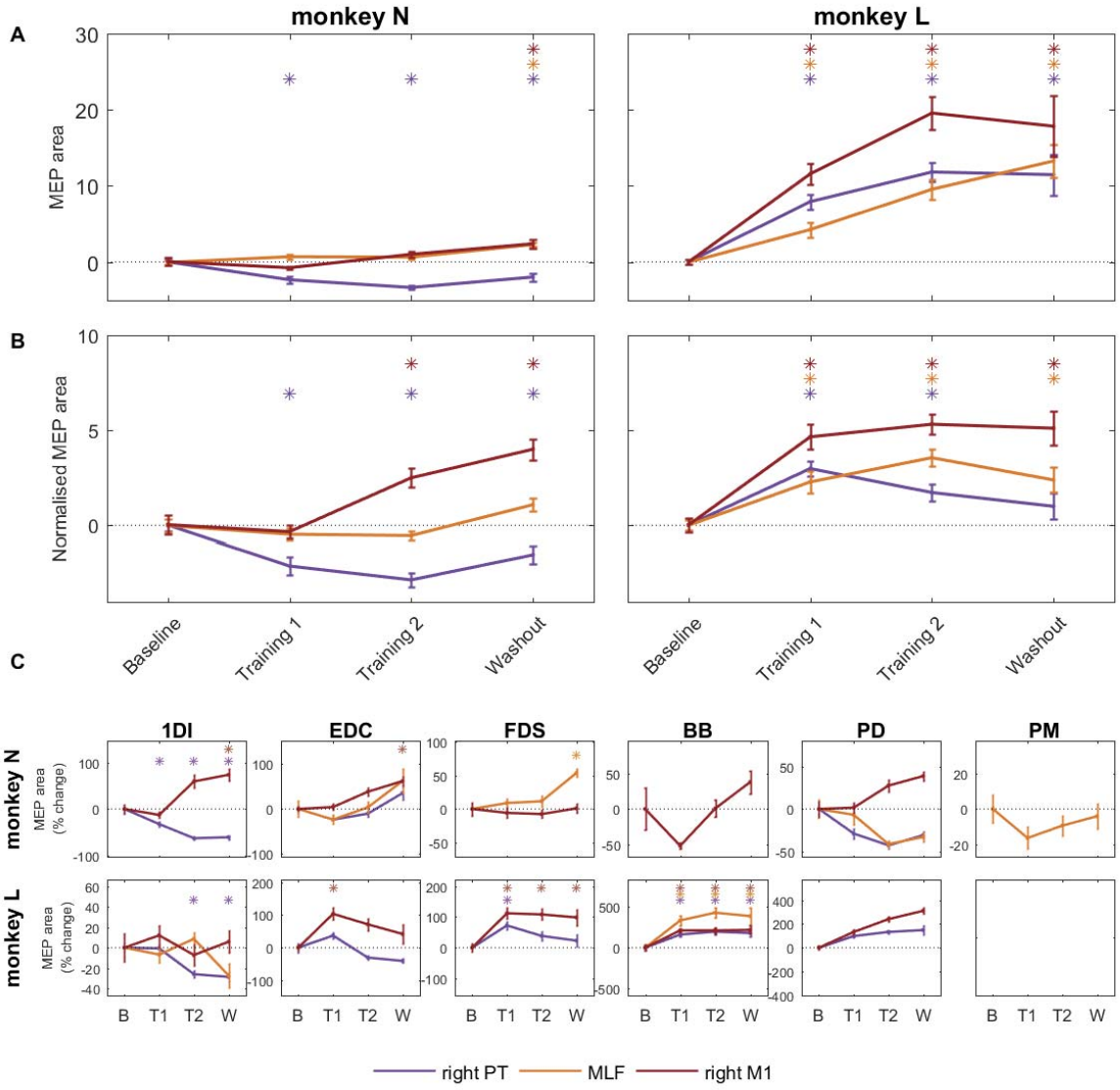

Figure 4-14. Long-term adaptations to strength training in the left (untrained) arm

Change in MEP size recorded from muscles on the left (untrained) arm relative to the initial assessment period. MEP area was calculated as the area under the curve above background EMG activity for a custom window for each muscle-stimulus combination. Asterisks represent a statistically significant change ($p<0.05$) in MEP size relative to the initial assessment stage. ***A.*** Changes in MEP size averaged across all muscles (1DI, EDC, FDS, BB, PD, PM) following Z-score transformation of individual muscle percentages. ***B.*** Same, but with normalisation of values relative to background EMG. ***C.*** Percentage change in MEP size for individual muscles normalised relative to background EMG across the four training stages: initial assessment (IA), training 1 (T1), training (T2) and washout (W). See Figure 4-1 for training stage details. Note that the arm was held in a restraint during these recordings.

Spinal adaptations

As expected, volleys were observed in the spinal cord recordings for all stimuli. In contrast, the field potentials were small even with the highest intensity stimuli when single stimuli were delivered. However, these field potentials, approximately 1ms after the volleys, were seen to grow with trains of three stimuli. Although the growth of a field with increasing number of stimuli would normally suggest a disynaptic connection, this is unlikely here due to the short latency relative to the volley. Instead, we propose that the field we recorded represents action potentials in the motoneurons and interneurons, which became more probable after stimulus trains due to temporal summation. This is supported by the field generally being concentrated within the regions corresponding to the ventral horn and intermediate zone.

The spinal data combined across both recording sites (rostral and caudal) and both monkeys show few significant differences between the left (untrained) and right (trained) sides of the cord for contralateral responses to PT stimulation (Figure 4-15). In contrast, RF stimulation resulted in a statistically significantly steeper volley-field gradient in the ventral horn on the right (trained) cord relative to the left (untrained) for all four equivalent recordings (Figure 4-15). This suggests that for a given reticular input, the right (trained) side of the cord generated a bigger output that the left (untrained) cord, which could be interpreted as an increase in synaptic efficacy. Similar results were observed regardless of whether the reticular volley was measured from the VLF or VMF. This likely relates to the significant correlation between volley amplitude recorded at these two sites (see Figure 4-16 for example), presumably due to similar activation of these two reticular pathways by our RF stimulus.

The results are less clear for ipsilateral stimulation. Ipsilateral PT stimulation resulted in a steeper volley-field gradient on the left (untrained) side of the cord, although this was not localised (Figure 4-15). Ipsilateral RF stimuli showed a similar effect to the contralateral stimuli, albeit a much weaker one, with an increase in volley-field gradient in the approximate region of the ventral horn and intermediate zone (Figure 4-15).

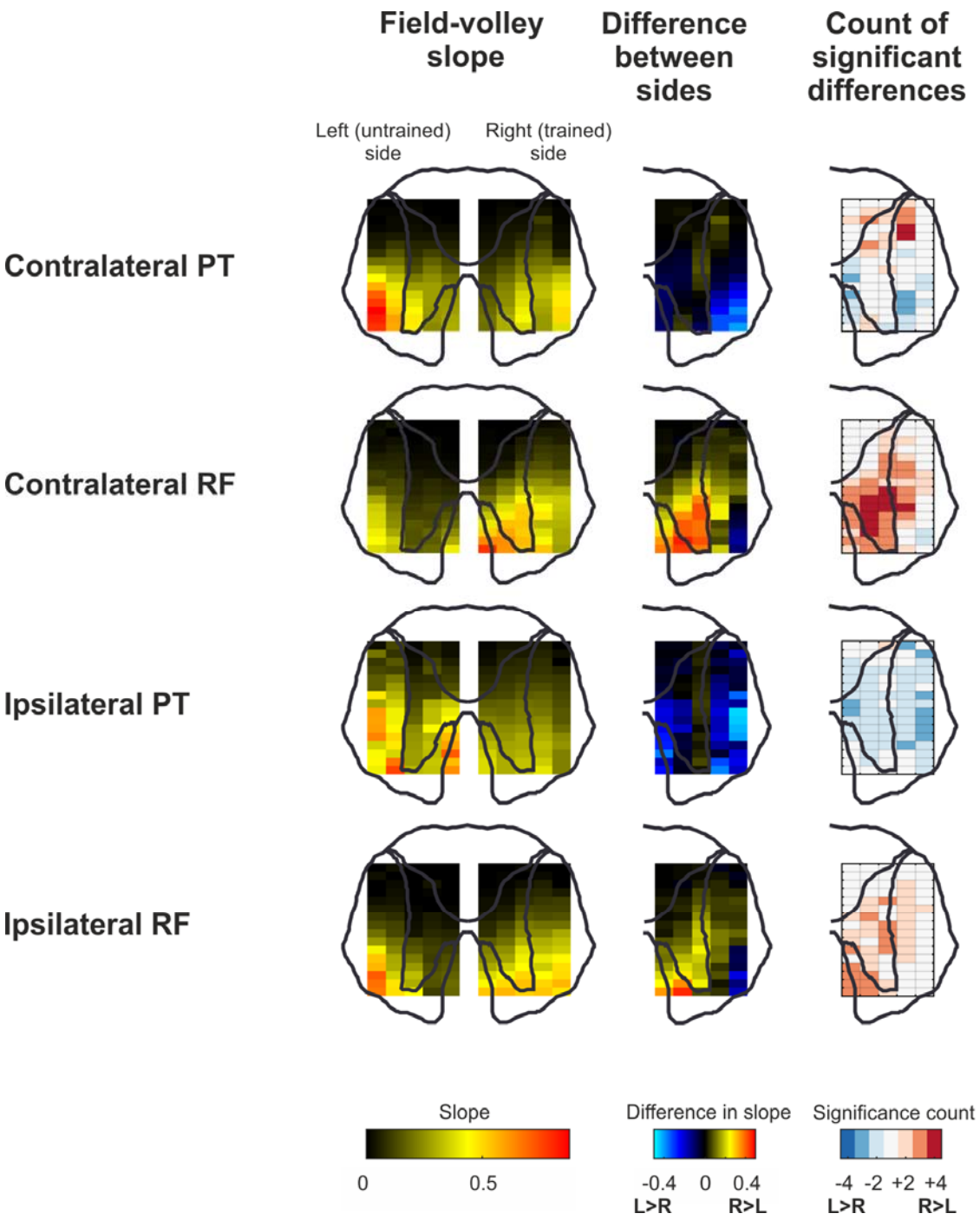

Figure 4-15. Spinal adaptations to strength training

Field-volley gradients are presented in the first column for contralateral PT volleys, contralateral RF volleys, ipsilateral PT volleys, and ipsilateral RF volleys. PT and RF volleys are measured from the areas corresponding to DLF and VLF, respectively (see Figure 4-5). The outline of the cord indicates the approximate location of each measurement. The second column shows the difference in gradient between the left and right side of the cord for each stimulus. The third column shows the statistical significance of this gradient difference (see Methods and Figure 4-6).

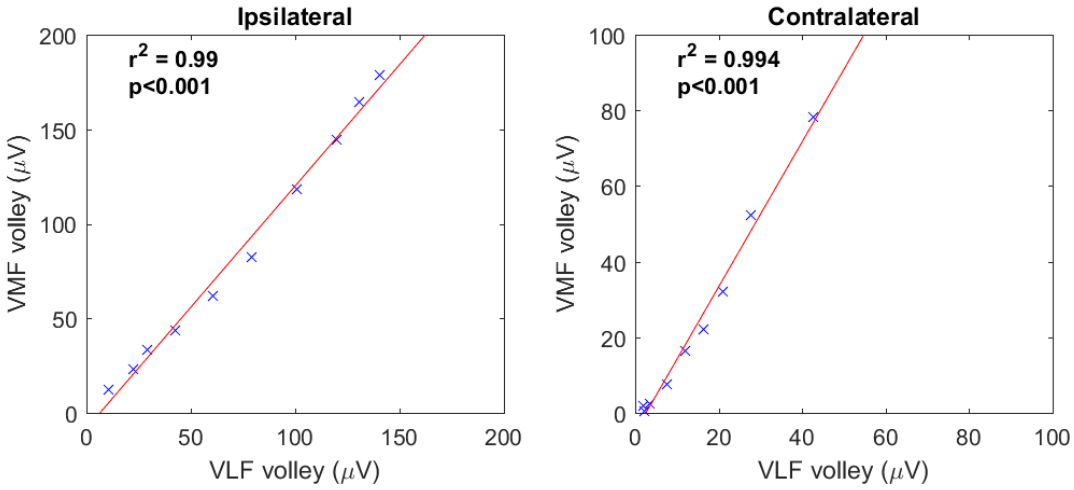

Figure 4-16. Correlation of volley amplitude for VLF and VMF

Example volley recordings made from sites corresponding to VLF and VMF (see Figure 4-5) for the left side of the cord at the caudal site of monkey N in response to ipsilateral (left panel) and contralateral (right panel) RF stimulation. Each data point shows a different stimulus intensity. A significant correlation was observed between VLF and VMF volleys (r^2 and p values shown on each panel).

Discussion

A fundamental feature of a strength training protocol is the demonstration of an increase in strength. This is straightforward to measure in human studies in which participants can be instructed to perform MVCs. Unsurprisingly, a recent meta-analysis reported an increase in strength in all examined strength training studies (Kidgell et al., 2017). However, in the absence of MVC measurements in our animal model, strength gains had to be inferred through other means.

Strength training typically consists of making repetitive movements against a substantial resistance, which could be defined as a load sufficient to induce fatigue – the reduction in force output from muscles following exercise. Fatigue can be assessed in our experiments by comparing stimulation effects. TMS studies have shown that low intensity contractions (10-50% MVC) can facilitate MEPs for 2-4 minutes post-exercise (Samii et al., 1996). With increasing force, and the emergence of fatigue, the facilitation decays rapidly and the response is instead dominated by a suppression that can last for up to 30 minutes (Brasil-Neto et al., 1993; Liepert et al., 1996; Samii et al., 1996). Based on the assumption that our M1 stimulation is comparable to TMS, with increasing load we would expect to see a shift from facilitation to suppression of MEPs, indicating that the task has progressed from low force to fatiguing

contractions. Although not statistically significant, this trend was observed in monkey N (Figure 4-10).

In contrast to TMS, strength training elicits an initial suppression of cervicomedullary MEPs (CMEPs) lasting approximately 1-4 minutes (Gandevia et al., 1999; Petersen et al., 2003), followed by a longer lasting facilitation (Nuzzo et al., 2016, 2018). Increasing the force of contraction from 50% to 100% MVC enhances the initial CMEP suppression (Petersen et al., 2003). Although we did not precisely time the interval between the strength training and post-training sessions, it was typically less than a minute. It is therefore possible that the observed PT MEP trend in both monkeys, from an increase in MEP size to a decrease in MEP size with increasing load, represents a shift in dominance from the later facilitation to the earlier suppression.

In combination, the reduction in background EMG and progression from facilitation to suppression of cortical MEPs in monkey N, along with the progression from facilitation to suppression of PT MEPs in both monkeys, provide support for the notion that the task was sufficiently fatiguing to constitute strength training.

Cortical and corticospinal contributions to strength training

The human strength training literature has made much use of the non-invasive techniques available to investigate the associated neural adaptation. Studies have predominantly focussed on TMS to assess cortical changes and reflex studies to examine spinal adaptations. Techniques to directly measure reticulospinal output non-invasively in humans are not currently available. In addition to intracortical and corticospinal circuitry, we were able to assess reticulospinal function in our animal model through stimulation of the MLF and RF, and the recording of EMG responses and spinal field potentials. The different synaptic locations at which changes might have occurred are indicated by the lower case letters in Figure 4-17, which are referenced in our consideration below.

The observed facilitation of M1 MEPs in the absence of a similar trend in PT MEPs suggests that neural adaptations occur at the cortical level (Figure 4-17*a*) with strength training. This is consistent with much of the human strength training literature. A recent meta-analysis reported a large effect of strength training interventions for decreasing short-interval intracortical

inhibition and a medium effect on reducing silent period duration (Kidgell et al., 2017), suggesting that strength training has an overall effect of reducing cortical inhibition.

The facilitation of M1 MEPs in the absence of a corresponding trend in PT MEPs also excludes the possibility that adaptations occurred at the corticomotoneuronal synapse (Figure 4-17*f*). In addition to our inconsistent MEP findings, we did not observe any significant differences in PT-elicited spinal field volleys between the right (trained) and left (untrained) side of the spinal cord. This suggests that either a bilateral adaptation has occurred, or that strength training does not have a significant effect on corticospinal synapses onto motoneurons or interneurons. We are unable to draw any conclusions about the disynaptic action of the corticospinal tract on motoneurons (Figure 4-17*e*) since this pathways is rarely activated by PT stimulation without attenuation of feedforward glycinergic inhibition from the pyramid with strychnine (Maier et al., 1997; Maier et al., 1998; Alstermark et al., 1999; Isa et al., 2006).

Reticulospinal contributions to strength training

We are not aware of any previous reports of reticulospinal adaptations with strength training. Our finding of a facilitation of MLF MEPs is therefore novel but perhaps not surprising. From the seminal work of Lawrence and Kuypers (1968b) it is evident that subcortical pathways contribute to strength. Following bilateral PT lesions, monkeys quickly recovered grip strength sufficient to climb the bars of their cage despite a lack of independent finger movements (Lawrence and Kuypers, 1968b). The authors commented that “The most striking change after the first four to six post-operative weeks was a progressive increase in their general strength” (Lawrence and Kuypers, 1968b). Given the absence of corticospinal projections in these animals, it is likely that this increase in strength was mediated by subcortical pathways. More recent work has directly implicated the reticulospinal tract in this recovery process, demonstrating through intracellular motoneuron recordings that reticulospinal projections can strengthen following corticospinal lesions (Zaaimi et al., 2012). Furthermore, a recent study proposed two separable systems for recovery following stroke, one contributing all of the strength some individuation, the second providing additional individuation. Lesion analysis suggests these two systems may respectively be reticulospinal and corticospinal in origin (Xu et al., 2017).

Another aspect of reticulospinal physiology implicating it in strength training is the extensive collateralisation of the RST (Peterson et al., 1975; Matsuyama et al., 1997) and thus its

disposition to activate muscle synergies. Strength training tasks typically involve gross movements requiring co-activation of several muscles, in contrast to the independent finger movements that may be associated with skill training. Our simple lever pulling task generated substantial EMG activity in all recorded muscles on the active arm (Figure 4-7), thus showing more similarity to the gross movements mediated by the reticulospinal tract (Davidson and Buford, 2004; Davidson and Buford, 2006) than the sophisticated individuation associated with corticospinal function (Zaaimi et al., 2018). It is therefore reasonable to suggest that repeated performance of the gross movements commonly associated with strength training are more likely to generate adaptive changes in the reticulospinal pathways.

We assessed reticulospinal function on a daily basis through stimulation of the MLF in awake behaving monkeys. Our results show an increase in the size of MLF MEPs with increasing weight in both monkeys, suggesting an increase in the synaptic efficacy of reticulospinal inputs to the spinal cord. In support of this, after a further three months of strength training, spinal recordings demonstrated a steeper gradient between volley and field amplitude for the right (trained) side of the cord relative to the left (untrained) side in the region corresponding to the intermediate zone and ventral horn. It is important to note that this method does not permit quantification of absolute changes in synaptic efficacy but instead simply provides a comparison between the two sides of the cord. It is therefore possible that the observed effect could be due to an increase in synaptic efficacy on the right side of the cord, a decrease on the left side of the cord, or perhaps a bilateral adaptation that was more pronounced on one side. Given the observed facilitation of MLF MEPs, we interpret this result as an increase in synaptic efficacy of descending reticulospinal projections onto either interneurons or motoneurons in the right (trained) side of the spinal cord. Alternatively, given that stimulus trains delivered to the PT or RF have been shown to produce a later volley thought to represent activation of corticoreticular and reticulo-reticular connections, respectively (Jankowska et al., 2003; Edgley et al., 2004; Fisher et al., 2015), it is possible that the ‘field’ we measured at the VLF is actually a supernumerary volley. Therefore, increased synaptic efficacy within the RF may also contribute to the observed changes in field potential.

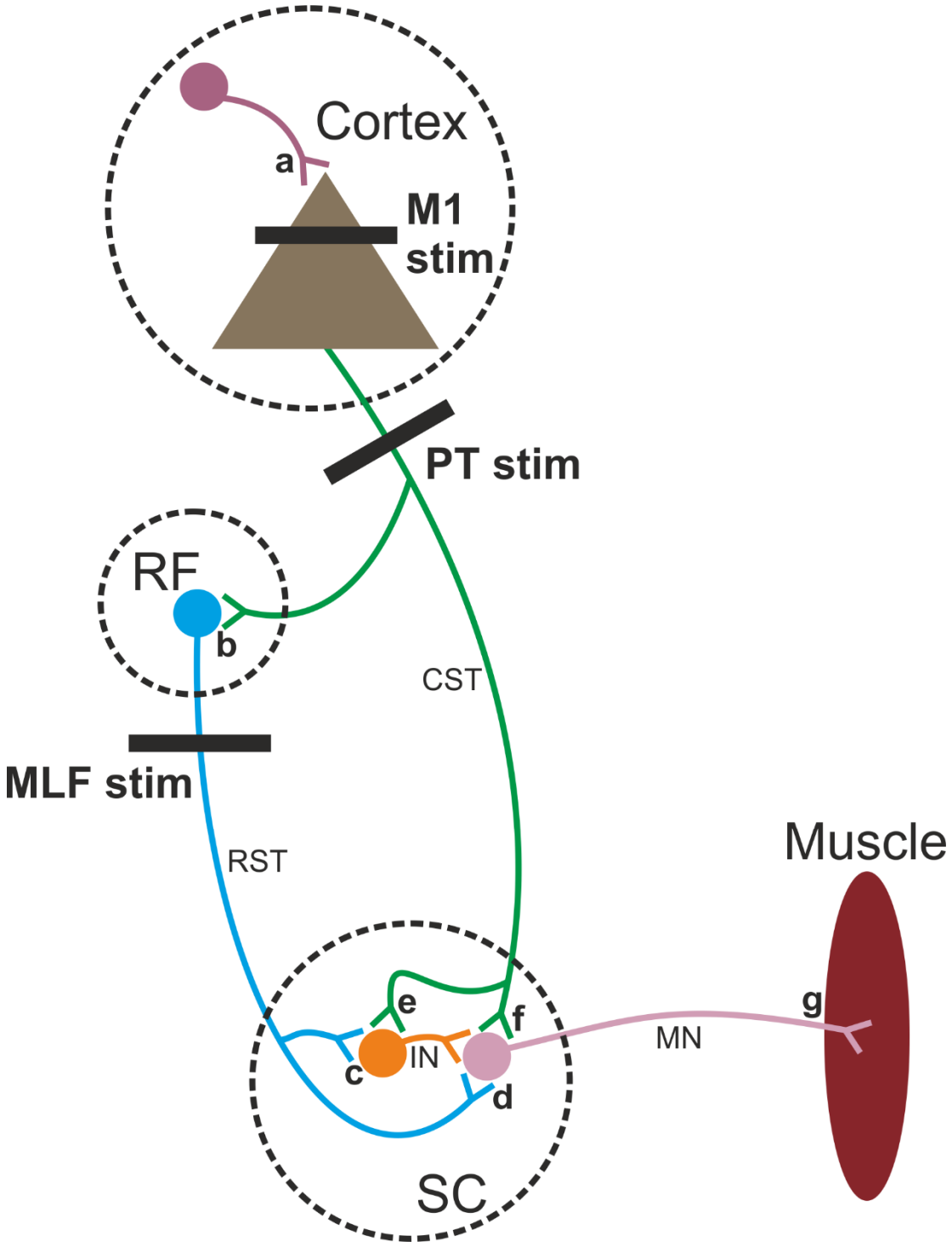

Figure 4-17. Schematic showing simplified pathways

Strength training may induce adaptive changes in ***(a)*** intracortical circuits, ***(b)*** corticoreticular connections, ***(c)*** reticulospinal projections to interneurons, ***(d)*** monosynaptic reticular projections to motoneurons, ***(e)*** corticospinal projections to interneurons, ***(f)*** corticomotoneuronal synapses, and/or ***(g)*** within the motor units themselves. See discussion.

The RST has been shown to form both monosynaptic and disynaptic connections with upper limb motoneurons (Riddle et al., 2009). We observed widespread differences in synaptic efficacy between the left (untrained) and right (trained) cord, which appeared concentrated in the intermediate zone rather than amongst the motor nuclei (Figure 4-15). This suggests that changes in reticulospinal output following strength training are more likely to occur at reticulospinal-interneuron synapses (Figure 4-17*c*) than reticulospinal-motoneuron synapses (Figure 4-17*d*).

We reject the hypothesis that the observed adaptations are entirely due to post-synaptic changes in either motoneurons or interneurons leading to a changes in excitability, since these both receive convergent inputs from reticulospinal and corticospinal projections (Riddle et al., 2009; Riddle and Baker, 2010). If post-synaptic adaptations were a dominant effect we would expect to see similar trends for both our reticular and corticospinal stimuli, which was not the case. Although a rodent model has demonstrated considerable changes in motoneuron properties following a strength training programme (Krutki et al., 2017) and similar adaptations may be occurring here, the differences between the MEPs observed with PT, MLF and M1 stimulation in our experiments suggest that motoneuron changes are not the dominant factor. There is the possibility that our results are due to an increase in motoneuron excitability and decrease in PT responses in the absence of any MLF and M1 changes, but this is unlikely, particularly when considered in combination with our spinal recordings.

Interestingly, we observed relatively similar trends in MEPs across all muscles examined. This is perhaps surprising in relation to the proximal-distal bias reported for corticospinal innervation. Given that corticospinal excitatory post-synaptic potentials (EPSPs) are greater in motoneurons innervating distal compared to proximal muscles (Porter and Lemon, 1993), whereas the amplitude of MLF-evoked EPSPs is similar across different muscle groups (Riddle et al., 2009), it could be expected that the relative size of PT and MLF MEPs would change from distal to proximal muscles. We observed no such distal to proximal trends. A possible explanation for this is activation of reticular pathways with the PT stimulus via cortico-reticular collaterals. Branching collaterals from the corticospinal tract project to the reticular formation in monkeys (Keizer and Kuypers, 1989) (Figure 4-17*b*). These corticoreticular connections can be activated with TMS (Fisher et al., 2012) and increasing evidence suggests they may be of importance in the recovery of strength following cortical injury (Darling et al., 2018; McPherson et al., 2018).

Cross-education effects

MEP recordings from the left (untrained) arm provide insight into the neural adaptations associated with cross-education. The increase in both M1 and MLF MEPs (Figure 4-14) indicates that neural adaptations are occurring in the untrained limb. Furthermore, although the respective reduction and increase in PT MEP size for monkey N and L contradict each other, they match the trends observed in the right (trained) arm of each monkey. Overall these findings suggest that cross-education occurs both at the level of the cortex and spinal cord; this is in agreement with a recent proposal that "neural adaptations to cross-education are due to structural and functional changes within the cortical motor and non-motor regions and subtle changes along the entire neuroaxis" (Frazer et al., 2018).

Cortical changes associated with cross-education have been studied in humans using both imaging and electrophysiological methods (Frazer et al., 2018). The former support the importance of interhemispheric pathways (Farthing et al., 2007; Palmer et al., 2013; Ruddy and Leemans, 2017) whereas the latter implicate increased corticospinal excitability (Kidgell et al., 2015), decreased corticospinal inhibition (Hendy et al., 2015; Coombs et al., 2016), reduced interhemispheric inhibition (Hortobagyi et al., 2011; Zult et al., 2016) and increased voluntary activation (Lee et al., 2009) in cross-education.

In contrast, few studies have examined spinal adaptations associated with cross-education (Frazer et al., 2018). Given that our PT and MLF electrodes were positioned amongst the axons of the CST and RST respectively, it can be assumed that any bilateral changes in the MEPs of these stimuli are due to spinal adaptations. We propose that commissural interneurons may mediate an element of cross-education. Reticulospinal projections have been shown to terminate on commissural interneurons, which in turn synapse onto contralateral motoneurons (Bannatyne et al., 2003; Jankowska et al., 2003; Edgley et al., 2004; Hammar et al., 2007). It is perhaps surprising that there has been little mention of the reticulospinal tract in cross-education given the bilateral actions of this pathway in both cats (Jankowska et al., 2003; Schepens and Drew, 2006b) and primates (Davidson et al., 2007).

It is important to note that although our task did generate some bilateral activation (Figure 4-7), particulary in more proximal muscles, there is not an obvious relationship between the active/inactive muscles on the left (untrained) and the changes in MEP size, thus making it

likely that the effects observed are due to a pure cross-education effect rather than active strength training in these muscles.

Summary

Strength training likely generates neural adaptations throughout the motor system, both unilaterally and bilaterally. We propose that for gross upper body movements eliciting significant co-activation, these adaptations primarily occur in intracortical and reticular networks. The latter likely consists of pre-synaptic changes at the synapses between descending reticulospinal projections and either motoneurons or interneurons. Although we cannot rule out adaptations in motoneurons, we suggest that these did not make a significant contribution in our strength training model. Furthermore, our results suggest corticospinal adaptations do not play a major role. These findings highlight reticulospinal pathways as a new contender in the strength training field.

CHAPTER V

General discussion

The human literature on motor neuroscience has focussed predominantly on the corticospinal tract (CST); a bias that reflects its position as the dominant descending pathway. However, the motor system consists of an extensive network of neurons and it is an overly simplistic view to limit the study of this to any single component. Instead, an integrated approach for studying the motor system is required; this should involve consideration of cortical networks, the multiple descending pathways, and spinal cord circuitry. It is unlikely that any of these components simply represents a relay station; instead, increasing evidence shows that in addition to the processing that occurs at the level of the cortex, brainstem motor pathways and interneuron circuits also actively modulate motor commands.

Our understanding of the motor system is largely attributable to animal experiments in which anatomy can be studied in detail and the activity of single neurons can be recorded in both awake and anaesthetised models. These experiments provide much insight into the motor systems of individual species, but the translation of findings across different species is limited due to both fundamental and subtle differences. For example, the corticomotoneuronal (CM) cells associated with independent finger movements are present only in primates and even within this group the CM system has developed to variable extents. Similarly, although rodents represent a readily available animal model, the CST in these animals differs to that of primates since it descends in the dorsal columns and can make a substantial ipsilateral contribution.

Therefore, although the findings of animal experiments can provide a conceptual framework of the motor system, the study of the human motor system requires the use of non-invasive techniques. The introduction of transcranial electrical stimulation (TES) and transcranial magnetic stimulation (TMS) in the 1980s has propelled the study of the human motor system, specifically the CST. Given the widespread use of these techniques and the increasing number of inferences about motor control that are made using them, it is important that we understand their underlying mechanisms. Crucially, TMS does not simply provide an on/off switch for the

CST but instead the responses evoked in muscles represent a complex interplay between interneuron circuits in the cortex and spinal cord.

The application of non-invasive techniques used in humans to animal models can provide a means of studying their specific mechanisms of action. Despite the considerable inter-species differences in the motor system, these experiments can still improve our understanding of non-invasive techniques when considered in the context of the human literature. To this end, we delivered TMS to anaesthetised macaques and recorded from individual corticospinal axons, thereby providing insight into the action of TMS on single cells. Our results differ from the population effects observed with epidural or electromyography recordings. In combination with the known heterogeneity of the CST, our findings further highlight the complexity of the responses evoked by TMS. It is also important to remember that the large, directional current induced in the cortex by transcranial stimulation is unlikely to mimic physiological excitation of the descending CST. Caution is therefore required in the interpretation of TMS experiments and the comparability of these findings to the physiological control of movement.

Non-invasive techniques can also be used to study the reticulospinal tract (RST). Although less widespread than those available for the CST, these techniques are increasingly being used to characterise this brainstem motor pathway in humans. For example, by combining startling auditory stimuli with a visually-guided reaching task, we propose to have modulated reticulospinal output. Furthermore, in line with the wealth of literature studying corticospinal plasticity, our results indicate that plastic effects can also be induced in the RST. In contrast to TMS, the sensory stimuli used in these experiments represent physiological activation of the motor system. However, they are unlikely to evoke a pure reticulospinal response and the extent of the involvement of other pathways is unknown.

The selective excitation of descending pathways is only possible in animal models through the use of surgical techniques. For example, electrodes can be implanted into the pyramidal tract to give a pure excitation of the CST. Reticulospinal isolation is more complex since the medial longitudinal fasciculus, in which the RST descends, also contains vestibulospinal and tectospinal fibres. Nonetheless, compared to the non-invasive techniques available in humans, the surgical methods commonly used in animal experiments are significantly more selective and so are of great value when comparing corticospinal and reticulospinal function. We applied such techniques to study the relative contributions of these two pathways to strength training.

To date, the strength training literature has focussed almost exclusively on the CST. Although it is well established that strength training induces neural adaptations, it is perhaps surprising that so much emphasis has fallen on a pathway whose most characteristic feature is the control of fine, fractionated movement. In contrast, there is evidence to suggest a reticulospinal role in strength-induced adaptations. To compare the adaptations that occur in these two pathways with strength training, two macaques were trained to perform a weight lifting task and the output of each pathway periodically assessed through stimulation of electrodes chronically implanted into their axon bundles, as well as epidural stimulation of the cortex. In support of the literature, the results demonstrate a considerable cortical adaptation; however, no consistent changes were recorded from the CST. Crucially, an increase in reticulospinal excitability was evident.

Having shown that the RST adapts during strength training, the next question to ask was whether neurons within the reticular formation code for force. Previous studies have shown that the firing rate of CM cells correlates with load for low force levels but can saturate at higher force levels (Cheney and Fetz, 1980; Maier et al., 1993). However, it is not known whether reticular cells show a similar relationship. To address this question and establish the relative contributions of the CST and RST to strength, we recorded from individual pyramidal tract neurons and reticular neurons whilst two macaques performed a weight lifting task with a range of loads, up to and including the equivalent of their bodyweight. Due to time constraints, the data collected in these experiments have not yet been analysed and are not presented in this thesis. Nonetheless, these recordings will provide unique insight into the neural mechanisms underlying strength.

In summary, our understanding of the motor system and the relative contribution of the CST and RST has advanced considerably since the macaque lesion studies performed 50 years ago. However, the failure to translate these findings into clinically relevant outcomes for patients with motor deficits highlights the significant gaps in our knowledge. This may relate to the corticospinal-centric view that has dominated the field, as well as inter-species differences. Only by bridging the gap between human and animal studies, and considering the complex interplay between all elements of the motor systems, can we advance our clinical and scientific understanding of movement.

REFERENCES

Akima H, Takahashi H, Kuno SY, Masuda K, Masuda T, Shimojo H, Anno I, Itai Y, Katsuta S (1999) Early phase adaptations of muscle use and strength to isokinetic training. Med Sci Sports Exerc 31:588-594.

Alstermark B, Isa T, Ohki Y, Saito Y (1999) Disynaptic pyramidal excitation in forelimb motoneurons mediated via C(3)-C(4) propriospinal neurons in the Macaca fuscata. J Neurophysiol 82:3580-3585.

Amassian VE, Eberle L, Maccabee PJ, Cracco RQ (1992) Modelling magnetic coil excitation of human cerebral cortex with a peripheral nerve immersed in a brain-shaped volume conductor: the significance of fiber bending in excitation. Electroencephalogr Clin Neurophysiol 85:291-301.

Anderson CT, Sheets PL, Kiritani T, Shepherd GM (2010) Sublayer-specific microcircuits of corticospinal and corticostriatal neurons in motor cortex. Nat Neurosci 13:739-744.

Armatas CA, Summers JJ, Bradshaw JL (1994) Mirror movements in normal adult subjects. J Clin Exp Neuropsychol 16:405-413.

Baker SN (2011) The primate reticulospinal tract, hand function and functional recovery. The Journal of physiology 589:5603-5612.

Baker SN, Perez MA (2017) Reticulospinal Contributions to Gross Hand Function after Human Spinal Cord Injury. J Neurosci 37:9778-9784.

Baker SN, Olivier E, Lemon RN (1995) Task-related variation in corticospinal output evoked by transcranial magnetic stimulation in the macaque monkey. J Physiol 488 (Pt 3):795-801.

Baker SN, Zaaimi B, Fisher KM, Edgley SA, Soteropoulos DS (2015) Pathways mediating functional recovery. Prog Brain Res 218:389-412.

Bannatyne BA, Edgley SA, Hammar I, Jankowska E, Maxwell DJ (2003) Networks of inhibitory and excitatory commissural interneurons mediating crossed reticulospinal actions. Eur J Neurosci 18:2273-2284.

Barker AT, Jalinous R, Freeston IL (1985) Non-invasive magnetic stimulation of human motor cortex. Lancet 1:1106-1107.

Berardelli A, Inghilleri M, Cruccu G, Manfredi M (1990) Descending volley after electrical and magnetic transcranial stimulation in man. Neurosci Lett 112:54-58.

Bernhard CG, Bohm E (1954) Cortical representation and functional significance of the corticomotoneuronal system. AMA Arch Neurol Psychiatry 72:473-502.

Berrevoets CE, Kuypers HG (1975) Pericruciate cortical neurons projecting to brain stem reticular formation, dorsal column nuclei and spinal cord in the cat. Neurosci Lett 1:257-262.

Bichot NP, Heard MT, Desimone R (2011) Stimulation of the nucleus accumbens as behavioral reward in awake behaving monkeys. J Neurosci Methods 199:265-272.

Bourbonnais D, Vanden Noven S, Carey KM, Rymer WZ (1989) Abnormal spatial patterns of elbow muscle activation in hemiparetic human subjects. Brain 112 (Pt 1):85-102.

Boyd SG, Rothwell JC, Cowan JM, Webb PJ, Morley T, Asselman P, Marsden CD (1986) A method of monitoring function in corticospinal pathways during scoliosis surgery with a note on motor conduction velocities. J Neurol Neurosurg Psychiatry 49:251-257.

Brasil-Neto JP, Pascual-Leone A, Valls-Sole J, Cammarota A, Cohen LG, Hallett M (1993) Postexercise depression of motor evoked potentials: a measure of central nervous system fatigue. Exp Brain Res 93:181-184.

Brebner JMT, Welford AT (1980) Reaction times. London: Academic Press.

Brown P, Rothwell JC, Thompson PD, Britton TC, Day BL, Marsden CD (1991) New observations on the normal auditory startle reflex in man Brain 114.

Buford JA, Davidson AG (2004) Movement-related and preparatory activity in the reticulospinal system of the monkey. Exp Brain Res 159:284-300.

Bunday KL, Tazoe T, Rothwell JC, Perez Ma (2014) Subcortical Control of Precision Grip after Human Spinal Cord Injury. J Neurosci 34:7341-7350.

Burke D, Hicks R, Gandevia SC, Stephen J, Woodforth I, Crawford M (1993) Direct comparison of corticospinal volleys in human subjects to transcranial magnetic and electrical stimulation. J Physiol 470:383-393.

Buys EJ, Lemon RN, Mantel GW, Muir RB (1986) Selective facilitation of different hand muscles by single corticospinal neurones in the conscious monkey. The Journal of physiology 381:529-549.

Carlsen A, Chua R, Inglis JT, Sanderson DJ, Franks IM (2004a) Prepared movements are elicited early by startle. J Mot Behav 36:253-264.

Carlsen AN, Maslovat D, Franks IM (2012) Preparation for voluntary movement in healthy and clinical populations: evidence from startle. Clin Neurophysiol 123:21-33.

Carlsen AN, Hunt MA, Inglis JT, Sanderson DJ, Chua R (2003) Altered triggering of a prepared movement by a startling stimulus. J Neurophysiol 89:1857-1863.

Carlsen AN, Chua R, Inglis JT, Sanderson DJ, Franks IM (2004b) Can prepared responses be stored subcortically? Exp Brain Res 159:301-309.

Carlsen AN, Chua R, Inglis JT, Sanderson DJ, Franks IM (2009) Differential effects of startle on reaction time for finger and arm movements. J Neurophysiol 101:306-314.

Carlsen AN, Maslovat D, Lam MY, Chua R, Franks IM (2011) Considerations for the use of a startling acoustic stimulus in studies of motor preparation in humans. Neurosci Biobehav Rev 35:366-376.

Carlton LG (1981) Processing visual feedback information for movement control. J Exp Psychol Hum Percept Perform 7:1019-1030.

Carroll TJ, Selvanayagam VS, Riek S, Semmler JG (2011) Neural adaptations to strength training: moving beyond transcranial magnetic stimulation and reflex studies. Acta Physiol (Oxf) 202:119-140.

Cerri G, Shimazu H, Maier MA, Lemon RN (2003) Facilitation from ventral premotor cortex of primary motor cortex outputs to macaque hand muscles. J Neurophysiol 90:832-842.

Cheney PD, Fetz EE (1980) Functional classes of primate corticomotoneuronal cells and their relation to active force. J Neurophysiol 44:773-791.

Coombs TA, Frazer AK, Horvath DM, Pearce AJ, Howatson G, Kidgell DJ (2016) Cross-education of wrist extensor strength is not influenced by non-dominant training in right-handers. Eur J Appl Physiol 116:1757-1769.

Cykowski MD, Coulon O, Kochunov PV, Amunts K, Lancaster JL, Laird AR, Glahn DC, Fox PT (2008) The central sulcus: an observer-independent characterization of sulcal landmarks and depth asymmetry. Cereb Cortex 18:1999-2009.

D'Ostilio K, Goetz SM, Hannah R, Ciocca M, Chieffo R, Chen JA, Peterchev AV, Rothwell JC (2016) Effect of coil orientation on strength-duration time constant and I-wave activation with controllable pulse parameter transcranial magnetic stimulation. Clin Neurophysiol 127:675-683.

Darling WG, Ge J, Stilwell-Morecraft KS, Rotella DL, Pizzimenti MA (2018) Hand Motor Recovery Following Extensive Frontoparietal Cortical Injury Is Accompanied by Upregulated Corticoreticular Projections in Monkey. 38:6323-6339.

Davidson AG, Buford JA (2004) Motor outputs from the primate reticular formation to shoulder muscles as revealed by stimulus-triggered averaging. J Neurophysiol 92:83-95.

Davidson AG, Buford JA (2006) Bilateral actions of the reticulospinal tract on arm and shoulder muscles in the monkey: stimulus triggered averaging. Exp Brain Res 173:25-39.

Davidson AG, Schieber MH, Buford JA (2007) Bilateral spike-triggered average effects in arm and shoulder muscles from the monkey pontomedullary reticular formation. J Neurosci 27:8053-8058.

Davis M, Gendelman DS, Tischler MD, Gendelman PM (1982) A primary acoustic startle circuit: lesion and stimulation studies. J Neurosci 2:791-805.

Day BL, Lyon IN (2000) Voluntary modification of automatic arm movements evoked by motion of a visual target. Exp Brain Res 130:159-168.

Day BL, Brown P (2001) Evidence for subcortical involvement in the visual control of human reaching. Brain 124:1832-1840.

Day BL, Dressler D, Maertens de Noordhout A, Marsden CD, Nakashima K, Rothwell JC, Thompson PD (1989) Electric and magnetic stimulation of human motor cortex: surface EMG and single motor unit responses. J Physiol 412:449-473.

Dean LR, Baker SN (2017) Fractionation of muscle activity in rapid responses to startling cues. J Neurophysiol 117:1713-1719.

Deliagina TG, Beloozerova IN, Zelenin PV, Orlovsky GN (2008) Spinal and supraspinal postural networks. Brain Res Rev 57:212-221.

Dewald JPA, Pope PS, Given JD, Buchanan TS, Rymer WZ (1995) Abnormal muscle coactivation patterns during isometric torque generation at the elbow and shoulder in hemiparetic subjects. Brain 118 (Pt 2):495-510.

Di Lazzaro V, Ziemann U (2013) The contribution of transcranial magnetic stimulation in the functional evaluation of microcircuits in human motor cortex. Front Neural Circuits 7:18.

Di Lazzaro V, Oliviero A, Profice P, Insola A, Mazzone P, Tonali P, Rothwell JC (1999a) Effects of voluntary contraction on descending volleys evoked by transcranial electrical stimulation over the motor cortex hand area in conscious humans. Exp Brain Res 124:525-528.

Di Lazzaro V, Oliviero A, Profice P, Insola A, Mazzone P, Tonali P, Rothwell JC (1999b) Direct demonstration of interhemispheric inhibition of the human motor cortex produced by transcranial magnetic stimulation. Exp Brain Res 124:520-524.

Di Lazzaro V, Oliviero A, Meglio M, Cioni B, Tamburrini G, Tonali P, Rothwell JC (2000) Direct demonstration of the effect of lorazepam on the excitability of the human motor cortex. Clin Neurophysiol 111:794-799.

Di Lazzaro V, Restuccia D, Oliviero A, Profice P, Ferrara L, Insola A, Mazzone P, Tonali P, Rothwell JC (1998a) Effects of voluntary contraction on descending volleys evoked by transcranial stimulation in conscious humans. J Physiol 508 (Pt 2):625-633.

Di Lazzaro V, Oliviero A, Profice P, Saturno E, Pilato F, Insola A, Mazzone P, Tonali P, Rothwell JC (1998b) Comparison of descending volleys evoked by transcranial magnetic and electric stimulation in conscious humans. Electroencephalogr Clin Neurophysiol 109:397-401.

Di Lazzaro V, Restuccia D, Oliviero A, Profice P, Ferrara L, Insola A, Mazzone P, Tonali P, Rothwell JC (1998c) Magnetic transcranial stimulation at intensities below active motor threshold activates intracortical inhibitory circuits. Exp Brain Res 119:265-268.

Di Lazzaro V, Oliviero A, Saturno E, Pilato F, Insola A, Mazzone P, Profice P, Tonali P, Rothwell JC (2001) The effect on corticospinal volleys of reversing the direction of current induced in the motor cortex by transcranial magnetic stimulation. Exp Brain Res 138:268-273.

Di Lazzaro V, Oliviero A, Mazzone P, Pilato F, Saturno E, Insola A, Visocchi M, Colosimo C, Tonali PA, Rothwell JC (2002) Direct demonstration of long latency cortico-cortical inhibition in normal subjects and in a patient with vascular parkinsonism. Clin Neurophysiol 113:1673-1679.

Di Lazzaro V, Oliviero A, Pilato F, Saturno E, Dileone M, Meglio M, Cioni B, Papacci F, Tonali PA, Rothwell JC (2004) Comparison of descending volleys evoked by transcranial and epidural motor cortex stimulation in a conscious patient with bulbar pain. Clin Neurophysiol 115:834-838.

Drew T, Dubuc R, Rossignol S (1986) Discharge patterns of reticulospinal and other reticular neurons in chronic, unrestrained cats walking on a treadmill. J Neurophysiol 55:375-401.

Dum RP, Strick PL (2005) Frontal lobe inputs to the digit representations of the motor areas on the lateral surface of the hemisphere. J Neurosci 25:1375-1386.

Edgley SA, Jankowska E, Hammar I (2004) Ipsilateral actions of feline corticospinal tract neurons on limb motoneurons. J Neurosci 24:7804-7813.

Edgley SA, Eyre JA, Lemon RN, Miller S (1997) Comparison of activation of corticospinal neurons and spinal motor neurons by magnetic and electrical transcranial stimulation in the lumbosacral cord of the anaesthetized monkey. Brain 120 (Pt 5):839-853.

Enoka RM (1988) Muscle strength and its development. New perspectives. Sports Med 6:146-168.

Farthing JP, Borowsky R, Chilibeck PD, Binsted G, Sarty GE (2007) Neuro-physiological adaptations associated with cross-education of strength. Brain Topogr 20:77-88.

Firmin L, Field P, Maier MA, Kraskov A, Kirkwood PA, Nakajima K, Lemon RN, Glickstein M (2014) Axon diameters and conduction velocities in the macaque pyramidal tract. J Neurophysiol 112:1229-1240.

Fischer B, Rogal L (1986) Eye-hand-coordination in man: a reaction time study. Biol Cybern 55:253-261.

Fisher KM, Zaaimi B, Baker SN (2012) Reticular formation responses to magnetic brain stimulation of primary motor cortex. The Journal of physiology 590:4045-4060.

Fisher KM, Jillani NE, Oluoch GO, Baker SN (2015) Blocking central pathways in the primate motor system using high-frequency sinusoidal current. J Neurophysiol 113:1670-1680.

Fitzpatrick RC, Day BL (2004) Probing the human vestibular system with galvanic stimulation. Journal of applied physiology (Bethesda, Md : 1985) 96:2301-2316.

Folland JP, Williams AG (2007) The adaptations to strength training : morphological and neurological contributions to increased strength. Sports Med 37:145-168.

Fox PT, Narayana S, Tandon N, Sandoval H, Fox SP, Kochunov P, Lancaster JL (2004) Column-based model of electric field excitation of cerebral cortex. Hum Brain Mapp 22:1-14.

Foysal KM, de Carvalho F, Baker SN (2016) Spike Timing-Dependent Plasticity in the Long-Latency Stretch Reflex Following Paired Stimulation from a Wearable Electronic Device. J Neurosci 36:10823-10830.

Frazer AK, Pearce AJ, Howatson G, Thomas K, Goodall S, Kidgell DJ (2018) Determining the potential sites of neural adaptation to cross-education: implications for the cross-education of muscle strength. Eur J Appl Physiol.

Gandevia SC, Petersen N, Butler JE, Taylor JL (1999) Impaired response of human motoneurones to corticospinal stimulation after voluntary exercise. J Physiol 521 Pt 3:749-759.

Geyer S, Ledberg A, Schleicher A, Kinomura S, Schormann T, Burgel U, Klingberg T, Larsson J, Zilles K, Roland PE (1996) Two different areas within the primary motor cortex of man. Nature 382:805-807.

Grantyn A, Grantyn R (1982) Axonal patterns and sites of termination of cat superior colliculus neurons projecting in the tecto-bulbo-spinal tract. Exp Brain Res 46:243-256.

Gribble PL, Everling S, Ford K, Mattar A (2002) Hand-eye coordination for rapid pointing movements. Arm movement direction and distance are specified prior to saccade onset. Exp Brain Res 145:372-382.

Gu C, Pruszynski JA, Gribble PL (2018) Done in 100 ms: path-dependent visuomotor transformation in the human upper limb. 119:1319-1328.

Gu C, Wood DK, Gribble PL, Corneil BD (2016) A Trial-by-Trial Window into Sensorimotor Transformations in the Human Motor Periphery. 36:8273-8282.

Hammar I, Stecina K, Jankowska E (2007) Differential modulation by monoamine membrane receptor agonists of reticulospinal input to lamina VIII feline spinal commissural interneurons. Eur J Neurosci 26:1205-1212.

Hammond GR (1973) Lesions of pontine and medullary reticular formation and prestimulus inhibition of the acoustic startle reaction in rats. Physiol Behav 10:239-243.

Hanajima R, Ugawa Y, Terao Y, Sakai K, Furubayashi T, Machii K, Kanazawa I (1998) Paired-pulse magnetic stimulation of the human motor cortex: differences among I waves. J Physiol 509 (Pt 2):607-618.

Hendy AM, Teo WP, Kidgell DJ (2015) Anodal Transcranial Direct Current Stimulation Prolongs the Cross-education of Strength and Corticomotor Plasticity. Med Sci Sports Exerc 47:1788-1797.

Hern JE, Landgren S, Phillips CG, Porter R (1962) Selective excitation of corticofugal neurones by surface-anodal stimulation of the baboon's motor cortex. J Physiol 161:73-90.

Hess CW, Mills KR, Murray NM (1987) Responses in small hand muscles from magnetic stimulation of the human brain. J Physiol 388:397-419.

Honeycutt CF, Kharouta M, Perreault EJ (2013) Evidence for reticulospinal contributions to coordinated finger movements in humans. J Neurophysiol 110:1476-1483.

Hortobagyi T, Richardson SP, Lomarev M, Shamim E, Meunier S, Russman H, Dang N, Hallett M (2011) Interhemispheric plasticity in humans. Med Sci Sports Exerc 43:1188-1199.

Illert M, Lundberg A, Padel Y, Tanaka R (1978) Integration in descending motor pathways controlling the forelimb in the cat. 5. Properties of and monosynaptic excitatory convergence on C3--C4 propriospinal neurones. Exp Brain Res 33:101-130.

Irvine DR, Jackson GD (1983) Auditory input to neurons in mesencephalic and rostral pontine reticular formation: an electrophysiological and horseradish peroxidase study in the cat. J Neurophysiol 49:1319-1333.

Isa T, Ohki Y, Seki K, Alstermark B (2006) Properties of propriospinal neurons in the C3-C4 segments mediating disynaptic pyramidal excitation to forelimb motoneurons in the macaque monkey. J Neurophysiol 95:3674-3685.

Jankowska E, Hammar I, Slawinska U, Maleszak K, Edgley SA (2003) Neuronal basis of crossed actions from the reticular formation on feline hindlimb motoneurons. J Neurosci 23:1867-1878.

Jinnai K (1984) Electrophysiological study on the corticoreticular projection neurons of the cat. Brain Res 291:145-149.

Jones DA, Rutherford OM (1987) Human muscle strength training: the effects of three different regimens and the nature of the resultant changes. J Physiol 391:1-11.

Keizer K, Kuypers HG (1989) Distribution of corticospinal neurons with collaterals to the lower brain stem reticular formation in monkey (Macaca fascicularis). Exp Brain Res 74:311-318.

Kidgell DJ, Bonanno DR, Frazer AK, Howatson G, Pearce AJ (2017) Corticospinal responses following strength training: a systematic review and meta-analysis. Eur J Neurosci 46:2648-2661.

Kidgell DJ, Frazer AK, Daly RM, Rantalainen T, Ruotsalainen I, Ahtiainen J, Avela J, Howatson G (2015) Increased cross-education of muscle strength and reduced corticospinal inhibition following eccentric strength training. Neuroscience 300:566-575.

Kischka U, Fajfr R, Fellenberg T, Hess CW (1993) Facilitation of motor evoked potentials from magnetic brain stimulation in man: a comparative study of different target muscles. J Clin Neurophysiol 10:505-512.

Komi PV (1986) Training of muscle strength and power: interaction of neuromotoric, hypertrophic, and mechanical factors. Int J Sports Med 7 Suppl 1:10-15.

Korn H, Faber DS (2005) The Mauthner cell half a century later: a neurobiological model for decision-making? Neuron 47:13-28.

Krutki P, Mrowczynski W, Baczyk M, Lochynski D, Celichowski J (2017) Adaptations of motoneuron properties after weight-lifting training in rats. J Appl Physiol (1985) 123:664-673.

Kumru H, Valls-Sole J (2006) Excitability of the pathways mediating the startle reaction before execution of a voluntary movement. Exp Brain Res 169:427-432.

Kumru H, Urra X, Compta Y, Castellote JM, Turbau J, Valls-Sole J (2006) Excitability of subcortical motor circuits in Go/noGo and forced choice reaction time tasks. Neurosci Lett 406:66-70.

Kurtzer IL (2014) Long-latency reflexes account for limb biomechanics through several supraspinal pathways. Front Integr Neurosci 8:99.

Kuypers HG (1981) Anatomy of Descending Pathways: American Physiological Society, Bethesda, MD

Lang CE, Schieber MH (2003) Differential impairment of individuated finger movements in humans after damage to the motor cortex or the corticospinal tract. J Neurophysiol 90:1160-1170.

Lang CE, Schieber MH (2004) Reduced muscle selectivity during individuated finger movements in humans after damage to the motor cortex or corticospinal tract. J Neurophysiol 91:1722-1733.

Lawrence DG, Kuypers HGJM (1968a) The functional organization of the motor system in the monkey. II. The effects of lesions of the descending brain-stem pathways. Brain 91:15-36.

Lawrence DG, Kuypers HGJM (1968b) The functional organization of the motor system in the monkey. I. The effects of bilateral pyramidal tract lesions. Brain 91:1-14.

Lee M, Carroll TJ (2007) Cross education: possible mechanisms for the contralateral effects of unilateral resistance training. Sports Med 37:1-14.

Lee M, Gandevia SC, Carroll TJ (2009) Unilateral strength training increases voluntary activation of the opposite untrained limb. Clin Neurophysiol 120:802-808.

Leitner DS, Powers AS, Hoffman HS (1980) The neural substrate of the startle response. Physiol Behav 25:291-297.

Lemon RN (1984) Methods for Neuronal Recording in Conscious Animals: Wiley

Lemon RN (2008) Descending pathways in motor control. Annu Rev Neurosci 31:195-218.

Liepert J, Kotterba S, Tegenthoff M, Malin JP (1996) Central fatigue assessed by transcranial magnetic stimulation. Muscle Nerve 19:1429-1434.

Liu CN, Chambers WW (1964) An experimental study of the cortico-spinal system in the monkey (Macaca mulatta). The spinal pathways and preterminal distribution of

degenerating fibers following discrete lesions of the pre- and postcentral gyri and bulbar pyramid. J Comp Neurol 123:257-283.

Maccabee PJ, Amassian VE, Eberle LP, Cracco RQ (1993) Magnetic coil stimulation of straight and bent amphibian and mammalian peripheral nerve in vitro: locus of excitation. J Physiol 460:201-219.

Maccabee PJ, Eberle L, Amassian VE, Cracco RQ, Rudell A, Jayachandra M (1990) Spatial distribution of the electric field induced in volume by round and figure '8' magnetic coils: relevance to activation of sensory nerve fibers. Electroencephalogr Clin Neurophysiol 76:131-141.

MacKinnon CD, Bissig D, Chiusano J, Miller E, Rudnick L, Jager C, Zhang Y, Mille ML, Rogers MW (2007) Preparation of anticipatory postural adjustments prior to stepping. J Neurophysiol 97:4368-4379.

Maier MA, Bennett KM, Hepp-Reymond MC, Lemon RN (1993) Contribution of the monkey corticomotoneuronal system to the control of force in precision grip. J Neurophysiol 69:772-785.

Maier MA, Illert M, Kirkwood PA, Nielsen J, Lemon RN (1998) Does a C3-C4 propriospinal system transmit corticospinal excitation in the primate? An investigation in the macaque monkey. J Physiol 511 (Pt 1):191-212.

Maier MA, Olivier E, Baker SN, Kirkwood PA, Morris T, Lemon RN (1997) Direct and indirect corticospinal control of arm and hand motoneurons in the squirrel monkey (Saimiri sciureus). J Neurophysiol 78:721-733.

Matsuyama K, Takakusaki K, Nakajima K, Mori S (1997) Multi-segmental innervation of single pontine reticulospinal axons in the cervico-thoracic region of the cat: anterograde PHA-L tracing study. J Comp Neurol 377:234-250.

Mayston MJ, Harrison LM, Stephens JA (1999) A neurophysiological study of mirror movements in adults and children. Ann Neurol 45:583-594.

McPherson JG, Chen A, Ellis MD, Yao J, Heckman CJ, Dewald JPA (2018) Progressive recruitment of contralesional cortico-reticulospinal pathways drives motor impairment post stroke. J Physiol 596:1211-1225.

Merton PA, Morton HB (1980) Stimulation of the cerebral cortex in the intact human subject. Nature 285:227.

Miranda PC, Correia L, Salvador R, Basser PJ (2007) Tissue heterogeneity as a mechanism for localized neural stimulation by applied electric fields. Phys Med Biol 52:5603-5617.

Mori S, Matsuyama K, Mori F, Nakajima K (2001) Supraspinal sites that induce locomotion in the vertebrate central nervous system. Adv Neurol 87:25-40.

Moritani T, deVries HA (1979) Neural factors versus hypertrophy in the time course of muscle strength gain. Am J Phys Med 58:115-130.

Nakamura H, Kitagawa H, Kawaguchi Y, Tsuji H (1996) Direct and indirect activation of human corticospinal neurons by transcranial magnetic and electrical stimulation. Neurosci Lett 210:45-48.

Nathan, Smith (1955) Long descending tracts in man. Brain: a journal of neurology 78:248-303.

Nelles G, Cramer SC, Schaechter JD, Kaplan JD, Finklestein SP (1998) Quantitative assessment of mirror movements after stroke. Stroke; a journal of cerebral circulation 29:1182-1187.

Ni Z, Charab S, Gunraj C, Nelson AJ, Udupa K, Yeh IJ, Chen R (2011) Transcranial magnetic stimulation in different current directions activates separate cortical circuits. J Neurophysiol 105:749-756.

Nuzzo JL, Barry BK, Gandevia SC, Taylor JL (2016) Acute Strength Training Increases Responses to Stimulation of Corticospinal Axons. Med Sci Sports Exerc 48:139-150.

Nuzzo JL, Barry BK, Gandevia SC, Taylor JL (2018) Effects of acute isometric resistance exercise on cervicomedullary motor evoked potentials. Scand J Med Sci Sports 28:1514-1522.

Nyberg-Hansen R (1964a) The location and termination of tectospinal fibers in the cat. Exp Neurol 9:212-227.

Nyberg-Hansen R (1964b) Origin and termination of fibers from the vestibular nuclei descending in the medial longitudinal fasciculus. An experimental study with silver impregnation methods in the cat. J Comp Neurol 122:355-367.

Onodera S, Hicks TP (2010) Carbocyanine dye usage in demarcating boundaries of the aged human red nucleus. PloS one 5:e14430.

Palmer HS, Haberg AK, Fimland MS, Solstad GM, Moe Iversen V, Hoff J, Helgerud J, Eikenes L (2013) Structural brain changes after 4 wk of unilateral strength training of the lower limb. J Appl Physiol (1985) 115:167-175.

Patton HD, Amassian VE (1954) Single and multiple-unit analysis of cortical stage of pyramidal tract activation. J Neurophysiol 17:345-363.

Perez MA, Rothwell JC (2015) Distinct influence of hand posture on cortical activity during human grasping. J Neurosci 35:4882-4889.

Perfiliev S, Isa T, Johnels B, Steg G, Wessberg J (2010) Reflexive limb selection and control of reach direction to moving targets in cats, monkeys, and humans. J Neurophysiol 104:2423-2432.

Peterchev AV, Goetz SM, Westin GG, Luber B, Lisanby SH (2013) Pulse width dependence of motor threshold and input-output curve characterized with controllable pulse parameter transcranial magnetic stimulation. Clin Neurophysiol 124:1364-1372.

Petersen NT, Taylor JL, Butler JE, Gandevia SC (2003) Depression of activity in the corticospinal pathway during human motor behavior after strong voluntary contractions. J Neurosci 23:7974-7980.

Peterson BW, Maunz RA, Pitts NG, Mackel RG (1975) Patterns of projection and braching of reticulospinal neurons. Exp Brain Res 23:333-351.

Philipp R, Hoffmann KP (2014) Arm movements induced by electrical microstimulation in the superior colliculus of the macaque monkey. J Neurosci 34:3350-3363.

Porter R, Lemon R (1993) Corticospinal function and voluntary movement: Oxford: Oxford UP.

Prentice SD, Drew T (2001) Contributions of the reticulospinal system to the postural adjustments occurring during voluntary gait modifications. Journal of neurophysiology 85:679-698.

Pruszynski AJ, King GL, Boisse L, Scott SH, Randall Flanagan J, Munoz DP (2010) Stimulus-locked responses on human arm muscles reveal a rapid neural pathway linking visual input to arm motor output. Eur J Neurosci 32:1049-1057.

Raghavan P, Petra E, Krakauer JW, Gordon AM (2006) Patterns of impairment in digit independence after subcortical stroke. J Neurophysiol 95:369-378.

Ralston DD, Ralston HJ, 3rd (1985) The terminations of corticospinal tract axons in the macaque monkey. J Comp Neurol 242:325-337.

Rathelot J-A, Strick PL (2009) Subdivisions of primary motor cortex based on cortico-motoneuronal cells. Proceedings of the National Academy of Sciences of the United States of America 106:918-923.

Reynolds RF, Day BL (2007) Fast visuomotor processing made faster by sound. J Physiol 583:1107-1115.

Riddle CN, Baker SN (2010) Convergence of pyramidal and medial brain stem descending pathways onto macaque cervical spinal interneurons. J Neurophysiol 103:2821-2832.

Riddle CN, Edgley SA, Baker SN (2009) Direct and indirect connections with upper limb motoneurons from the primate reticulospinal tract. The Journal of neuroscience : the official journal of the Society for Neuroscience 29:4993-4999.

Rosenthal J, Waller HJ, Amassian VE (1967) An analysis of the activation of motor cortical neurons by surface stimulation. J Neurophysiol 30:844-858.

Rosenzweig ES, Brock JH, Culbertson MD, Lu P, Moseanko R, Edgerton VR, Havton LA, Tuszynski MH (2009) Extensive spinal decussation and bilateral termination of cervical corticospinal projections in rhesus monkeys. The Journal of comparative neurology 513:151-163.

Rothkegel H, Sommer M, Paulus W, Lang N (2010) Impact of pulse duration in single pulse TMS. Clin Neurophysiol 121:1915-1921.

Rothwell J, Burke D, Hicks R, Stephen J, Woodforth I, Crawford M (1994) Transcranial electrical stimulation of the motor cortex in man: further evidence for the site of activation. J Physiol 481 (Pt 1):243-250.

Rothwell JC (2006) The startle reflex, voluntary movement, and the reticulospinal tract. Supplements to Clinical neurophysiology 58:223-231.

Ruddy KL, Leemans A (2017) Structural and Functional Cortical Connectivity Mediating Cross Education of Motor Function. 37:2555-2564.

Rushton WA (1927) The effect upon the threshold for nervous excitation of the length of nerve exposed, and the angle between current and nerve. J Physiol 63:357-377.

Sakai K, Ugawa Y, Terao Y, Hanajima R, Furubayashi T, Kanazawa I (1997) Preferential activation of different I waves by transcranial magnetic stimulation with a figure-of-eight-shaped coil. Exp Brain Res 113:24-32.

Sakai ST, Davidson AG, Buford JA (2009) Reticulospinal neurons in the pontomedullary reticular formation of the monkey (Macaca fascicularis). Neuroscience 163:1158-1170.

Sale DG (1988) Neural adaptation to resistance training. Med Sci Sports Exerc 20:S135-145.

Salvador R, Silva S, Basser PJ, Miranda PC (2011) Determining which mechanisms lead to activation in the motor cortex: a modeling study of transcranial magnetic stimulation using realistic stimulus waveforms and sulcal geometry. Clin Neurophysiol 122:748-758.

Samii A, Wassermann EM, Ikoma K, Mercuri B, Hallett M (1996) Characterization of postexercise facilitation and depression of motor evoked potentials to transcranial magnetic stimulation. Neurology 46:1376-1382.

Sasaki S, Isa T, Pettersson LG, Alstermark B, Naito K, Yoshimura K, Seki K, Ohki Y (2004) Dexterous finger movements in primate without monosynaptic corticomotoneuronal excitation. J Neurophysiol 92:3142-3147.

Schepens B, Drew T (2004a) Independent and convergent signals from the pontomedullary reticular formation contribute to the control of posture and movement during reaching in the cat. J Neurophysiol 92:2217-2238.

Schepens B, Drew T (2004b) Independent and convergent signals from the pontomedullary reticular formation contribute to the control of posture and movement during reaching in the cat. Journal of neurophysiology 92:2217-2238.

Schepens B, Drew T (2006a) Descending signals from the pontomedullary reticular formation are bilateral, asymmetric, and gated during reaching movements in the cat. Journal of neurophysiology 96:2229-2252.

Schepens B, Drew T (2006b) Descending signals from the pontomedullary reticular formation are bilateral, asymmetric, and gated during reaching movements in the cat. J Neurophysiol 96:2229-2252.

Schepens B, Stapley P, Drew T (2008) Neurons in the pontomedullary reticular formation signal posture and movement both as an integrated behavior and independently. J Neurophysiol 100:2235-2253.

Shimazu H, Maier MA, Cerri G, Kirkwood PA, Lemon RN (2004) Macaque ventral premotor cortex exerts powerful facilitation of motor cortex outputs to upper limb motoneurons. J Neurosci 24:1200-1211.

Siegmund GP, Inglis JT, Sanderson DJ (2001) Startle response of human neck muscles sculpted by readiness to perform ballistic head movements. J Physiol 535:289-300.

Soechting JF, Lacquaniti F (1983) Modification of trajectory of a pointing movement in response to a change in target location. J Neurophysiol 49:548-564.

Sommer M, Ciocca M, Chieffo R, Hammond P, Neef A, Paulus W, Rothwell JC, Hannah R (2018) TMS of primary motor cortex with a biphasic pulse activates two independent sets of excitable neurones. Brain Stimul 11:558-565.

Soteropoulos DS, Baker SN (2006) Cortico-cerebellar coherence during a precision grip task in the monkey. J Neurophysiol 95:1194-1206.

Soteropoulos DS, Edgley SA, Baker SN (2011) Lack of evidence for direct corticospinal contributions to control of the ipsilateral forelimb in monkey. The Journal of neuroscience : the official journal of the Society for Neuroscience 31:11208-11219.

Soteropoulos DS, Williams ER, Baker SN (2012) Cells in the monkey ponto-medullary reticular formation modulate their activity with slow finger movements. J Physiol 590:4011-4027.

Stefan K, Kunesch E, Cohen LG, Benecke R, Classen J (2000) Induction of plasticity in the human motor cortex by paired associative stimulation. Brain 123 Pt 3:572-584.

Steriade M (1996) Arousal: revisiting the reticular activating system. Science 272:225-226.

Stuphorn V, Hoffmann KP, Miller LE (1999) Correlation of primate superior colliculus and reticular formation discharge with proximal limb muscle activity. J Neurophysiol 81:1978-1982.

Taylor JL, Gandevia SC (2004) Noninvasive stimulation of the human corticospinal tract. J Appl Physiol (1985) 96:1496-1503.

Taylor JL, Allen GM, Butler JE, Gandevia SC (1997) Effect of contraction strength on responses in biceps brachii and adductor pollicis to transcranial magnetic stimulation. Exp Brain Res 117:472-478.

Tokimura H, Di Lazzaro V, Tokimura Y, Oliviero A, Profice P, Insola A, Mazzone P, Tonali P, Rothwell JC (2000) Short latency inhibition of human hand motor cortex by somatosensory input from the hand. J Physiol 523 Pt 2:503-513.

Ueno S, Tashiro T, Harada K (1988) Localized stimulation of neural tissues in the brain by means of a paired configuration of time-varying magnetic fields. Journal of Applied Physics 64:5862-5864.

Valls-Sole J, Rothwell JC, Goulart F, Cossu G, Munoz E (1999) Patterned ballistic movements triggered by a startle in healthy humans. J Physiol 516 (Pt 3):931-938.

Valls-Solé J, Valldeoriola F, Molinuevo JL, Cossu G, Nobbe F (1999) Prepulse modulation of the startle reaction and the blink reflex in normal human subjects. Exp Brain Res 129:49-56.

Valls-Solé J, Solé A, Valldeoriola F, Muñoz E, Gonzalez LE, Tolosa ES (1995) Reaction time and acoustic startle in normal human subjects. Neurosci Lett 195:97-100.

Werner W (1993) Neurons in the primate superior colliculus are active before and during arm movements to visual targets. The European journal of neuroscience 5:335-340.

Wilson VJ, Wylie RM, Marco LA (1968) Organization of the medial vestibular nucleus. J Neurophysiol 31:166-175.

Witham CL, Fisher KM, Edgley SA, Baker SN (2016) Corticospinal Inputs to Primate Motoneurons Innervating the Forelimb from Two Divisions of Primary Motor Cortex and Area 3a. J Neurosci 36:2605-2616.

Xu J, Ejaz N, Hertler B, Branscheidt M, Widmer M, Faria AV, Harran MD, Cortes JC, Kim N, Celnik PA, Kitago T, Luft AR, Krakauer JW, Diedrichsen J (2017) Separable systems for recovery of finger strength and control after stroke. 118:1151-1163.

Yeo SS, Chang MC, Kwon YH, Jung YJ, Jang SH (2012) Corticoreticular pathway in the human brain: diffusion tensor tractography study. Neurosci Lett 508:9-12.

Yeomans JS, Frankland PW (1995) The acoustic startle reflex: neurons and connections. Brain Res Brain Res Rev 21:301-314.

Yoshino-Saito K, Nishimura Y, Oishi T, Isa T (2010) Quantitative inter-segmental and inter-laminar comparison of corticospinal projections from the forelimb area of the primary motor cortex of macaque monkeys. Neuroscience 171:1164-1179.

Zaaimi B, Dean LR, Baker SN (2018) Different contributions of primary motor cortex, reticular formation, and spinal cord to fractionated muscle activation. 119:235-250.

Zaaimi B, Edgley SA, Soteropoulos DS, Baker SN (2012) Changes in descending motor pathway connectivity after corticospinal tract lesion in macaque monkey. Brain 135:2277-2289.

Zhou S (2000) Chronic neural adaptations to unilateral exercise: mechanisms of cross education. Exerc Sport Sci Rev 28:177-184.

Zijdewind I, Kernell D (2001) Bilateral interactions during contractions of intrinsic hand muscles. J Neurophysiol 85:1907-1913.

Zult T, Goodall S, Thomas K, Solnik S, Hortobagyi T, Howatson G (2016) Mirror Training Augments the Cross-education of Strength and Affects Inhibitory Paths. Med Sci Sports Exerc 48:1001-1013.